12-20-2009

Comparative Analysis of Marine Structural End Connections

Bret Silewicz
University of New Orleans

Comparative Analysis of Marine Structural End Connections

A Thesis

Submitted to the Graduate Faculty of the
University of New Orleans
in partial fulfillment of the
requirements for the degree of

Master of Science
in
Engineering
Civil Engineering

by

Bret A. Silewicz

B.S., University of New Orleans, 2004

December 2009

Acknowledgements

Dr. Mattei, Professor of Civil Engineering supervised the preparation of this thesis, beginning with the approval of the topic and ending with the approval of the content. Additional members of the thesis committee were: Dr. Engin Egeseli, Adjunct Professor of Civil Engineering; and Dr. Lothar Birk, Associate Professor of Naval Architecture and Marine Engineering.

All members of the thesis committee took great interest in the work and provided academic support in the form of guidance and assistance. This thesis could not have been completed without the effort of these individuals.

Table of Contents

List of Figures and Tables

Nomenclature

a	Long Edge Distance (in.)
b	Short Edge Distance (in.)
c	constant
c_s	constant scaled
c_f	constant for fixed member - 12
E	Young's Modulus (psi)
F	Allowable Stress at a Specified Location (psi)
FEA	Finite Element Analysis
F_x	Yield Stress (psi) – 36,000 psi
HVM	Hencky Von Mises Stress Criteria
I_x	Moment of Inertia about x-axis (in^4)
I_y	Moment of Inertia about y-axis (in^4)
I_{xy}	Product Moment of Inertia about x-axis (in^4)
I_{minor}	Moment of Inertia about Minor Axis (in^4)
I_{major}	Moment of Inertia about Major Axis (in^4)
l	Length of Member (in.)
M	Moment about a Specified Location (in-lbs)
M_x	Moment about x-axis (in-lbs)
M_y	Moment about y-axis (in-lbs)
M_n	Yield Moment (in-lbs)
p	Uniform load (psi)
q	Distributed Load (psi)
t	Plate Thickness (in.)
w	Uniform Load (psi)
x	Distance along x-axis to area of concern (in.)
y	Vertical Deformation (in.)
y	Distance along y-axis to area of concern (in.)
α	Roark's Constant for Plate Deformation
β	Roark's Constant for Plate Deformation
β_2	Roark's Constant for Plate Deformation
Δ	Vertical Deformation (in.)
σ	Normal Stress (psi)

Abstract

Numerous structural end connections are utilized everyday in the marine industry for ship design and/or maintenance. End connection design has been developed in earlier vessel designs and adapted as a general standard for all vessels being designed / built at a facility. Usually the supporting calculations developed to analyze the structural end connection are not available for engineers to re-examine. Furthermore, young engineers employ un-proven end connections in their designs, using the justification "It has been done like this in the past, it should work." In this thesis, the author concentrates on finite element analysis for thirteen typical end connections used in the marine industry and correlated the shear and moment transfer to an AISC developed empirical beam equation for comparison. The author will rely on first principle equations and finite element analysis to prove the efficiency of various end connections, and draw comparative conclusions per each end connection analyzed.

Keywords: Marine Structural End Connections, Finite Element Analysis

Chapter 1 – Introduction

Numerous structural end connections are used in the marine industry for ship or facility construction and maintenance. Traditionally, end connection design has been developed from earlier vessel designs and adapted as general standards for all vessels being built at a shipyard. Usually, the supporting calculations developed to validate the structural end connections are not available for designers and engineers to reexamine or prove. The reliance on standards and classification society rules has allowed practical structural design to move away from engineering first principles. In recent years, the development of more user friendly Finite Element Analysis (FEA) software has allowed the engineer to use the computer to take on the computational work of analysis. In doing so, the structural designer essentially gets back to first principles, but uses the computer software to work out the tedious calculations.

Now, there could be the temptation to custom design every end connection and validate it using FEA; however, for shipyard economics, it is still wise to depend on a set of standard end connection details that can be used for various structural conditions rather than a wide variety of unique ones.

This thesis will present three criteria for determining the efficiency of thirteen various structural end connections widely used in the marine industry. The three criteria will also be used to evaluate two baseline end conditions whose fixity will be by definition and called "Baseline Fixed" and "Baseline Fixed Edge Support". It is hoped that by comparing the results of the two theoretical conditions to the thirteen practical standards, a validation will be confirmed.

The end connections were evaluated based on three criteria which analyzed Von Mises stress, nodal rotation, and "c" factors. The first criterion collects the maximum stress at both the

end connection and midspan of the beam. From the obtained results, a percent difference is calculated giving the reader a basis for comparisons. The second criterion compared the nodal rotation at the end connection and at the mid span of the beam. Another set of percent differences was calculated for this criterion. The final criteria developed a “c” factor for comparison reasons. The “c” factor represents a constant used in the empirical equation to calculate the moment on a section for a given end connection, i.e. 8 or 12 if ends are free to rotate or are constrained against rotation. From the three criteria, the reader can draw various conclusions on the end connection analyzed.

The calculations will be based on a representative beam consisting of deck plating, bulkhead plating, a vertical bulkhead stiffener, and a deck stiffener. The deck stiffener and vertical bulkhead stiffener are connected via thirteen various end connection consisting from chocks and brackets to simple web attachment. Both the deck stiffener and vertical bulkhead stiffener are the same section, a 6”x4”x3/8” angle, a common size member used in the marine industry. Also, the deck plating and vertical bulkhead plating are the same thickness, 3/8”.

The results of the comparison will be assessed to determine if reliance on the represented shipyard standards is feasible given checks on a case per case basis.

Chapter 2 – Validation of FEA

One of the most important steps in any analysis is the validation of the method/software. Finite element analysis programs will run any model a designer and/or engineer creates, but is the model accurately represented? Dr. Engin Egeseli of the University of New Orleans, always enforces a simple principle to his students when describing computer modeling, "GIGO; Garbage In = Garbage Out".

A simple validation process can be used to determine if the model is accurately described in regards to mesh size, aspect ratio and warp angle. Aspect ratio and warp angle have set upper limits set by general finite element modeling techniques. The aspect ratio, which is the long edge of the element divided by the short edge of the element, can not exceed 2.0. The warp angle of an element can be described as the maximum out-of-plane angle between any two triangles that you can divide a quad element into [11]. The warp angle cannot exceed 135 degrees, without giving faulty output. The mesh size used in a model is the designer and/or engineer's decision based on the amount of accuracy desired for the model. A larger mesh size will yield a larger error, but takes less computer memory and time to solve. While a denser mesh size will yield a smaller error, but take large computer memory and longer time to solve. A "happy medium" will need to be achieved to keep a model size manageable. Areas of less concern can be modeled with a coarser mesh, while areas of concern can have a more refined mesh size, yielding more accurate results in the areas of interest.

The validation process used in determining the maximum mesh size of the end connections analyzed was determined by modeling three simple models. The following sub sections describe the three FEA models and the obtained results.

FEA Validation - Plate Model

The first of the three models created was of a simple plate. The end constraints, or boundary conditions, were varied with either a simply supported edge or fully fixed edges around the entire perimeter of the plate. The mesh of the model was also varied from coarse to fine to determine the best percent difference from a closed form solution to the finite element solution.

An arbitrary plate size was used for this part of the validation process. The plate size analyzed was 18 inches by 12 inches by 3/8 inch thick. A 5 psi uniform load was applied to the entire surface of the rectangular plate. ALGOR Finite Element Suite was used in creating and compiling the models.

For the closed form solution, reference [5] was used to calculate the maximum deflection at the center of the supported plate. Reference [5] gives the following equations:

For rectangular plate with all edges simply supported and loaded uniformly over the entire plate

$$\sigma_{\max} = \sigma_b = \frac{\beta q b^2}{t^2} \tag{1}$$

and

$$y_{\max} = \frac{-\alpha q b^4}{E t^3} \tag{2}$$

where σ Normal Stress (psi)
y Vertical Deformation (in.)
β 0.4851 for a = 18”, & b = 12”
α 0.0838 for a = 18”, & b = 12”
q Distributed Load (psi)
E Young’s Modulus (psi)
t Plate Thickness (in.)

For rectangular plate with all edges fixed and loaded uniformly over the entire plate. The equations are:

$$\sigma_{max} = \frac{\beta_2 q b^2}{t^2} \tag{3}$$

and

$$y_{max} = \frac{-\alpha q b^4}{E t^3} \tag{4}$$

where σ Normal Stress (psi)
y Vertical Deformation (in.)
β_2 0.4518 for a = 18" & b = 12"
α 0.0239 for a = 18" & b = 12"
q Distributed Load (psi)
E Young's Modulus (psi)
t Plate Thickness (in.)

A comparison was developed for each boundary condition per mesh size, and the FEA model and results are shown in figures 1, 2, 3, and 4, and tables 1, 2, 3, 4, 5, and 6.

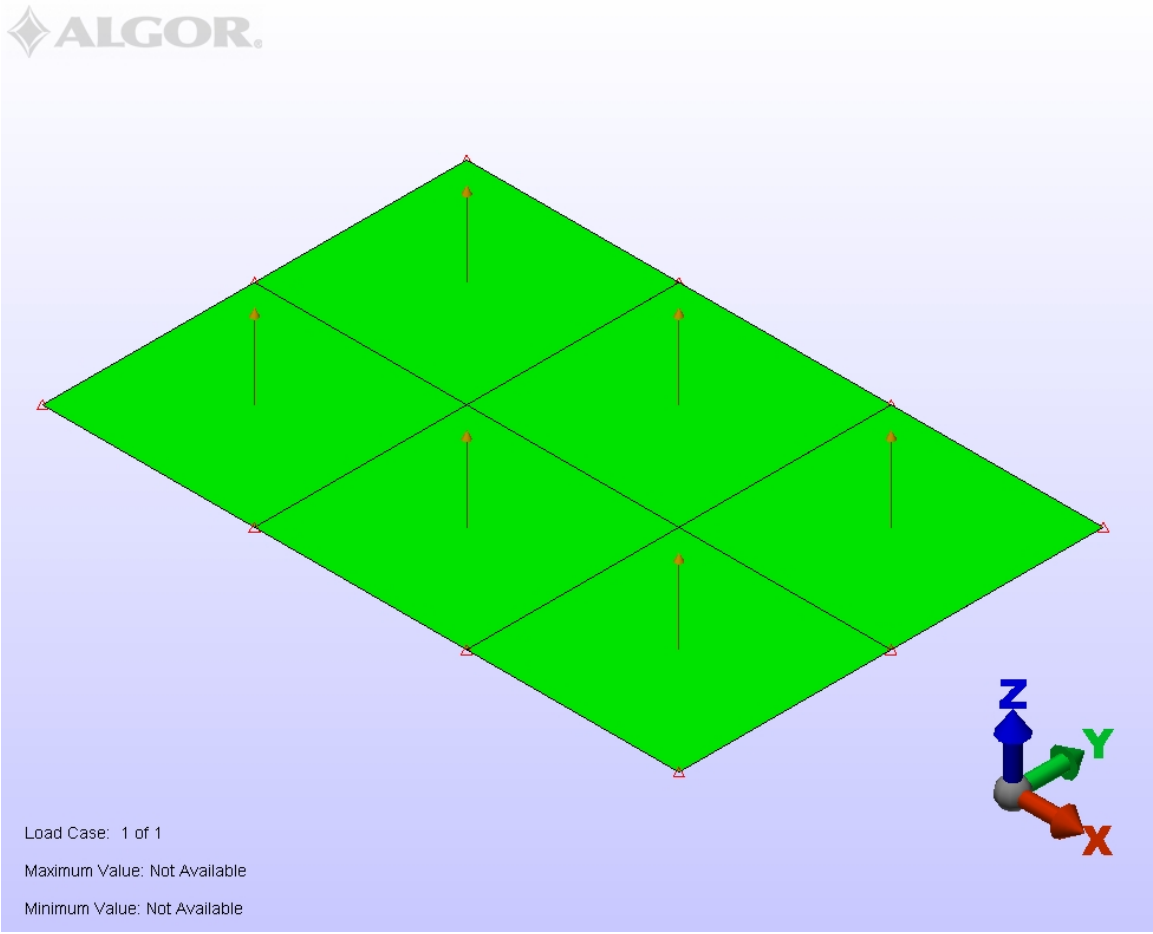

Figure 1 – Simply Supported Plate FEA Model

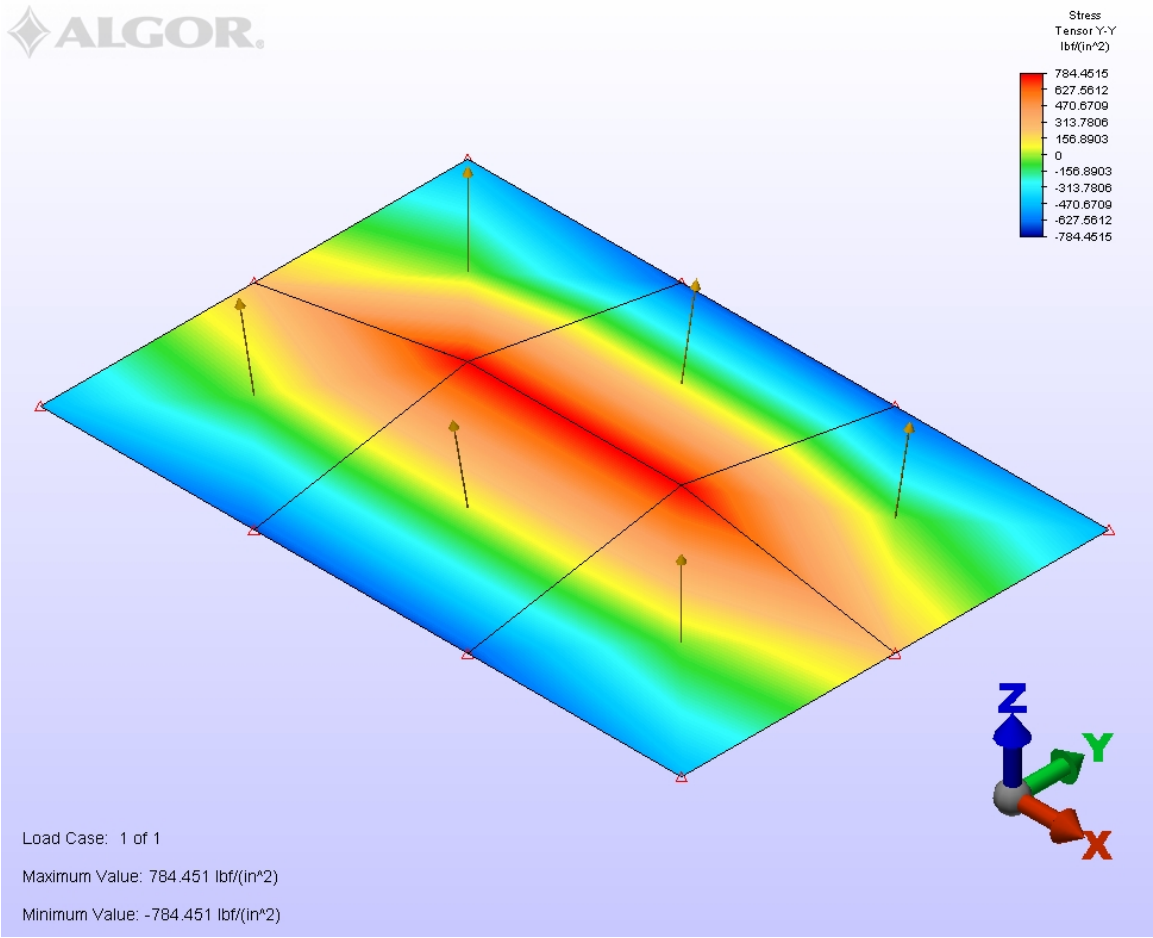

Figure 2 – Simply Supported Plate FEA Stress Results

Plate Verification Model Simply Supported End Constraints FEA Results

	FEA Model Results			
Element Size (Long x Short)	HVM (psi)	Δ (in.)	$f_{v\text{-}v}$ (psi)	$f_{x\text{-}x}$ (psi)
3x2	1,472	0.00359	1,654	1,084
6x4	2,098	0.00522	2,389	1,508
9x6	2,115	0.00544	2,417	1,504
12x8	2,151	0.00562	2,463	1,510
18x12	2,162	0.00570	2,477	1,511
48x32	2,169	0.00575	2,486	1,511

Table 1 - Simply Supported Plate Model FEA Results

Plate Verification Model Simply Supported End Constraints Deflection Percent Difference Results

Element Size (Long x Short)	FEA Δ (in.)	Closed Form Δ (in.)	Percent Difference
3x2	0.00359	0.00568	36.88%
6x4	0.00522	0.00568	8.14%
9x6	0.00544	0.00568	4.25%
12x8	0.00562	0.00568	1.08%
18x12	0.00570	0.00568	-0.29%
48x32	0.00575	0.00568	-1.21%

Table 2 - Simply Supported Plate Model Deformation Comparison

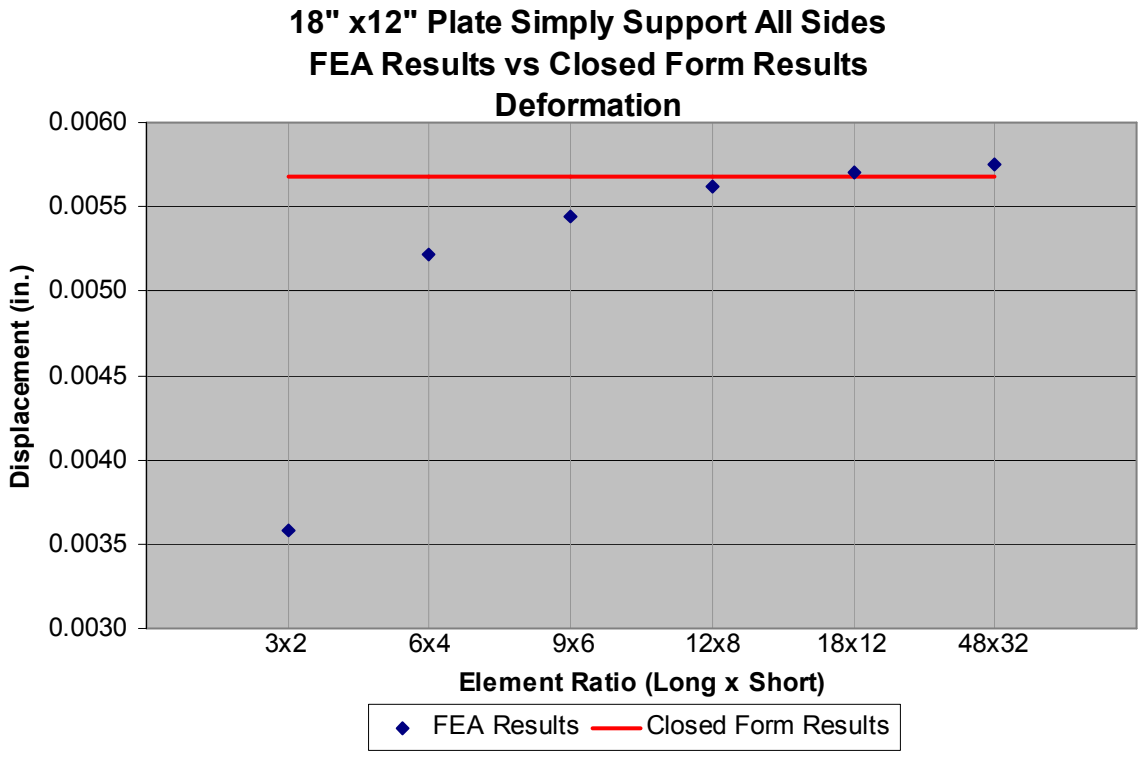

Figure 3 - Simply Supported Plate All Sides - FEA vs. Closed Form - Deformation

Plate Verification Model Simply Supported End Constraints Normal Stress Percent Difference Results

Element Size (Long x Short)	FEA $f_{y\text{-}y}$ (psi)	Closed Form σ_{max} (psi)	Percent Difference
3x2	1,654	2,484	33.40%
6x4	2,389	2,484	3.82%
9x6	2,417	2,484	2.70%
12x8	2,463	2,484	0.82%
18x12	2,477	2,484	0.28%
48x32	2,486	2,484	-0.09%

Table 3 - Simply Support Plate Model Stress Comparison

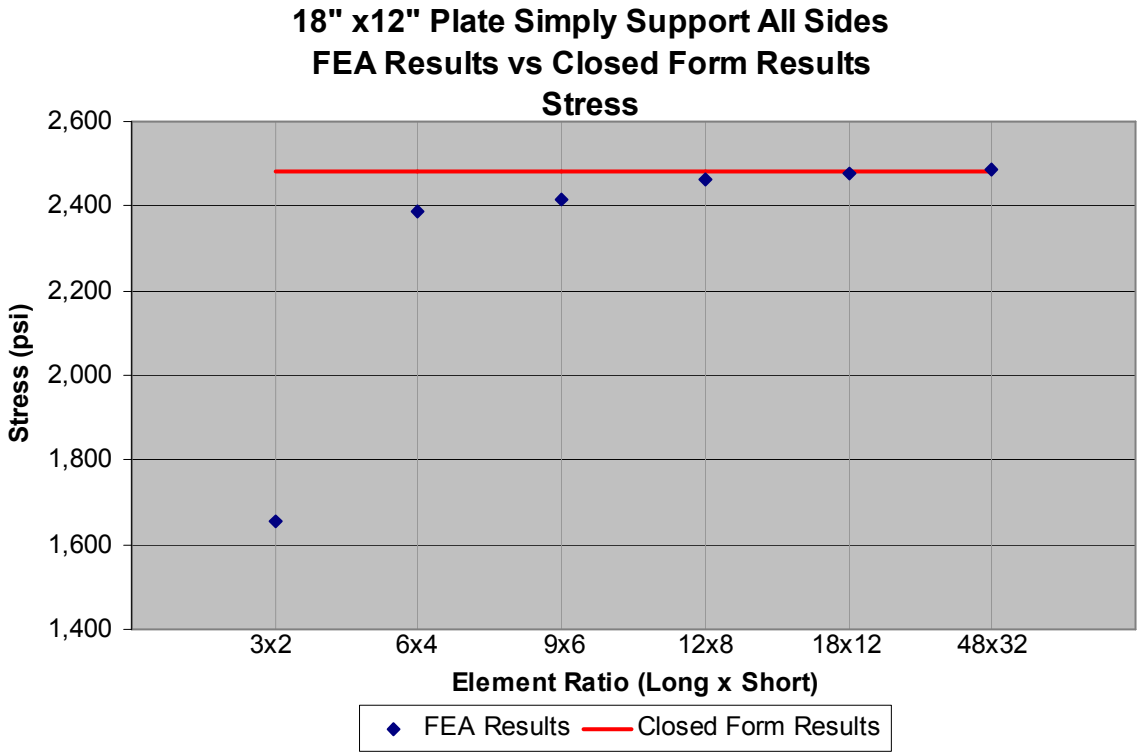

Figure 4 - Simply Supported Plate All Sides - FEA vs. Closed Form - Stress

Plate Verification Model Fixed End Constraints FEA Results

	FEA Model Results			
Element Size (Long x Short)	HVM (psi)	Δ (in.)	f_{y-y} (psi)	f_{x-x} (psi)
3x2	761	0.00138	784	437
6x4	1,463	0.00156	1,653	1,221
9x6	966	0.00157	1,111	630
12x8	979	0.00161	1,128	624
18x12	978	0.00163	1,128	618
48x32	975	0.00164	1,127	613

Table 4 - Fixed Supported Plate All Sides - FEA vs. Closed Form – FEA Results

Plate Verification Model Fixed End Constraints Deflection Percent Difference Results

Element Size (Long x Short)	FEA Δ (in.)	Closed Form Δ (in.)	Percent Difference
3x2	0.00138	0.00162	14.58%
6x4	0.00156	0.00162	3.97%
9x6	0.00157	0.00162	3.04%
12x8	0.00161	0.00162	0.39%
18x12	0.00163	0.00162	-0.41%
48x32	0.00164	0.00162	-0.97%

Table 5 - Fixed Supported Plate All Sides - FEA vs. Closed Form – Deformation

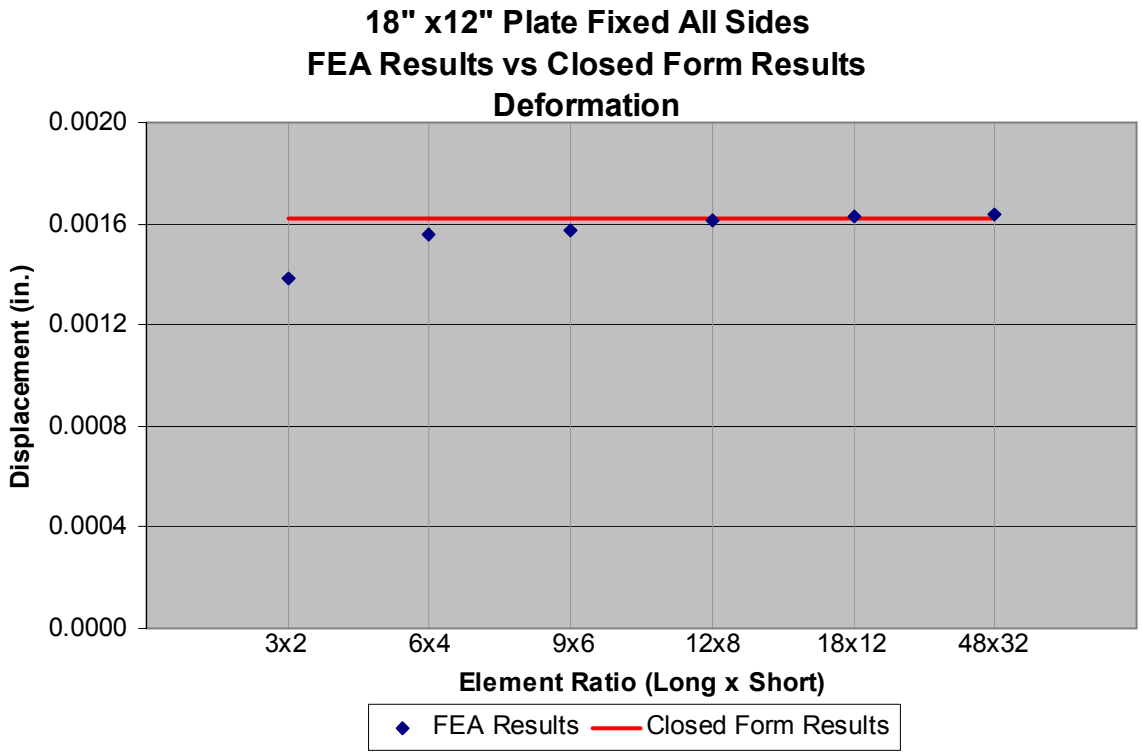

Figure 5 - Fixed Supported Plate All Sides - FEA vs. Closed Form - Deformation

Plate Verification Model Fixed End Constraints Normal Stress Percent Difference Results

Element Size (Long x Short)	FEA $f_{y\text{-}y}$ (psi)	Closed Form σ_{max} (psi)	Percent Difference
3x2	784	1,121	30.04%
6x4	1,653	1,121	-47.41%
9x6	1,111	1,121	0.90%
12x8	1,128	1,121	-0.63%
18x12	1,128	1,121	-0.59%
48x32	1,127	1,121	-0.54%

Table 6- Fixed Supported Plate All Sides - FEA vs. Closed Form – Stress

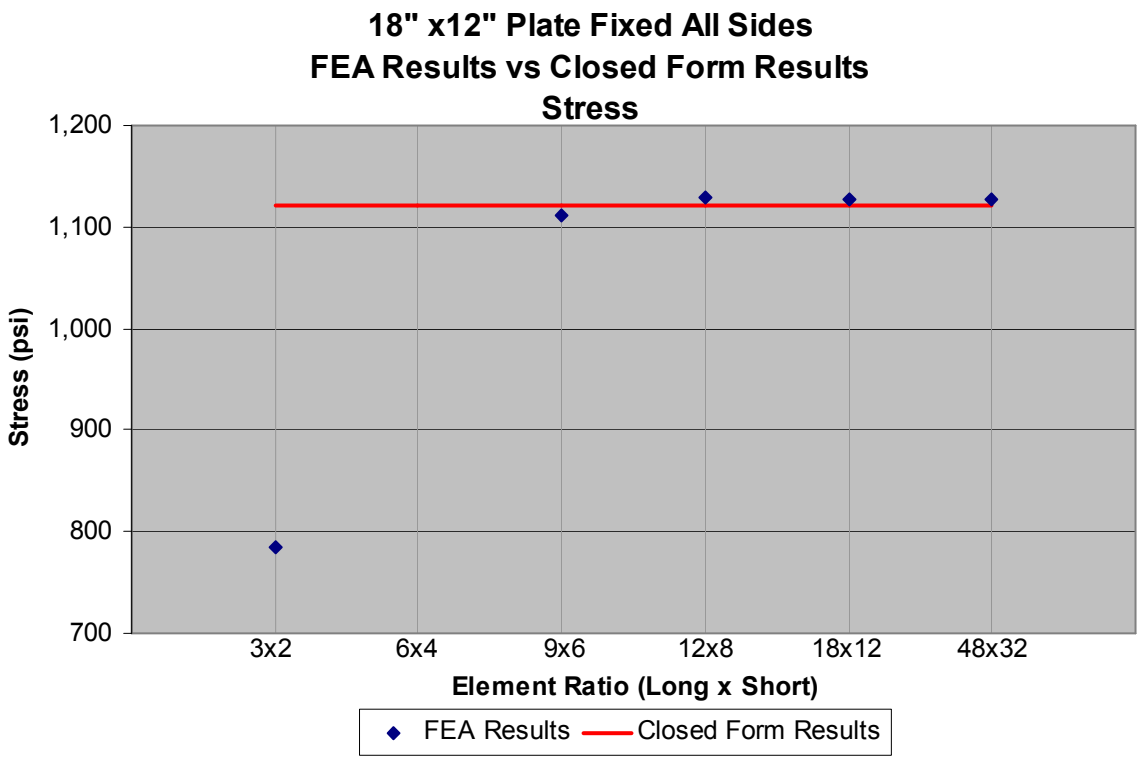

Figure 6- Fixed Supported Plate All Sides - FEA vs. Closed Form - Stress

FEA Validation – Cantilever Beam Model

A second model was created to determine the optimal mesh density of the web of a stiffener. This model represented a 120 inch long cantilevered member, fixed on one side, and free on the other. A 10 lbs. load was placed at the edge of the free side of the stiffener, and again the model was run with varying mesh densities. the mesh size was altered from a coarse to a fine mesh, and the percent difference was calculated by the finite element results to a closed form results. The closed form results were calculated as follow. From Reference [11] the equation for the deflection of a cantilevered beam in consideration of shear deflection

$$\Delta = \frac{pl^3}{3EI}\left[1 + 0.71\left(\frac{h}{l}\right)^2 - 0.10\left(\frac{h}{l}\right)^3\right] \tag{5}$$

where Δ Vertical Deformation (in.)
p Uniform load (psi)
l Length of Member (in.)
E Young's Modulus (psi)
I the inertia in the axis of the deflection (in^4)
h the height of the member (in.)

The maximum normal stress of the member can be calculated by the following equation;

$$\sigma_{max} = \frac{M}{S_x} \tag{6}$$

The FEA model and typical results are shown in figures 6, 7, 8 and 9 and tables 8, 9 and 10.

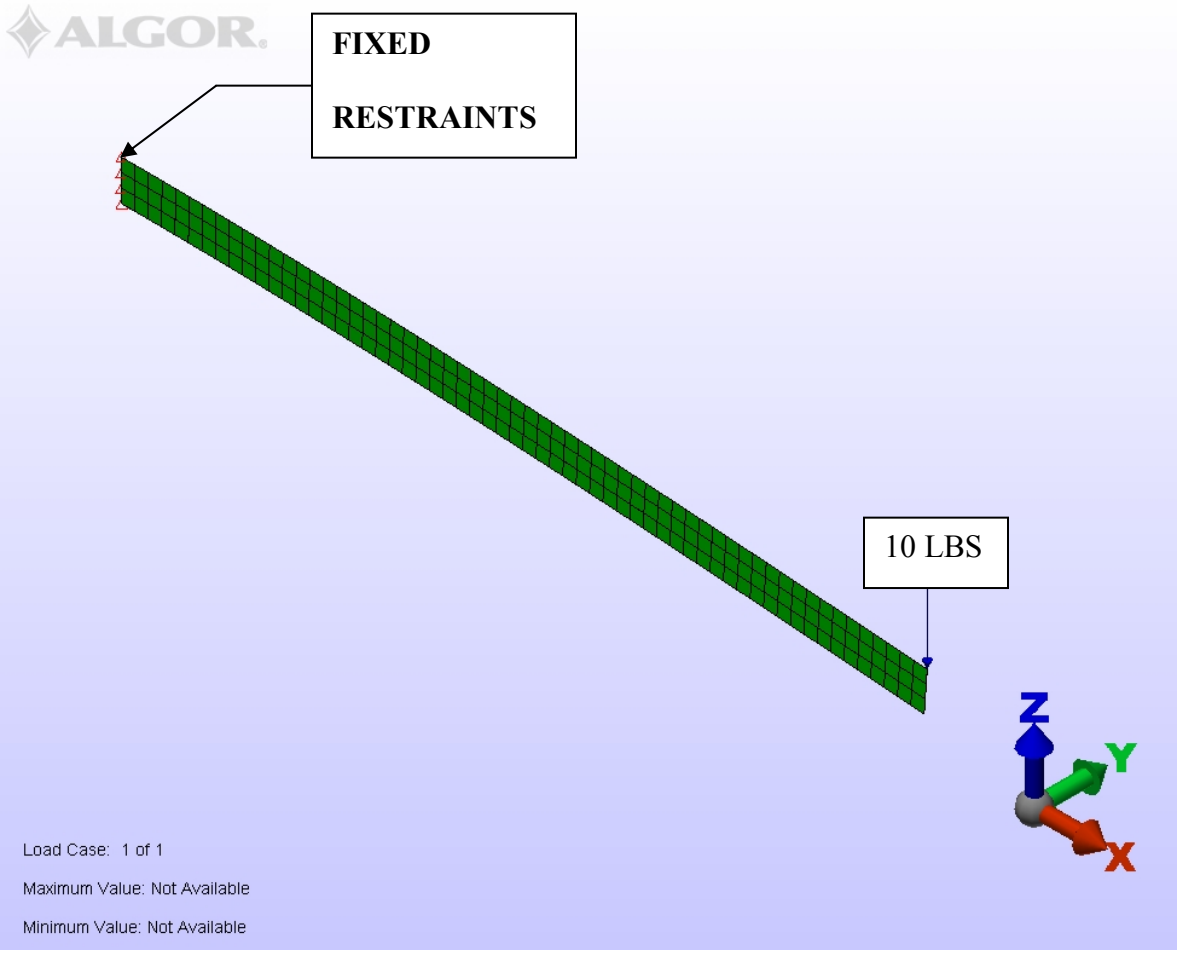

Figure 7 - 6"x3/8" FB Validation FEA Model

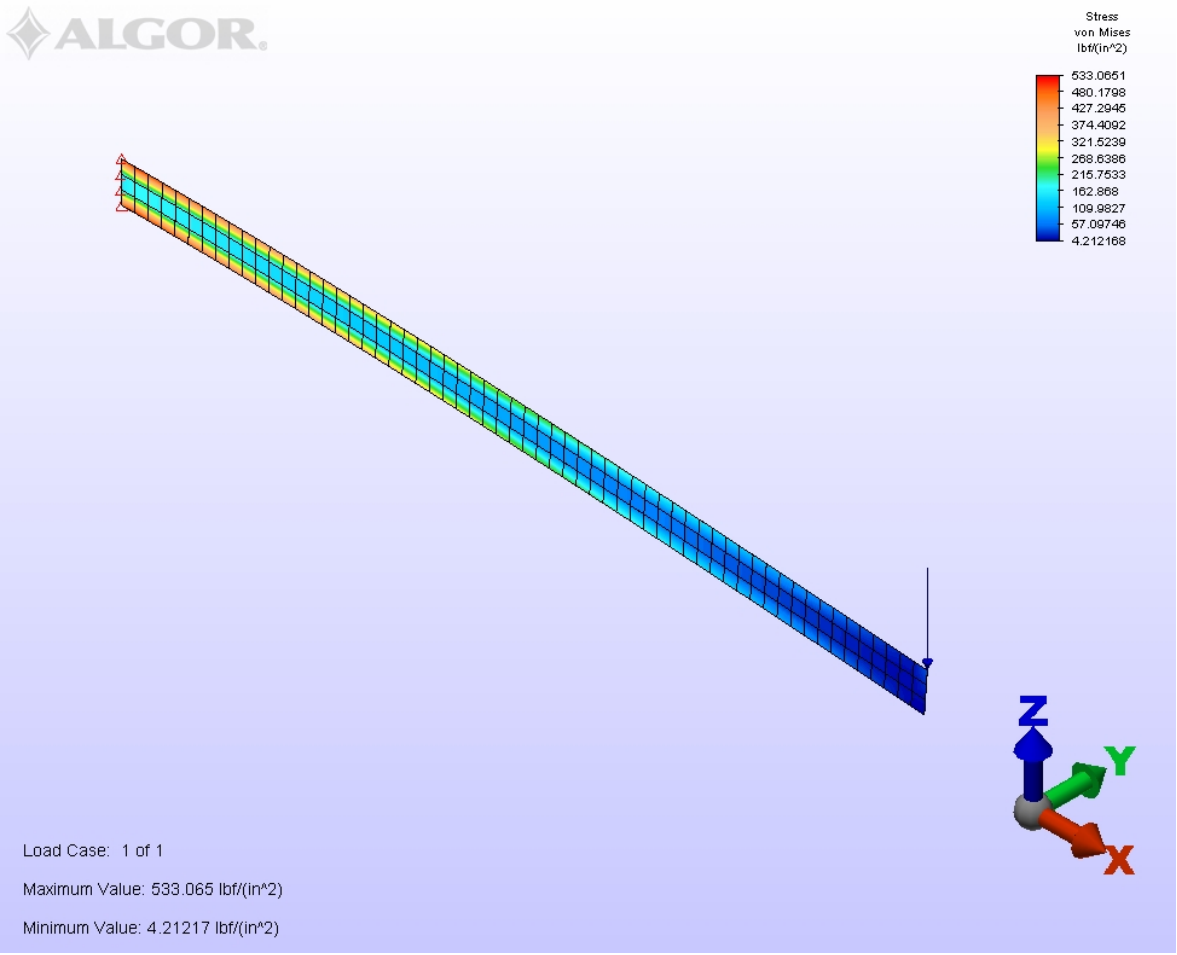

Figure 8 - 6"x3/8" FB Validation FEA Model Stress Plot

A comparison was developed for per mesh size, and the results are shown below;

	FEA Model Results	
Element Size	Δ (in.)	$f_{x\text{-}x}$ (psi)
20x1	0.029476	506.67
40x2	0.029451	507.08
60x3	0.029462	507.38
80x4	0.029469	506.85
120x6	0.029475	506.70
320x16	0.029484	506.66

Table 7 – Cantilever Beam - FEA Results

Beam Validation Model Deflection Percent Difference Results

Element Size	FEA Δ (in.)	Closed Form Δ (in.)	Percent Difference
20x1	0.029476	0.029477	0.00%
40x2	0.029451	0.029477	-0.09%
60x3	0.029462	0.029477	-0.05%
80x4	0.029469	0.029477	-0.03%
120x6	0.029475	0.029477	-0.01%
320x16	0.029484	0.029477	0.02%

Table 8 - Cantilever Beam - FEA vs. Closed Form – Deformation

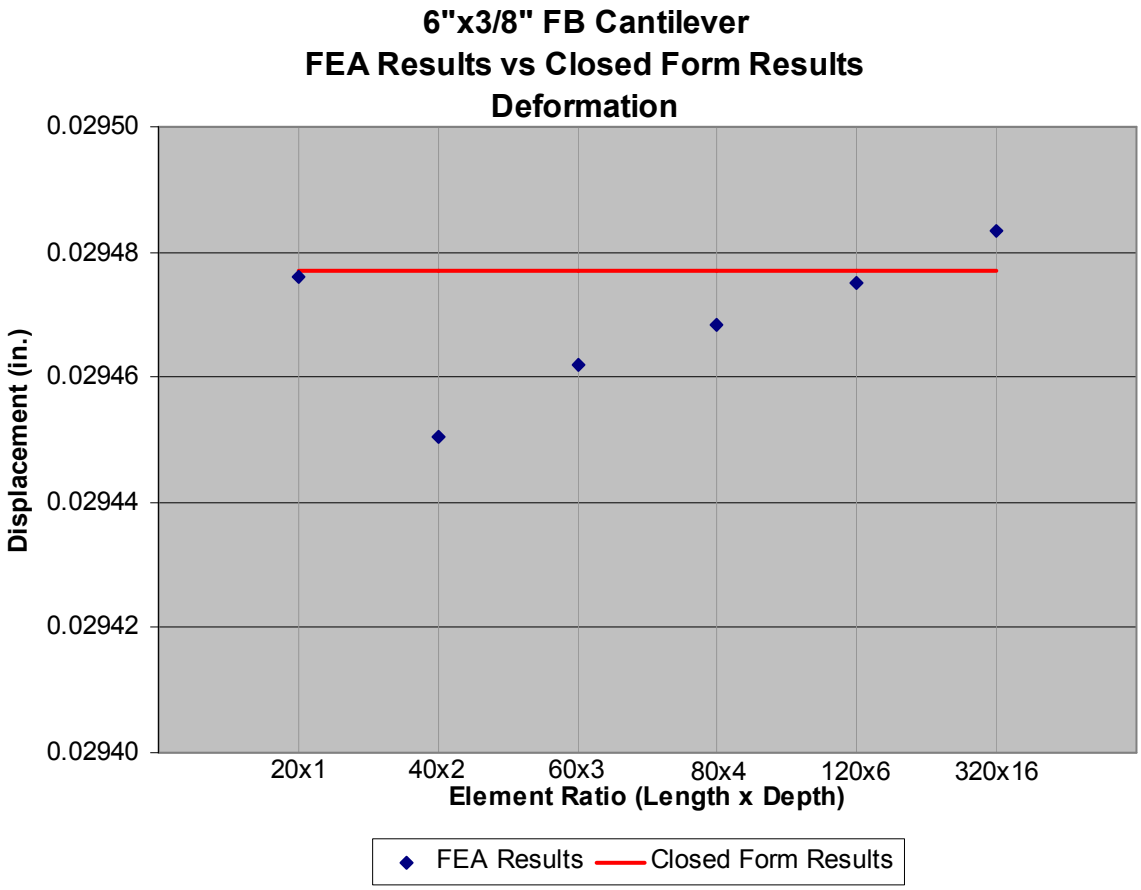

Figure 9 - Cantilever Beam - FEA vs. Closed Form - Deformation

Beam Validation Model Stress Percent Difference Results

Element Size	FEA f_{x-x} (psi)	Closed Form σ_{max} (psi)	Percent Difference
20x1	506.67	506.67	0.00%
40x2	507.08	506.67	0.08%
60x3	507.24	506.67	0.11%
80x4	506.85	506.67	0.04%
120x6	506.70	506.67	0.01%
320x16	506.66	506.67	0.00%

Table 9 - Cantilever Beam - FEA vs. Closed Form – Stress

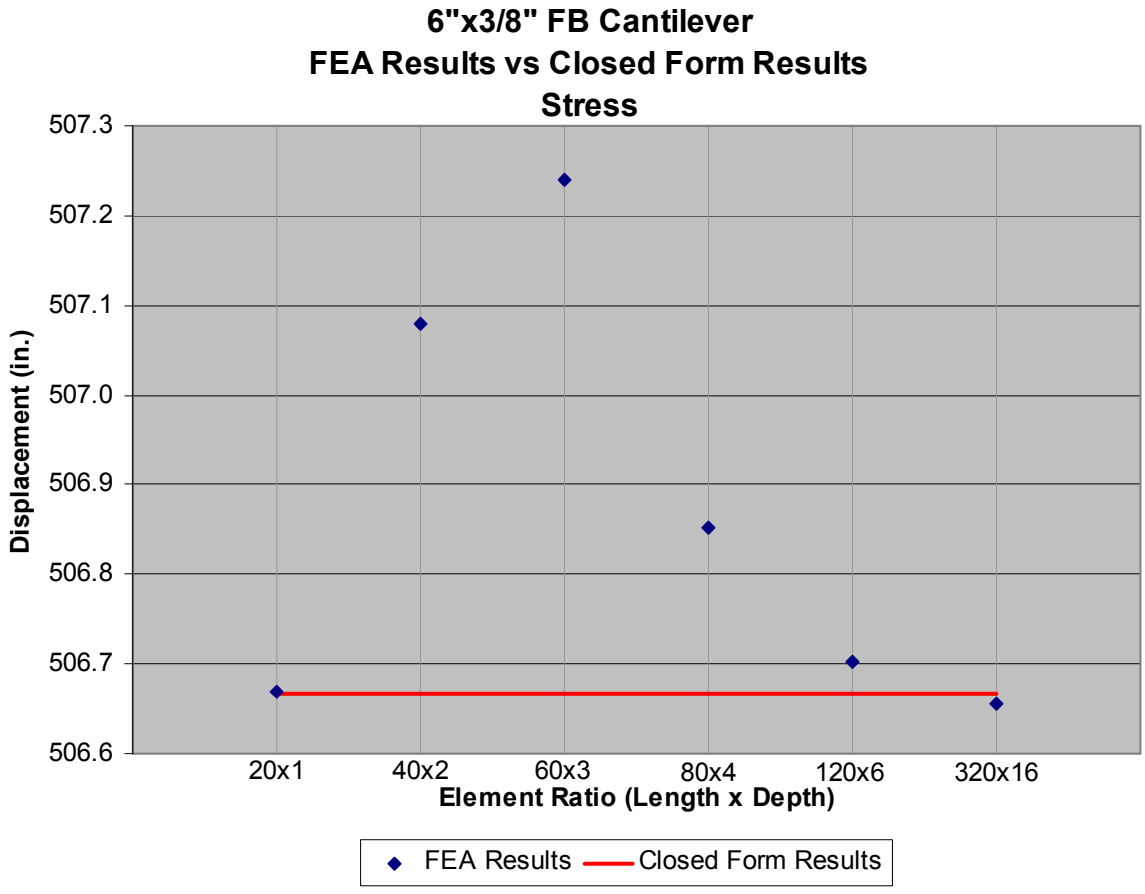

Figure 10 - Cantilever Beam - FEA vs. Closed Form - Stress

This step of the validation process shows that the optimal mesh density for the web of a cantilevered member is 60 elements long by 3 elements deep.

FEA Validation – L6"x4"x3/8" Model

A third model was created just like the previous two, except that the model represented a 6"x4"x3/8" angle. The length of the section is 120 inches. Both the section and length are the equivalent to the end connection models used to create the comparisons. Again the mesh size was altered from a coarse to a fine mesh, and the percent difference was calculated by the finite element results to closed form results. The closed form results were calculated using the following equation from reference [2] for the deflection of a beam fixed at both ends and uniformly load distributed along the length of the member.

$$\Delta_{\max} = \frac{wl^4}{384EI} \tag{7}$$

Where Δ Vertical Deformation (in.)
w Uniform Load (psi)
l Length of Member (in.)
E Young's Modulus (psi)
I the inertia in the axis of the deflection (in^4)

In the case of an un-balanced (unsymmetrical) section, "I" will be substituted for the major and minor inertias. Therefore equation (7) will be split into two directions, the deflection in the major axis and the deflection in the minor axis. Thus re-writing the equations

$$\Delta_{major} = \frac{wl^4}{384EI_{major}} \tag{8}$$

and

$$\Delta_{\min or} = \frac{wl^4}{384EI_{\min or}} \tag{9}$$

The total deflection of the un-symmetric section will therefore be calculated as

$$\Delta = \sqrt{\Delta_{major}^2 + \Delta_{\min or}^2} \tag{10}$$

The FEA model and typical results are shown in figures 11 and 12.

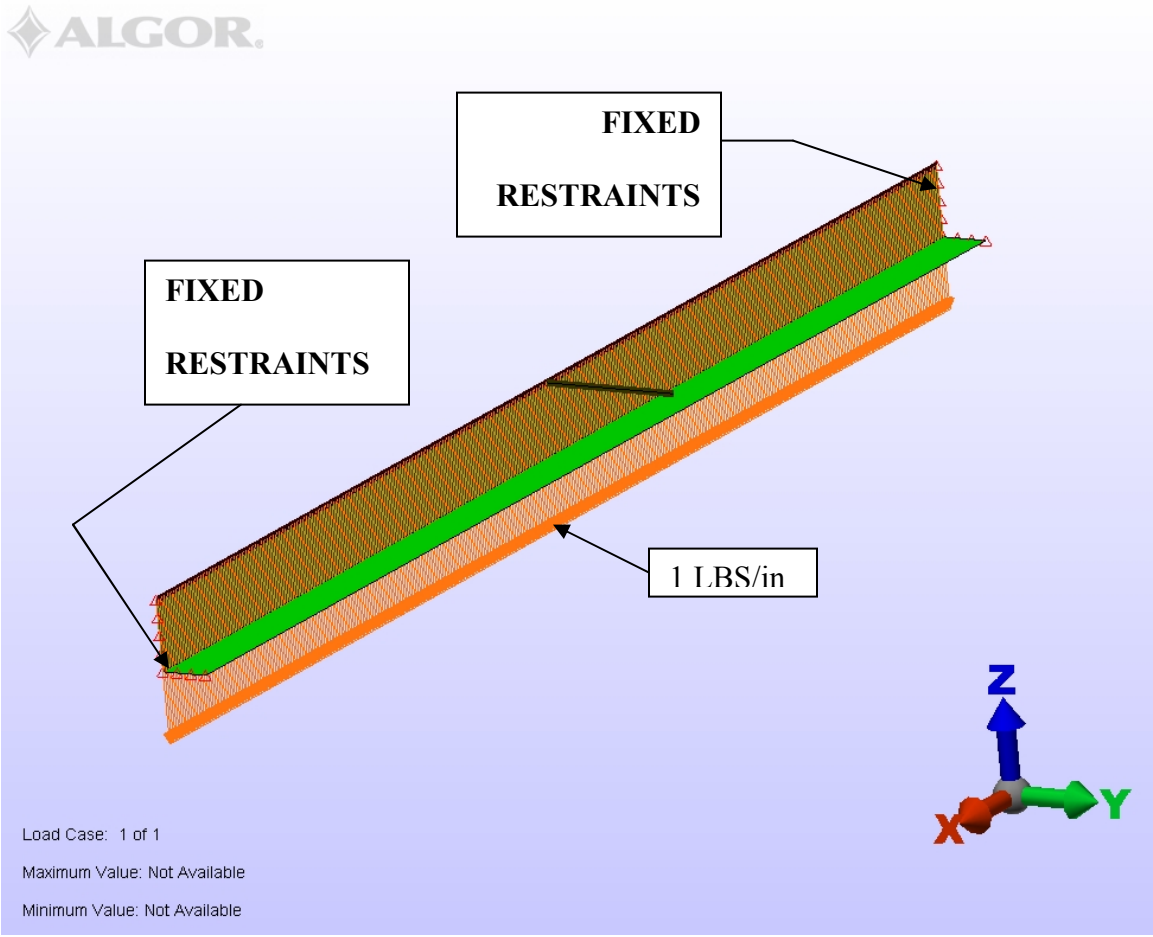

Figure 11 - L6"x4"x3/8" Validation FEA Model

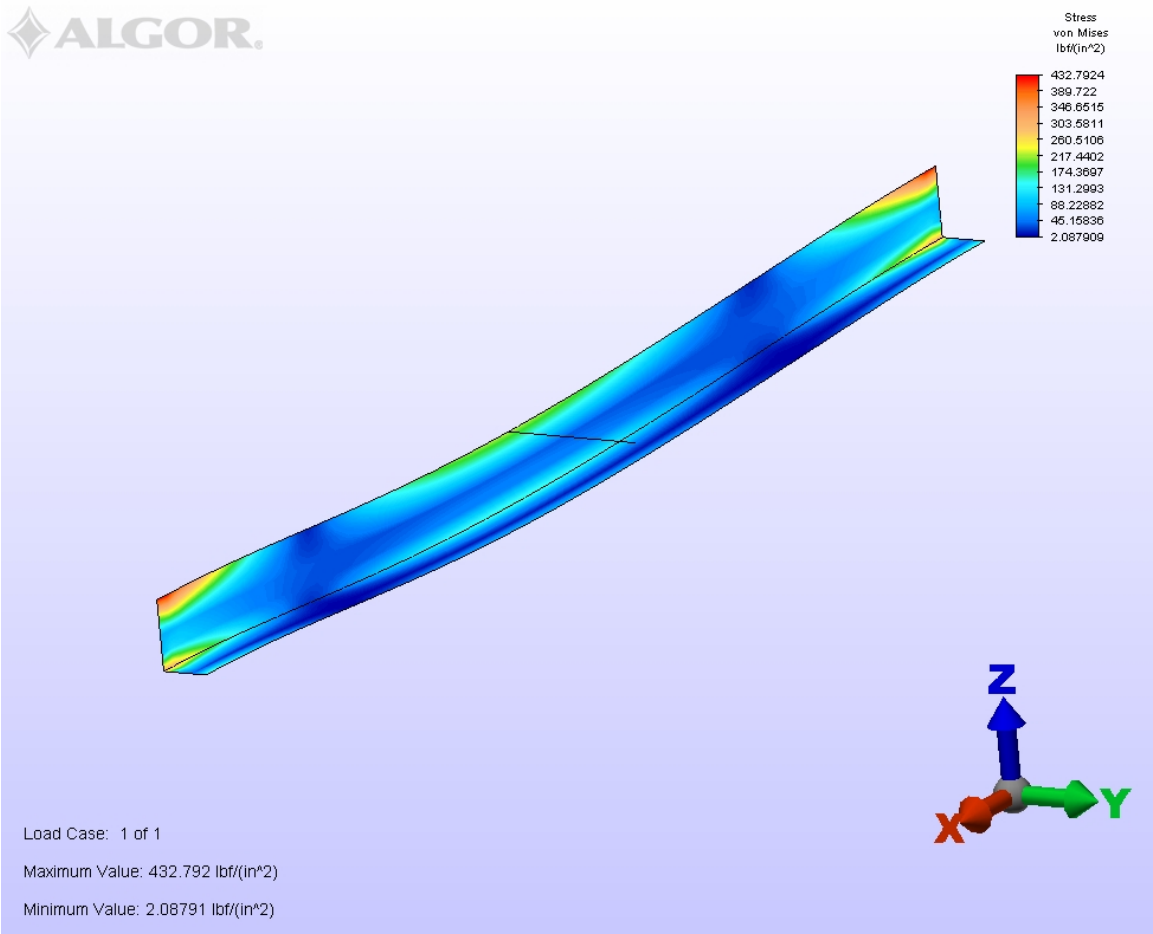

Figure 12 - L6"x4"x3/8" Validation FEA Model Stress Plot

A comparison was developed for each boundary condition per mesh size, and the results are shown in figure 13 and 14 and tables 11, 12, and 13.

Beam Validation Model Fixed End Constraints FEA Results

		FEA Model Results			
		Midspan			Ends
		Web		Flange	Shear
Element Size	Δ (in.)	f_{x-x} Top Avg Mem (psi)	f_{x-x} Knuckle Avg Mem (psi)	f_{x-x} Toe Avg Mem (psi)	f_{x-z} Avg Mem (psi)
60x3x2	0.003025	-227.56	170.03	-83.94	23.99
80x4x3	0.003029	-226.62	170.29	-84.03	22.75
120x6x4	0.003033	-226.78	170.40	-84.09	25.93
320x16x11	0.003035	-228.22	170.46	-84.13	22.92

Table 10 - L6"x4"x3/8" - FEA Results

Beam Validation Model Fixed End Constraints Deflection Percent Difference Results

Element Size (Length x Web x Flange)	FEA Δ (in.)	Closed Form Δ (in.)	Percent Difference
60x3x2	0.00303	0.00299	1.15%
80x4x3	0.00303	0.00299	1.28%
120x6x4	0.00303	0.00299	1.39%
320x16x11	0.00304	0.00299	1.48%

Table 11 - L6"x4"x3/8" - FEA vs. Closed Form - Deformation

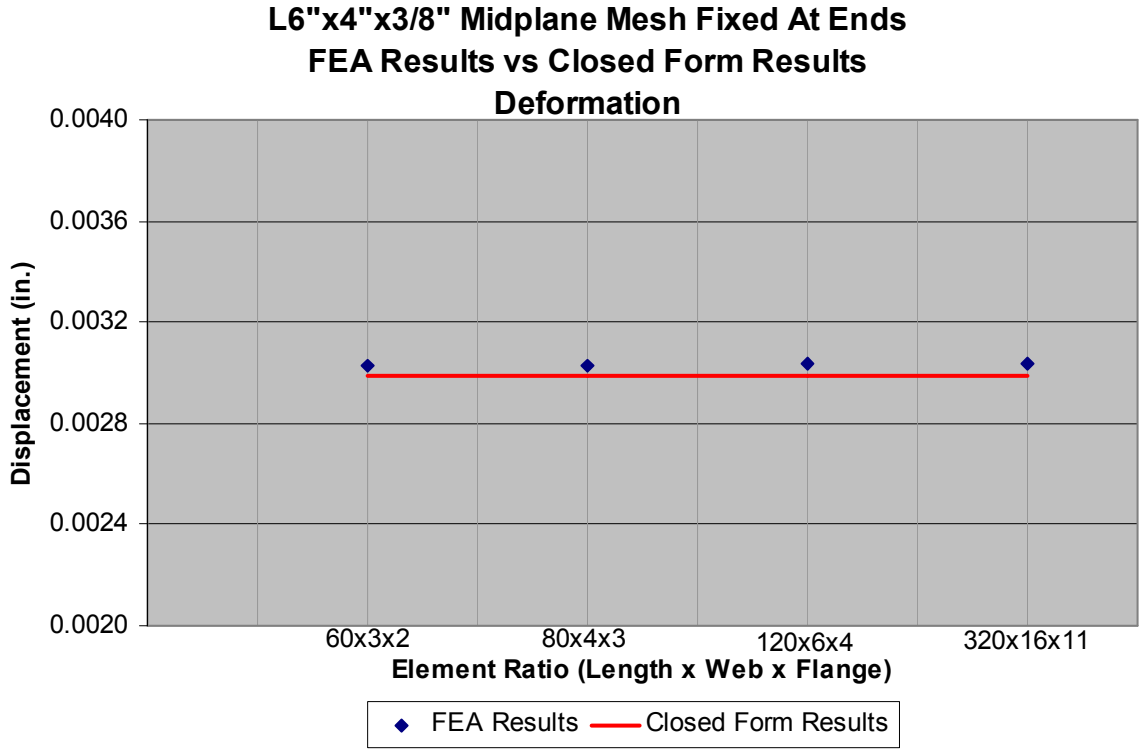

Figure 13 - L6"x4"x3/8" - FEA vs. Closed Form - Deformation

Beam Validation Model Fixed End Constraints Normal Stress Percent Difference Results

Element Size (Length x Web x Flange)	FEA $f_{y\text{-}y}$ (psi)	Closed Form σ_{max} (psi)	Percent Difference
60x3x2	-227.56	-227.85	0.13%
80x4x3	-226.62	-227.85	0.54%
120x6x4	-226.78	-227.85	0.47%
320x16x11	-228.22	-227.85	-0.16%

Table 12 - L6"x4"x3/8" - FEA vs. Closed Form - Stress

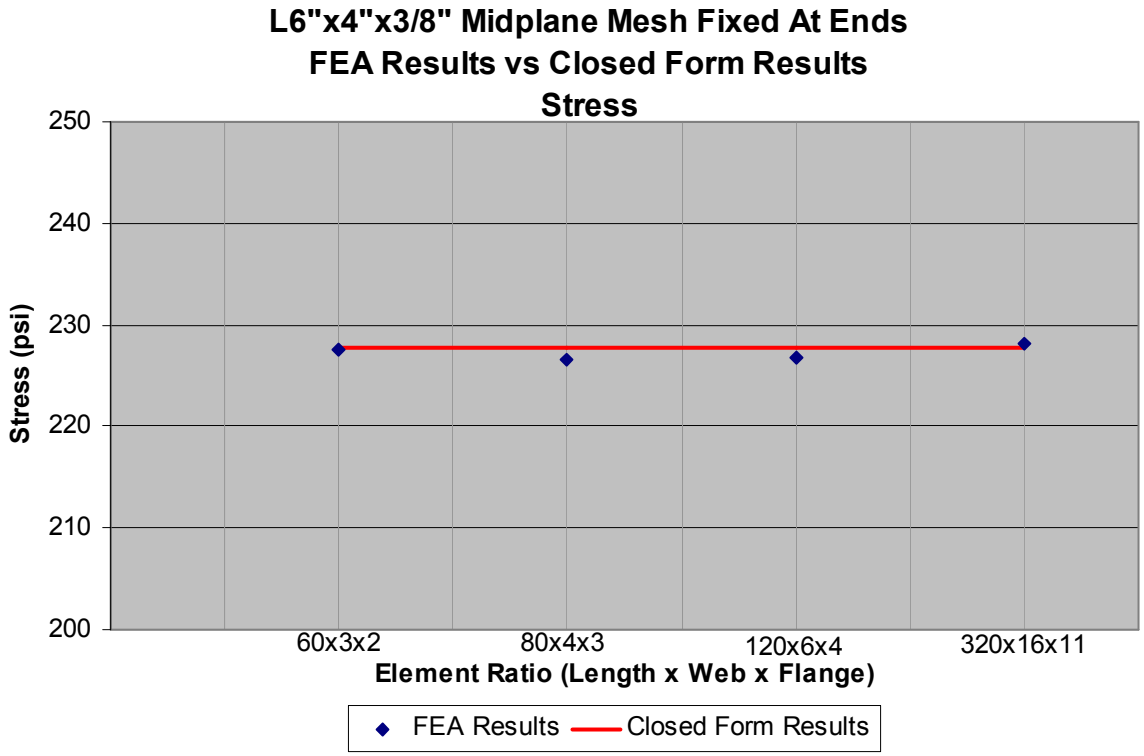

Figure 14 - L6"x4"x3/8" - FEA vs. Closed Form - Stress

Once all percent differences were calculated, the decision of which mesh size to be used to create the individual end connection models could be made. In terms of a simple rectangular plate model with varying end constraints. The percent difference shows that the denser the mesh, the lower the percent difference. In terms of a fixed beam model representing an angle, the above statement does not hold true. The percent difference for the coarser 60 elements long by 3 elements deep on the web, and 2 elements wide on the flange result in a lowest percent

difference. And the denser the mesh, the larger the percent difference grew. Looking at the actual deflection outputted from the finite element model, the deflection is the same up to the fifth decimal place, which is not practical to hold in basic structure calculations. The percent difference for the coarser plate model was not that great, and the difference could be tolerated. Therefore, the coarser 60 elements long by 3 elements deep on the web, and 2 elements wide on the flange was used to create the individual end connection models.

Chapter 3 – Modeling Criteria

Using Algor Finite Element Suite, thirteen various end connections were created, analyzed, and compared against a baseline model. A plate model of each end connection was created using the same mesh size and properties to ensure a proper comparison. The only variation in the mesh size was in areas in way of the connection where a perfect square mesh could not be used. The mesh size was determined with the methodology of Chapter 2.

For the sole purpose of creating a comparison, the thirteen end connections models and the baseline model used for the comparison maintained identical model properties. Therefore the only changes in each model were the end connection. The bulkhead, bulkhead stiffener, deck, and deck stiffener are identical for all models. A common plate thickness and stiffener size used in the marine field were chosen to create all the models. The plate is 3/8" thick grade "A" material, and the stiffeners are 6"x4"x3/8" angles, grade "A". Grade "A" material is carbon steel with a yield stress of 36 ksi.

The end restraints applied to each model are the same for every model. As shown in the table below, the restraints are given in table 14 and figure 15.

	Constraint					
	Translation			Rotation		
Side	T_x	T_y	T_z	R_x	R_y	R_z
A		x		x		x
B	x				x	x
C		x		x		x
D			x	x	x	
E		x		x		x
F		x		x		x
G			x	x	x	

Table 13 - Typical FEA Model End Constraints

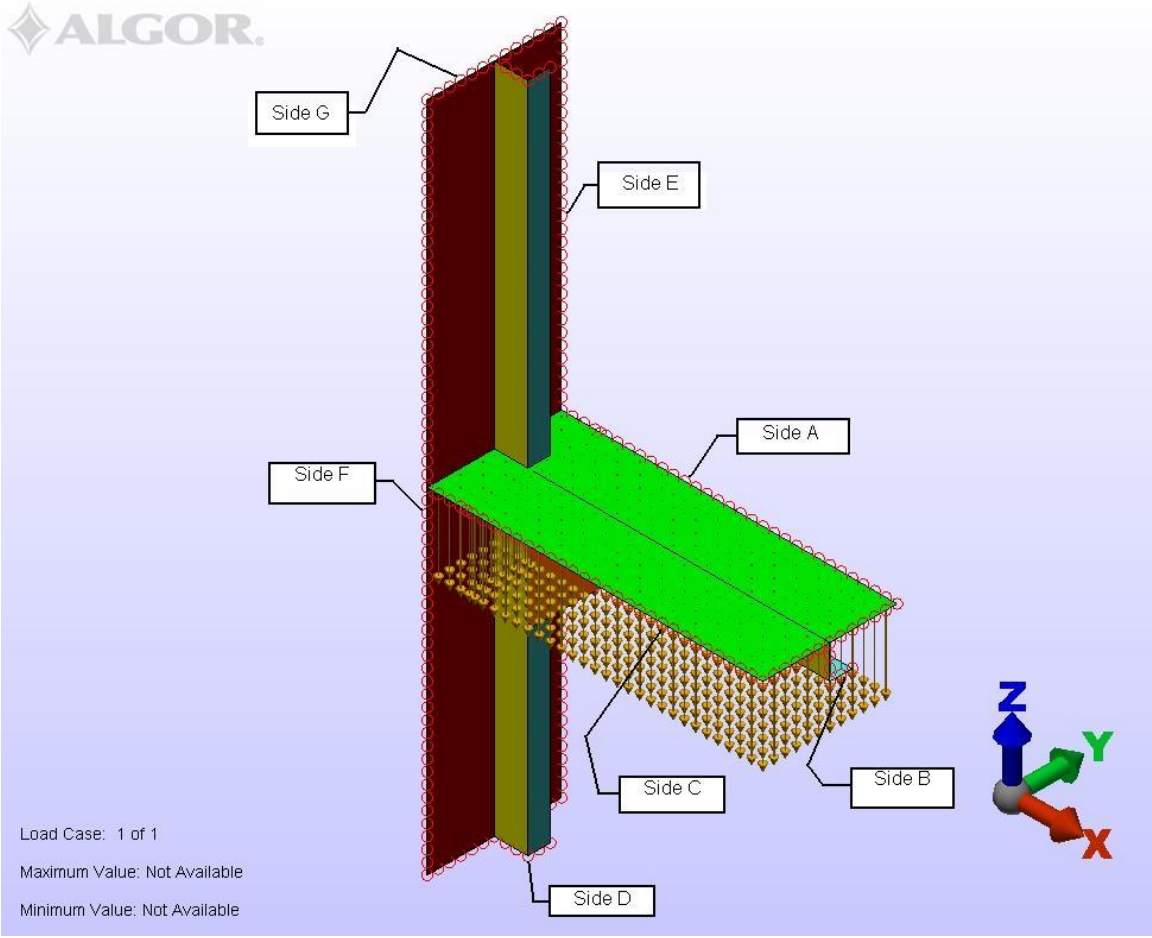

Figure 15 - Typical FEA Model End Constraints

The end constraints were chosen so that sides “A” and “C” are symmetric and the model is being mirrored infinitely in the positive and negative y-axis. Sides “D” and “G” are constrained so that the model is mirrored about the x-axis. Side “B” is constrained so that the model is mirrored about the y-axis.

Chapter 4 – Comparison Criteria

Each of the 13 different end connections analyzed was compared to the baseline models by three different criteria. The three different criteria were Von Mises Stress, End Rotation, and "c" Factors. Explanations of these three criteria are listed below. The baseline model represents a 100% fixed end connection eliminating all translations and rotations at the ends of the beam. The figure below shows the areas where the stress output was selected and compared.

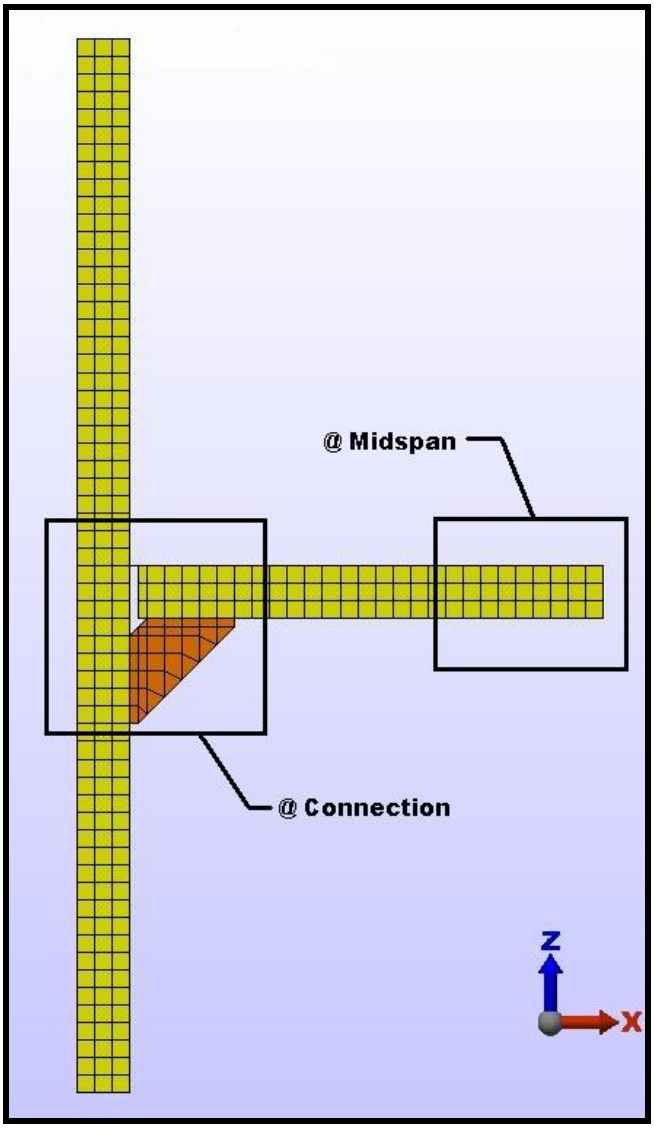

Figure 16 - Areas of Concern for Stress Results

Each criterion is described in the following sections.

Stress Criteria

From each model, Von Mises stress was calculated from the application of a 10 psi uniform load on the deck of the model, and recorded for two locations of the frame. The first location was at the midspan of the beam and the second location was at the end connection. The stresses were then compared against the baseline models, and a percent difference at the desired location was calculated and used as a comparison criteria. Results for this criterion can be viewed in Chapter 5, 6, and 7.

Rotation Criteria

The node rotation angle was calculated from the application of a 10 psi uniform load on the deck of the model, and recorded per each model analyzed at the midspan and at the joint. The node rotation angles were then compared to the baseline model by a percent difference at the desired location. Results for this criterion can be viewed in Chapter 5, 6, and 7.

"c" Factor Criteria

By loading each model with an increasing uniform load *p* until a stress concentration of 36 ksi was reached, the maximum uniform load the beam/end connection can withstand was determined. From AISC 13th Ed, Table 3-23, "Shears, Moments, and Deflection tables, the maximum moment for a beam fixed at both ends – uniformly distributed loads", the moment at midspan and at the end is calculated as

$$M = \frac{wl^2}{c} \tag{11}$$

where M Moment about a Specified Location (in-lbs)
w Uniform Load (psi)
l Length of Member (in.)
c = 12 at the ends and 24 at the center,

Manipulating equation (11), to solve for "c" and replacing M for M_n, the maximum constant "c" can be determined to achieve yield, thus giving equation (12).

$$c = \frac{wl^2}{M_n} \tag{12}$$

From reference [9] the normal stress distribution on a given section of beam subjected to unsymmetrical bending is

$$\sigma_{zz} = -\left[\frac{M_y I_x + M_x I_y}{I_x I_y - I_{xy} I_{xy}}\right]x + \left[\frac{M_x I_y + M_y I_{xy}}{I_x I_y - I_{xy} I_{xy}}\right]y \tag{13}$$

Substituting σ_{zz} for F_x, M_x for M_n, and $M_y = 0$ reduces equation (13) to

$$M_n = \left[\frac{F_x\left(I_x I_y - I_x{}^2{}_y\right)}{-I_{xy}(x) + I_y(y)}\right] \tag{14}$$

Combining equation (12) and (14) will determine the constant "c" for a uniform load "*p*" per end connection analyzed. The combined equation is

$$c = \frac{wl^2}{\left[\frac{F_x\left(I_x I_y - I_x{}^2{}_y\right)}{-I_{xy}(x) + I_y(y)}\right]} \tag{15}$$

Since a baseline finite element model was used as a contrast to compare the various end connections analyzed, the calculated constant "c" from equation (15) did not produce the constant of 12 as stated in equation (11). Thus, a scaling factor was developed to achieve a truly

fixed constant “c” of 12 at the end connection of the baseline model. The scaling factor was developed with the following equation;

$$c_s = \frac{c \times c_f}{c} \tag{16}$$

Where c_s constant scaled
c_f constant for fixed member - 12

Chapter 5 – Baseline Models

To create a contrast to compare to, a baseline model was created using Algor finite element suite. The baseline model represents a truly fixed model where all translations and rotations are constrained at the ends of the section. The finite element model can be seen below in figure (17). The mesh density and node locations are identical to the 13 end connection models created for the comparison.

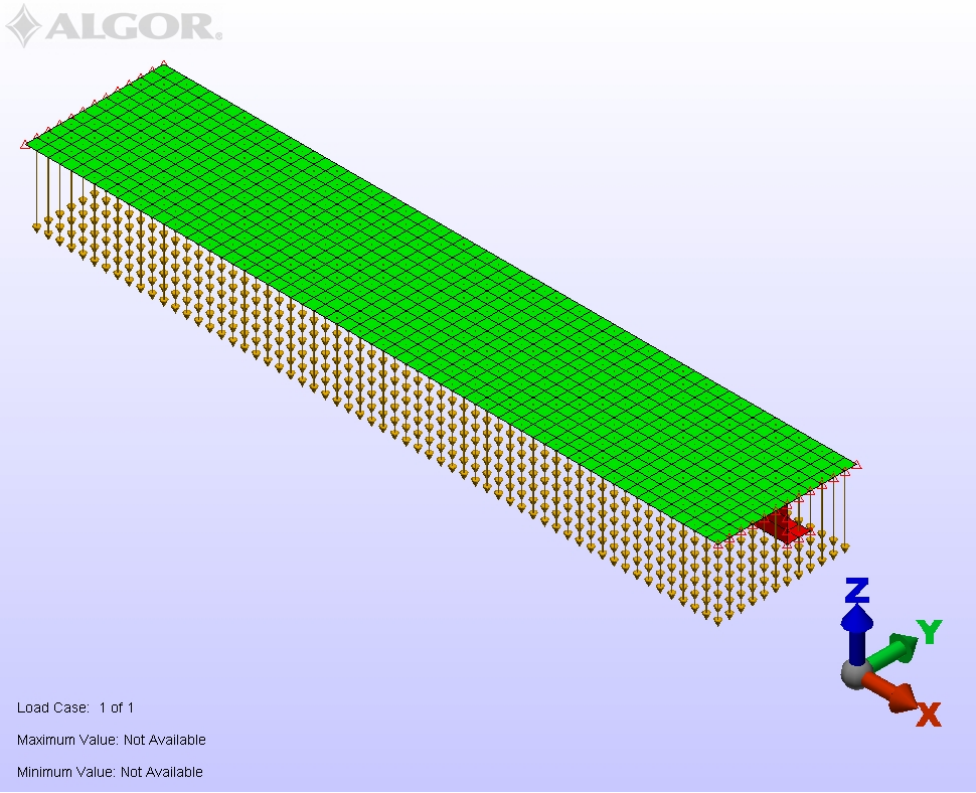

Figure 17 - Baseline FEA Model

Using the same deck uniform load applied to the end connection models for the purpose of the Stress Criteria and Rotation Criteria, the model was compiled and the output is displayed below in figure (18) and (19).

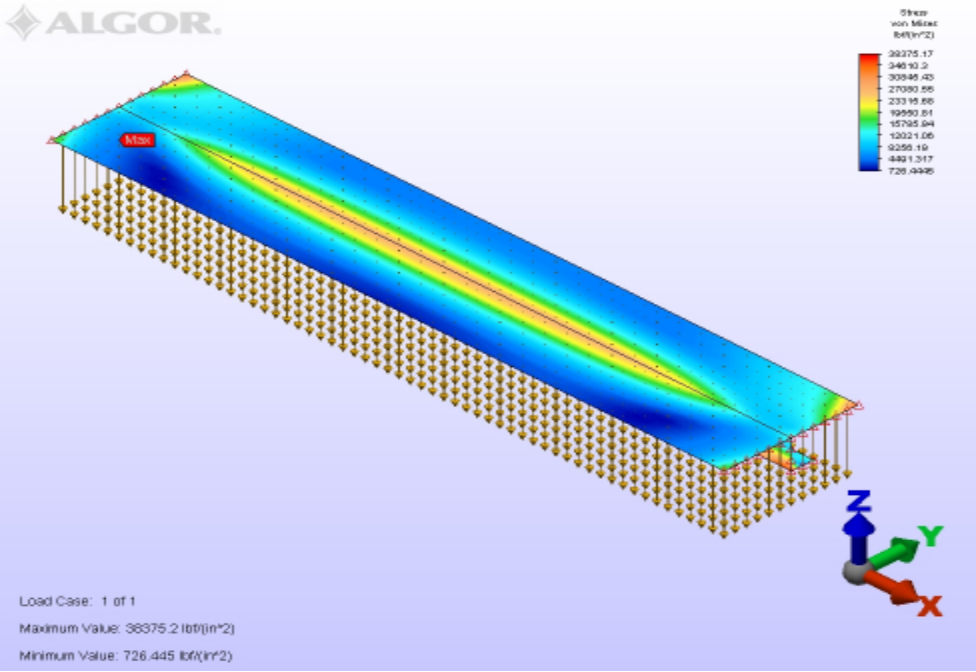

Figure 18 - Baseline FEA Model Stress Results – Plan View

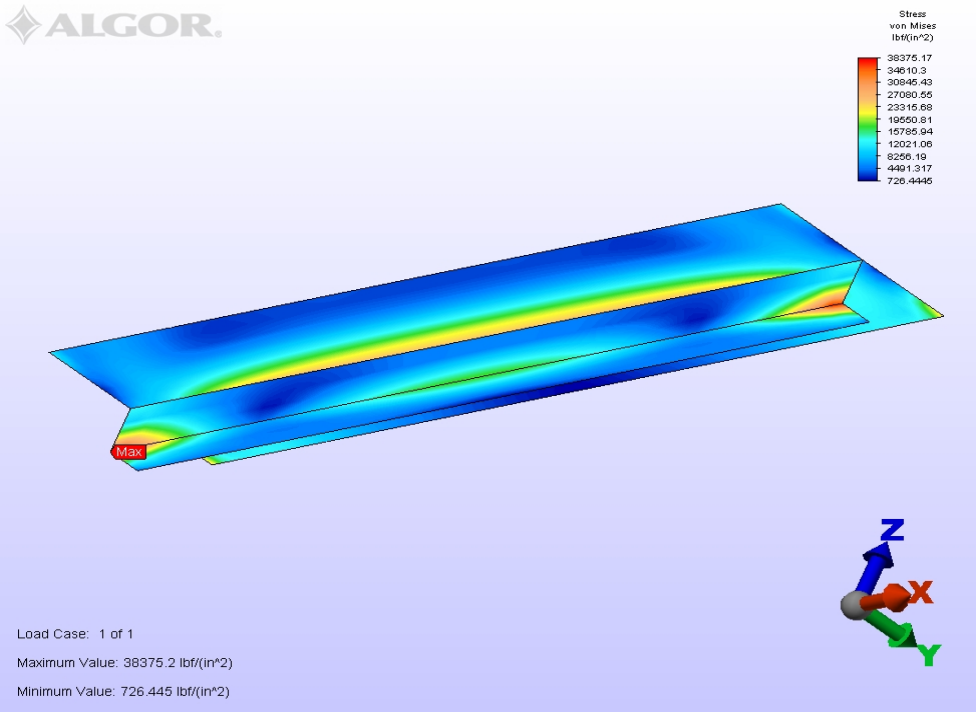

Figure 19 - Baseline FEA Model Stress Results – Bottom View

The uniform load on the deck of the model was also varied to achieve a 36 ksi stress concentration, or yield. This stress concentration was recorded and used in the calculation of the 'c' Factor Criteria.

The results for this model are;

Max Stress at the Connection	38,375.2	psi
Max Stress at Midspan	27,575.4	psi
Max Rotation Angle at the Connection	1.71733	degrees
Max Rotation Angle at Midspan	1.96403	degrees
Max Deck Uniform load to Yield	9.381	psi

Table 14 - Baseline FEA Model Summary

Please note that the nodal rotation for a fully fixed member should be 0 degrees at the end connection, and 0 degrees at the midspan of the member. For the purpose of the analysis, the nodal rotations were taken in the general areas of the end connection and midspan as displayed in figure (16).

The sole purpose of the baseline model was to simulate a truly fixed end connection in the finite element suite to contrast with the 13 end connection models. The ideal shear and moment can be represented by the following diagram from reference [2].

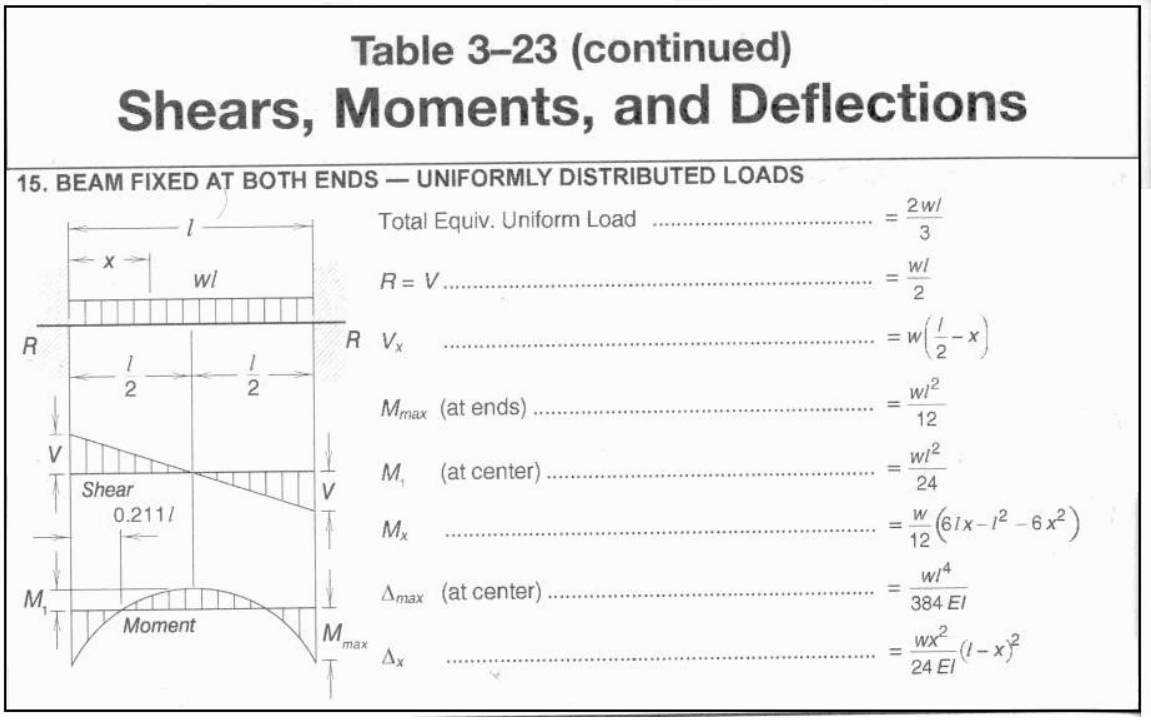

Figure 20 - AISC 13th Ed. Table 3-23; Shears, Moment, and Deflections [2]

One can take note that for a truly fixed beam the moment at the ends and midspan can be calculated as:

$$M_{ends} = \frac{wl^2}{12} \tag{15}$$

$$M_{midspan} = \frac{wl^2}{24} \tag{16}$$

Therefore the ‘c’ factor is 12 and 24 for the ends and midspan respectively.

Since each of the 13 end connection models analyzed for the purpose of this thesis contained edge supports in the y-axis, a second baseline model was created with again truly fixed end constraints in rotation and translation, but also containing the following end constraints;

Constraint					
Translation			Rotation		
T_x	T_y	T_z	R_x	R_y	R_z
	x		**x**		**x**

Table 15 - Baseline with Edge Support End Constraints

For the purpose of this paper, this second baseline model will be called, "Baseline Model with Edge Supports". The mesh density and node locations are identical to the baseline model stated above. The “Baseline Model with Edge Supports" is shown in figure (21). Notice the circles at the y-axis boundary of the model. These circles are the constraints shown in Table (16).

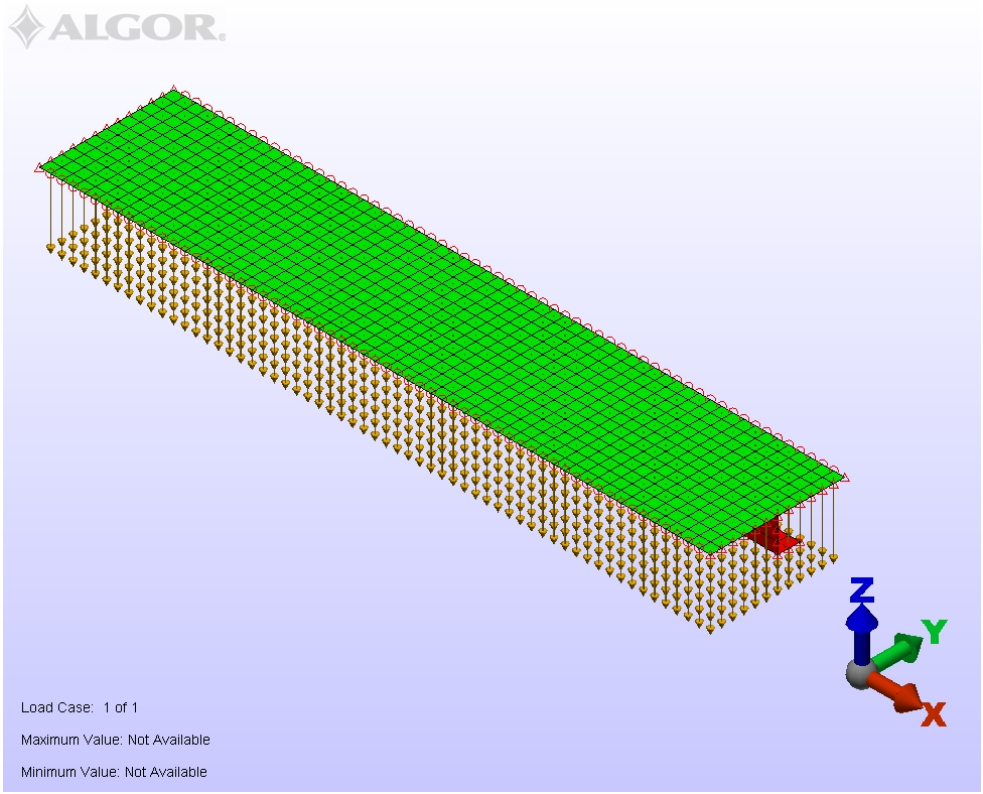

Figure 21 - Baseline with Edge Support FEA Model

The "Baseline Model with Edge Supports" also was loaded with the same uniform deck load applied to the end connection models for the purpose of the Stress Criteria and Rotation Criteria. The model was compiled and the output is displayed in figures (22) and (23).

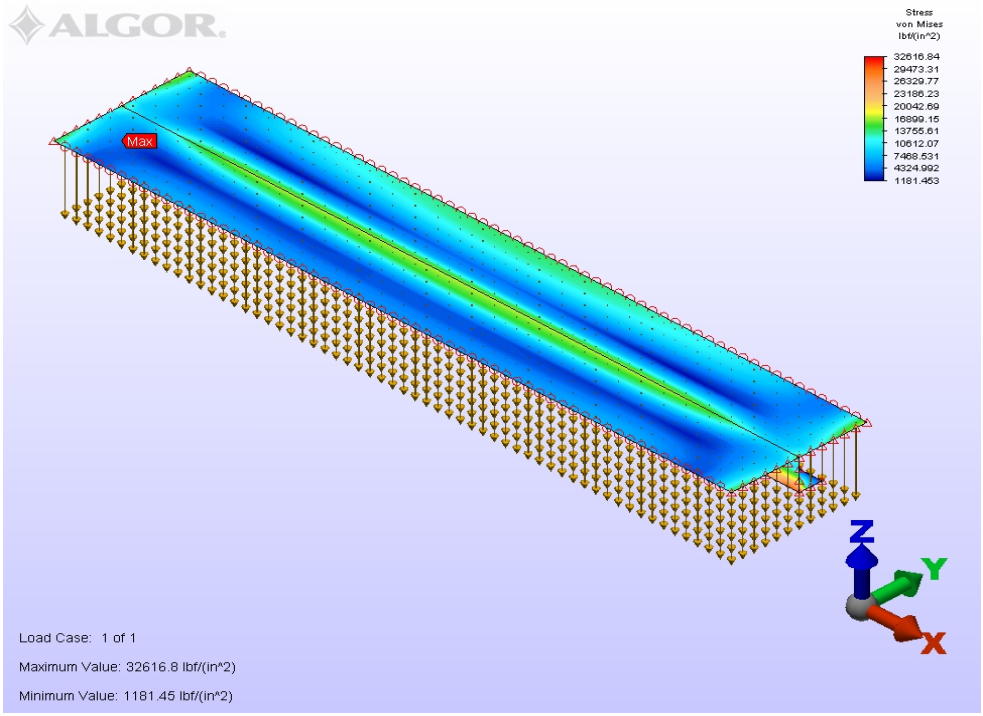

Figure 22 - Baseline with Edge Support FEA Model Stress Results - Plan View

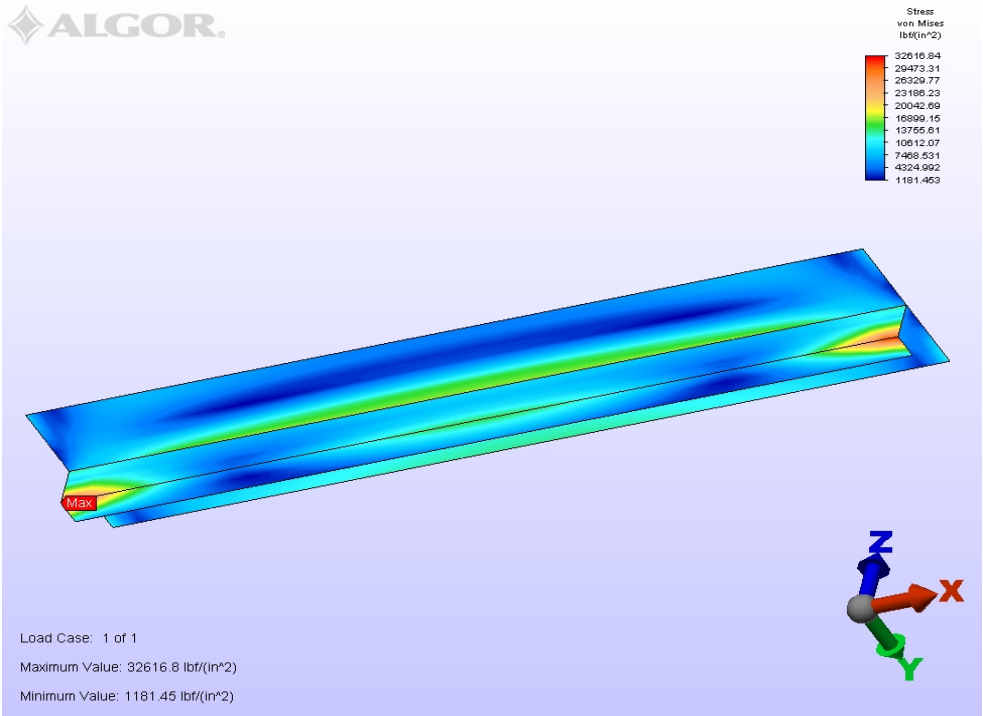

Figure 23 - Baseline with Edge Support FEA Model Stress Results - Bottom View

As done before on the baseline model, the uniform load on the deck was varied to achieve a 36 ksi stress concentration. This stress concentration was recorded and used in the 'c' Factor Criteria.

The results for this model are as shown;

Max Stress at the Connection	32,616.8	psi
Max Stress at Midspan	17,311.8	psi
Max Rotation Angle at the Connection	0.43426	degrees
Max Rotation Angle at Midspan	0.89733	degrees
Max Deck Uniform load to Yield	11.655	psi

Table 16 - Baseline with Edge Support FEA Model Summary

Chapter 6 - End Connections Analyzed

Thirteen various end connections have been analyzed for the purpose of this thesis paper. The thirteen end connections analyzed are common structural end connections used in the commercial marine field. The following chapter is organized in sub-sections of each end connection analyzed. A description of each end connection with sketches, figures of FEA output and results for each criterion are given in each sub-section. Chapter 7 will summarize all the results and give comparisons per each model.

Sniped End Connection

One of the cheapest and easiest end connections to fabricate is a sniped end connection. In this connection, the flange of the deck stiffener is cut back at a 30 to 45 degree angle. The web of the deck stiffener will hit hard to the web of the vertical bulkhead stiffener. When the flange is not connected, a full moment connection is not produced. Only shear and a little moment transfer will carry thru the web to the vertical bulkhead stiffener. The model analyzed has a flange sniped at a 45 degree angle. Figure (23) displays the end connection.

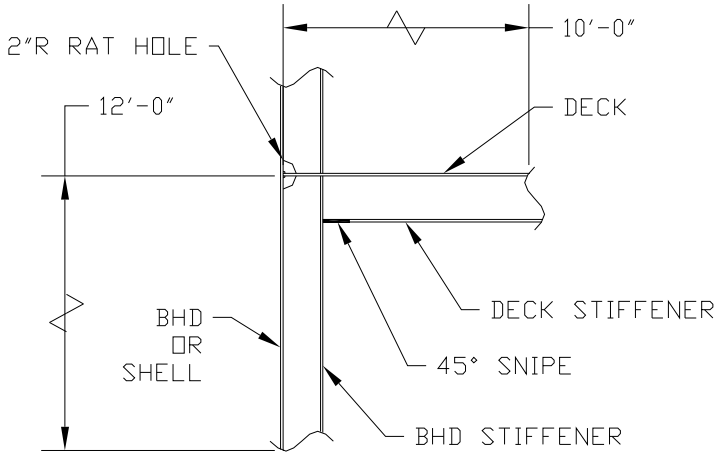

Figure 24 - Sniped End Connection Detail Sketch

The following model was produced to obtain results in Von Mises stress, node rotation, and max uniform load to produce material yielding.

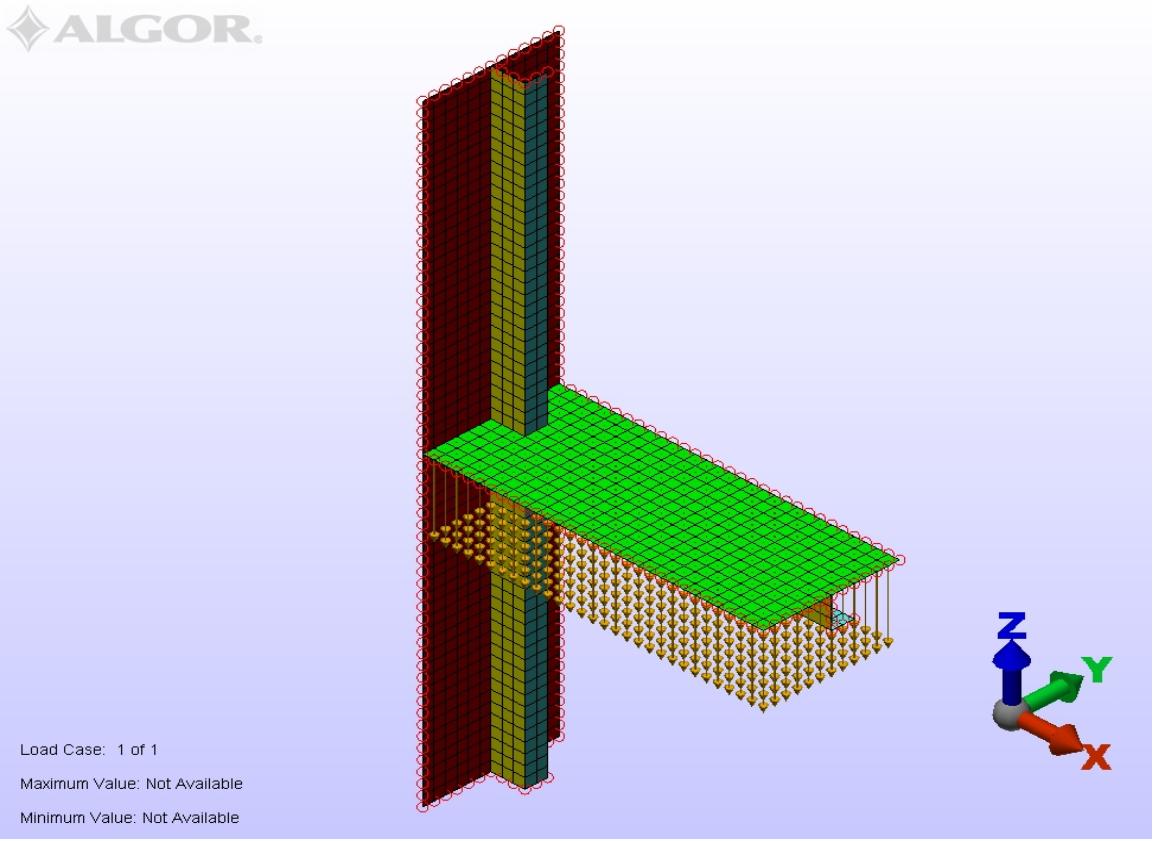

Figure 25 - Sniped End Connection FEA Model - Plane View

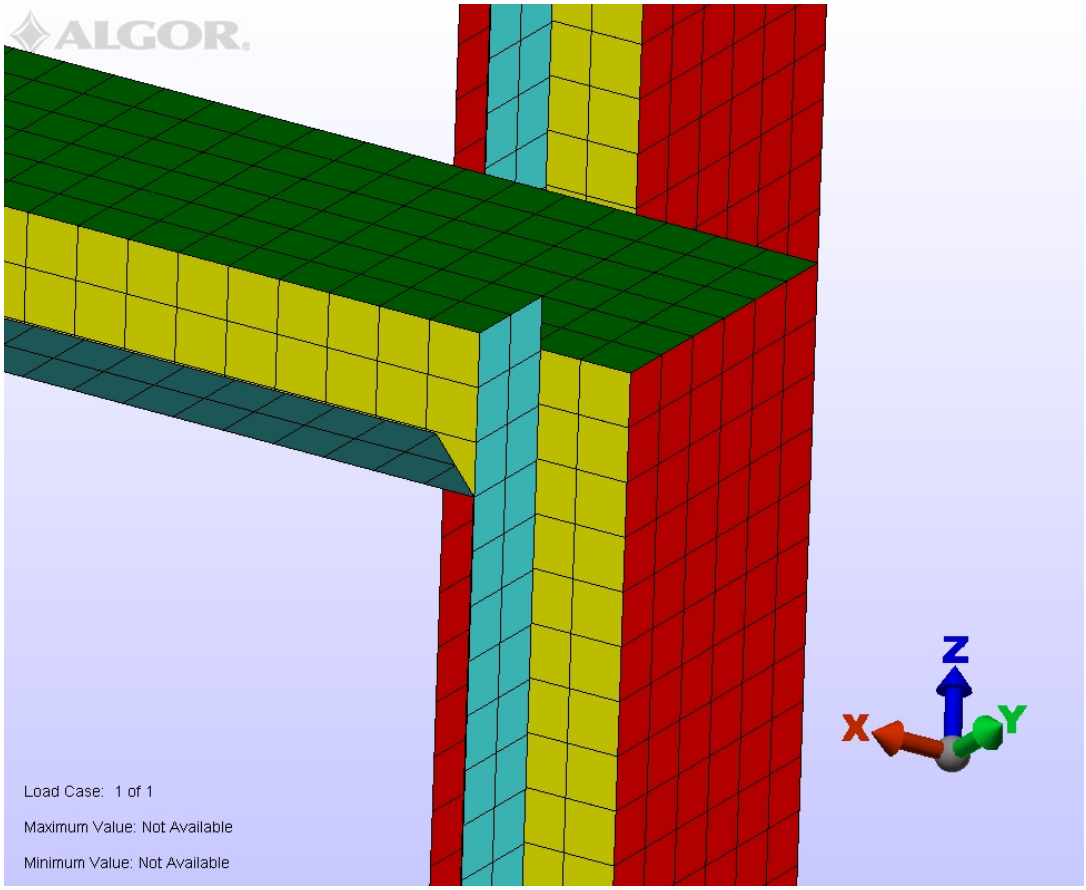

Figure 26 - Sniped End Connection FEA Model - Connection View

The Von Mises stress results are shown in the figures (27), (28), and (29).

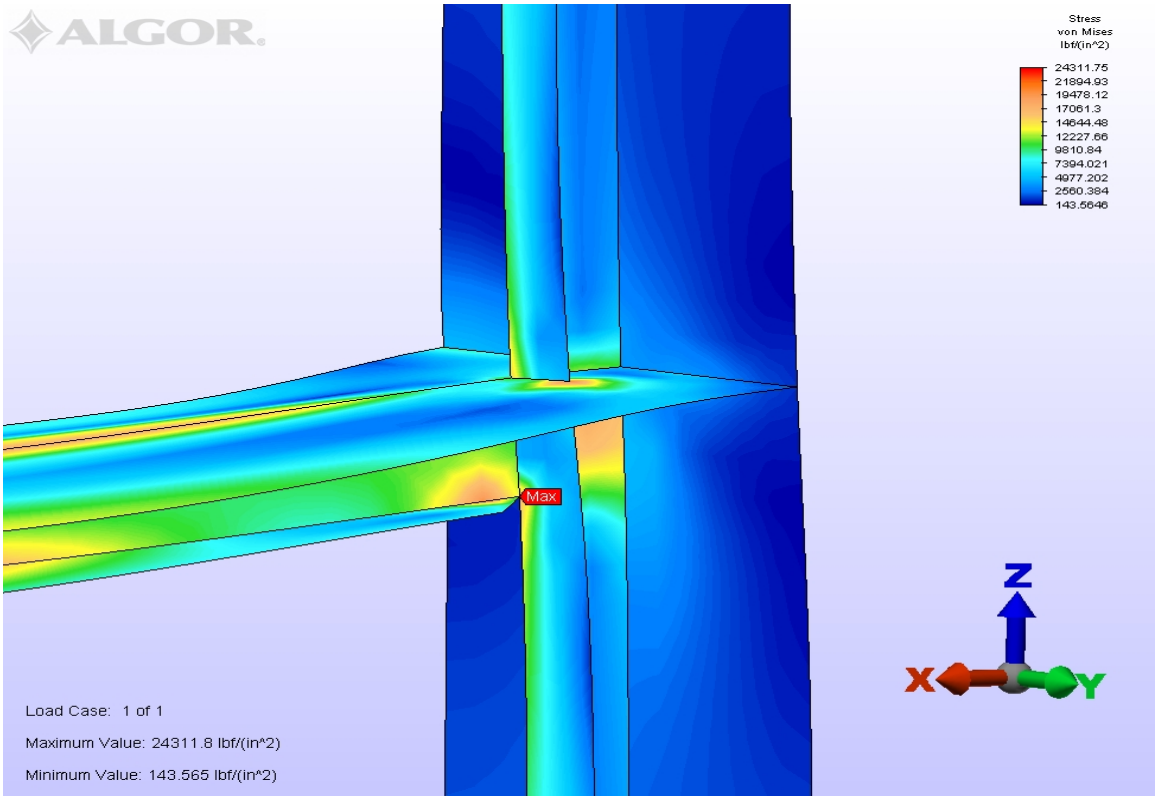

Figure 27 - Sniped End Connection FEA Model - Stress Plot

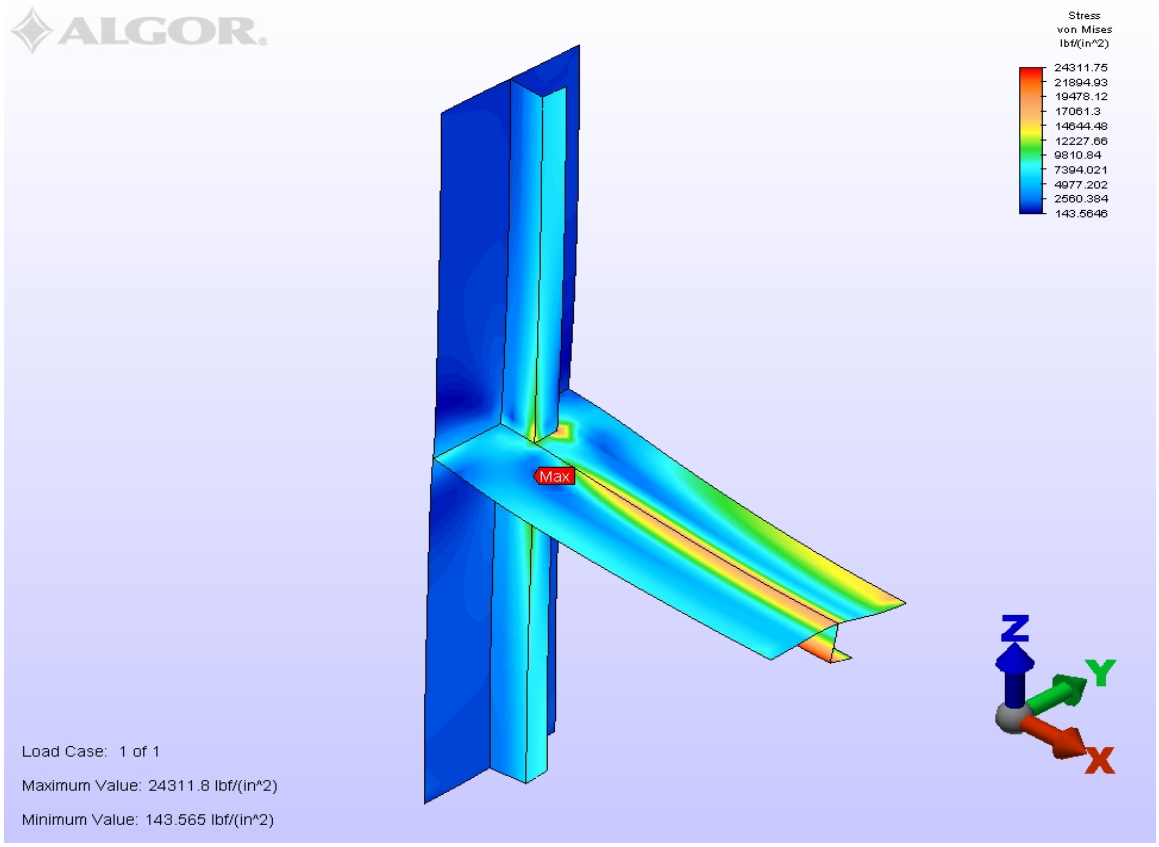

Figure 28 - Sniped End Connection FEA Model - Stress Plot

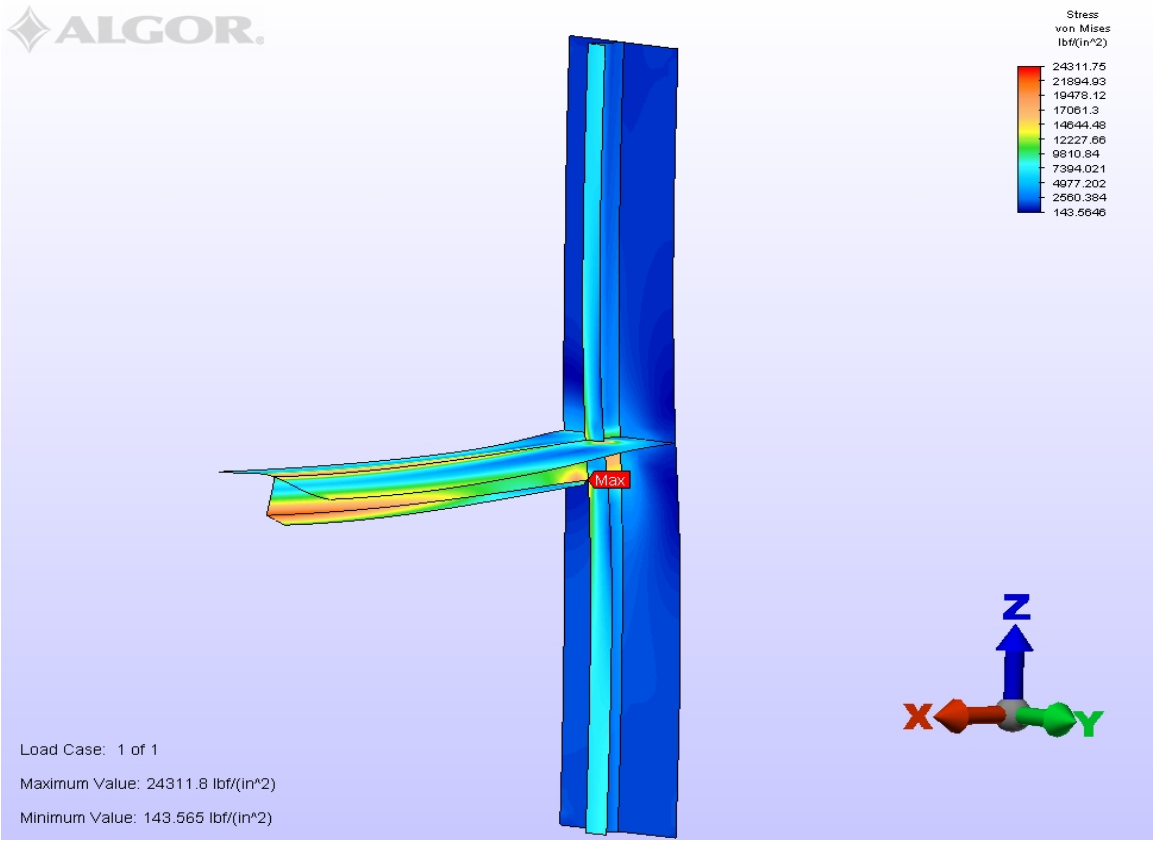

Figure 29 - Sniped End Connection FEA Model - Stress Plot

The following data was collected for comparison,

Max Stress at the Connection	24,311.80	psi
Max Stress at Midspan	24,147.03	psi
Max Rotation Angle at the Connection	0.5637	degrees
Max Rotation Angle at Midspan	0.7870	degrees
Max Deck Uniform load to Yield	14.81	psi

Table 17 - Sniped End Connection FEA Model - Summary

As one can notice, the max stress occurs at the end connection where the extreme fiber of the deck stiffener meets the web of the vertical bulkhead stiffener.

Flat Bar Chock Connection

A simple method to create a moment transfer from the deck beam to the vertical bulkhead stiffener is to back up the flange with a flat bar of matching flange thickness. The flat bar would be installed directly in-line with the flange of the deck stiffener in the space between the bulkhead, web of the bulkhead stiffener, and flange of the bulkhead stiffener. The flat bar would be welded with a continuous bead of weld all around the flat bar periphery. This type of connection requires field fit up of the flat bar in the above mentioned zone, and welding in tight spots. Figure (30) displays the end connection.

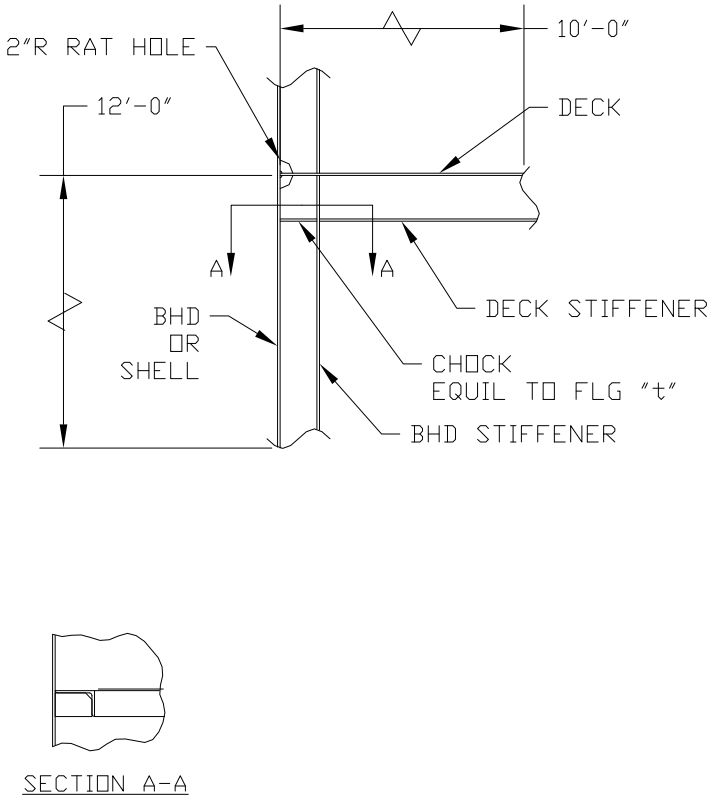

Figure 30 - Flat Bar Chock Detail Sketch

The following model was produced to obtain results in Von Mises stress, node rotation, and max deck uniform load to produce material yielding.

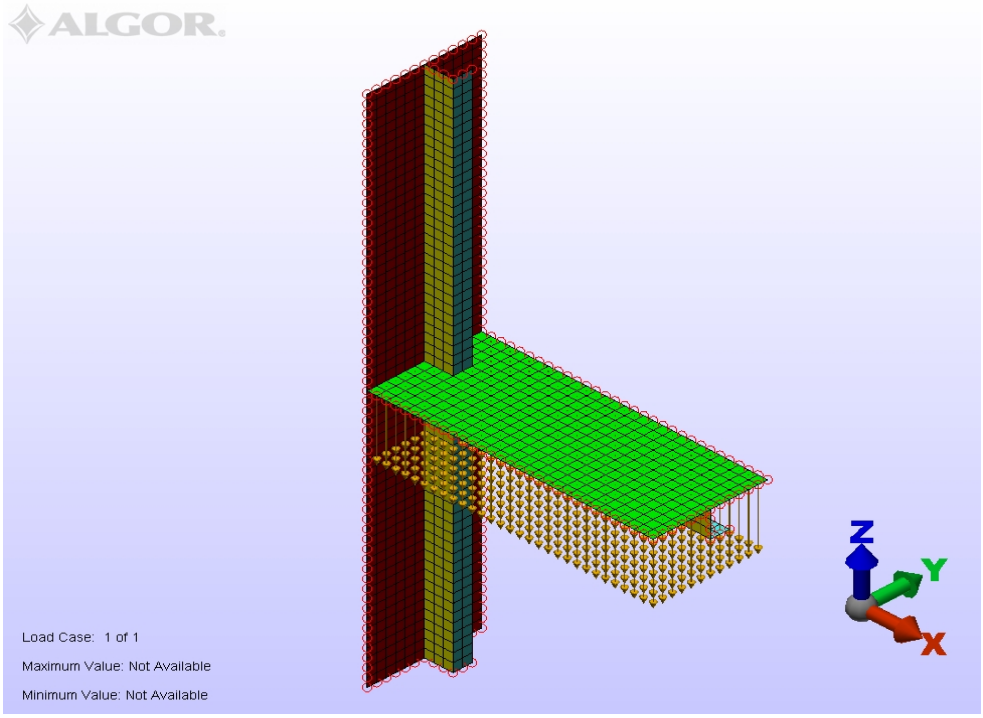

Figure 31 - Flat Bar Chock FEA Model - Plan View

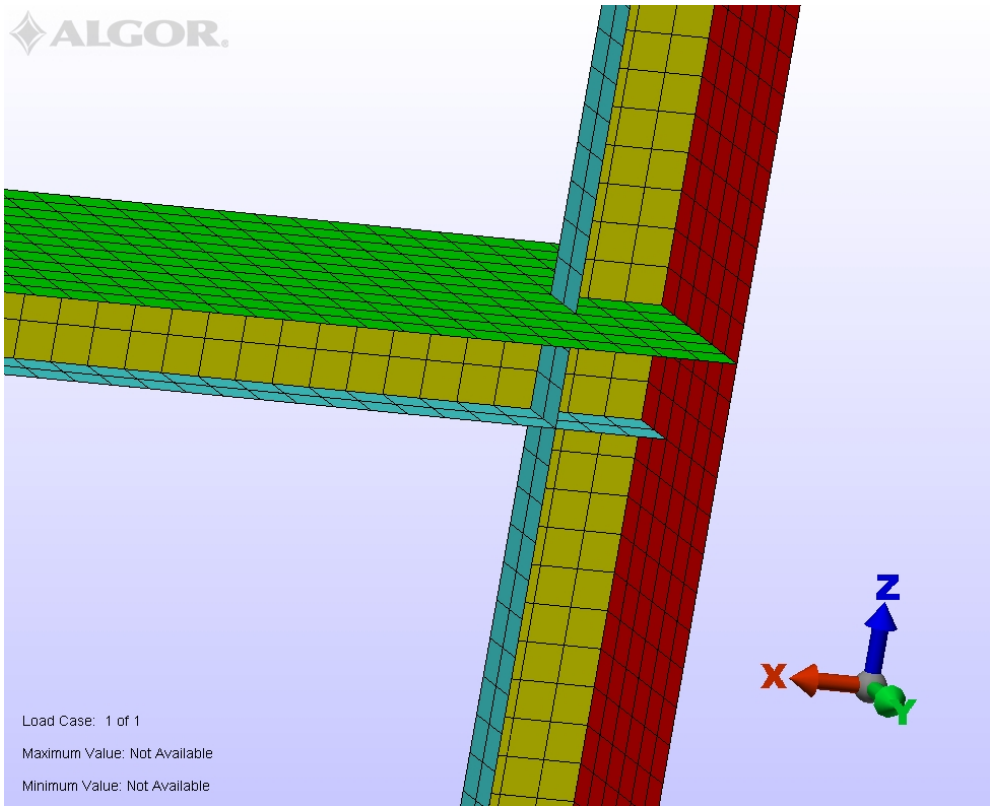

Figure 32 - Flat Bar Chock FEA Model - Connection View

The Von Mises stress results are shown in figures (33), (34), and (35).

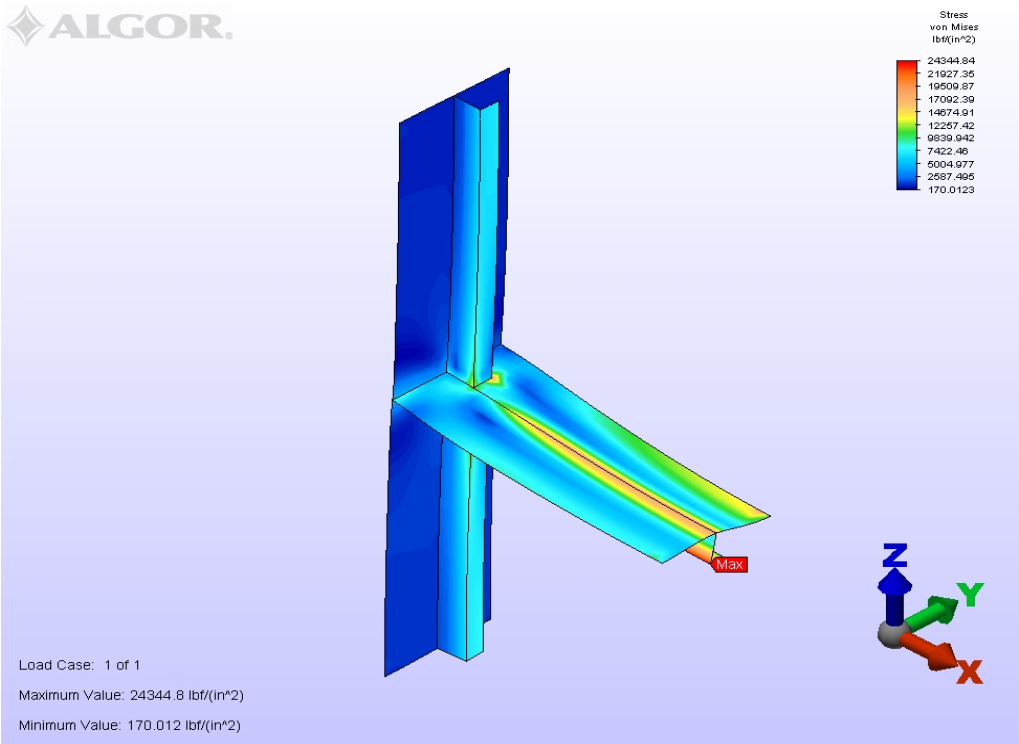

Figure 33 - Flat Bar Chock FEA Model - Stress Plot

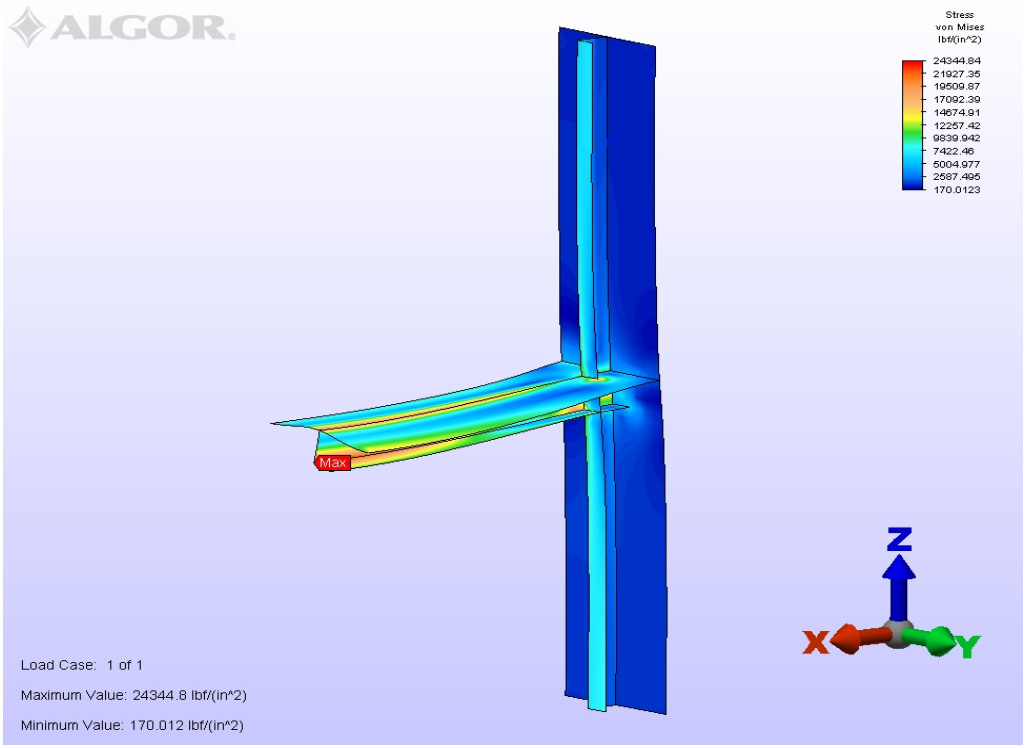

Figure 34 - Flat Bar Chock FEA Model - Stress Plot

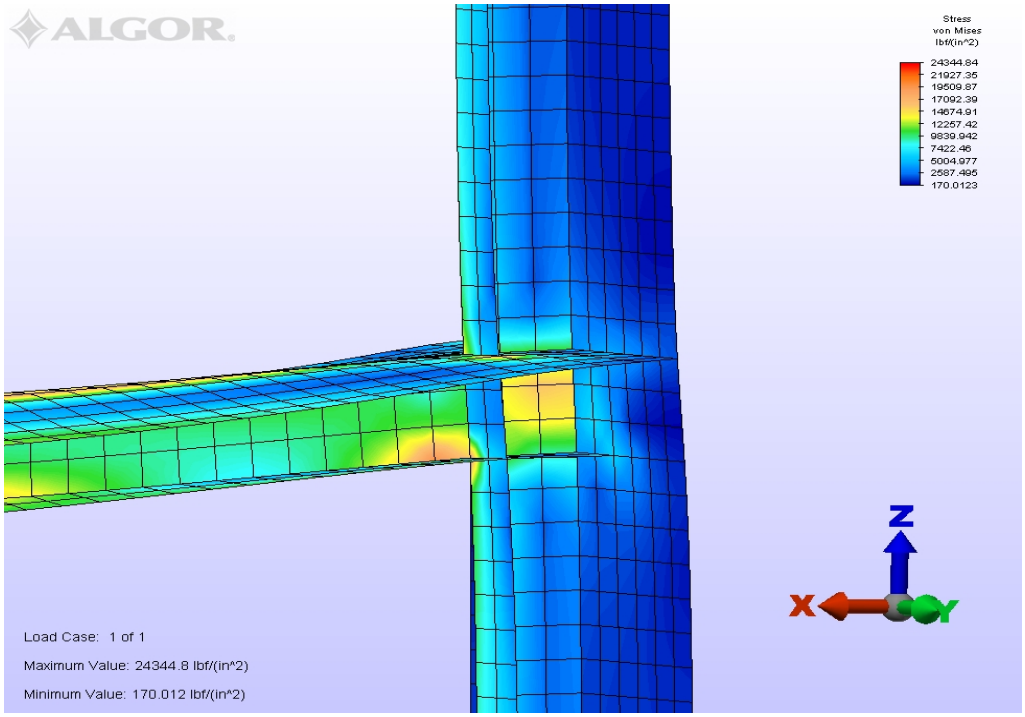

Figure 35 - Flat Bar Chock FEA Model - Stress Plot

The following data was collected for comparison,

Max Stress at the Connection	22,613.86	psi
Max Stress at Midspan	24,344.84	psi
Max Rotation Angle at the Connection	0.5289	degrees
Max Rotation Angle at Midspan	0.7131	degrees
Max Deck Uniform load to Yield	14.79	psi

Table 18 - Flat Bar Chock FEA Model - Summary

The max stress occurs at the midspan of the stiffener, where the web of the member joins the flange of the member.

Tapered Chock Connection

Another method to create a moment transfer from the deck beam to the vertical bulkhead stiffener is to back up the flange with a tapered chock matching the flange thickness. The tapered chock, like the flat bar chock, would be installed directly in-line with the flange of the deck stiffener in the space between the bulkhead, web of the bulkhead stiffener, and flange of the bulkhead stiffener. The flat bar would be welded with a continuous bead of weld all around the flat bar peripheral. But un-like the flat bar chock, only two sides of the chock require welding. This type of connection requires either NC cutting of the bracket, or a skilled laborer to cut the chock out of plate. Welding, once again would be required in tight spaces. Figure (36) displays the end connection.

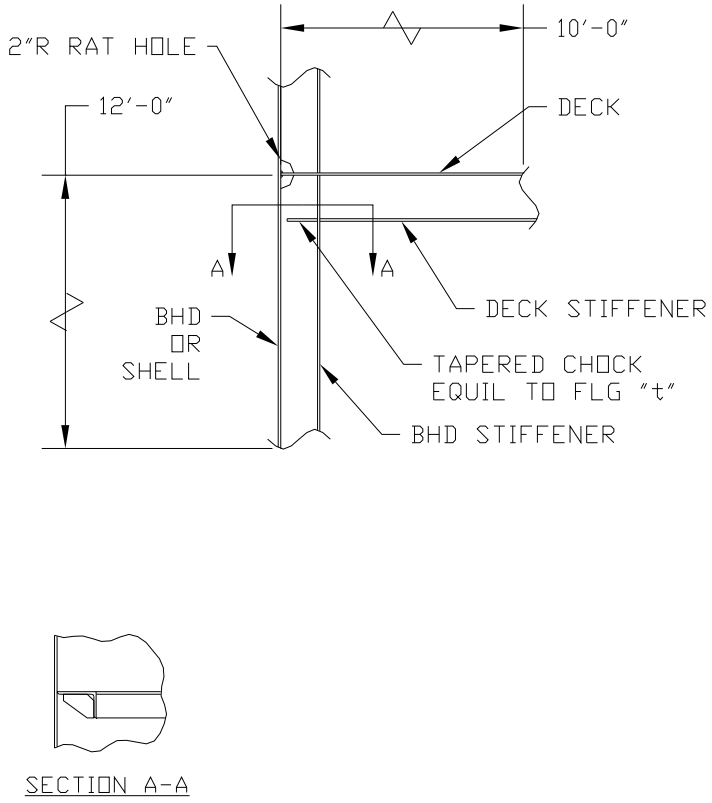

Figure 36 - Tapered Chock Detail Sketch

The following model was produced to obtain results in Von Mises stress, node rotation, and max deck uniform load to produce material yielding.

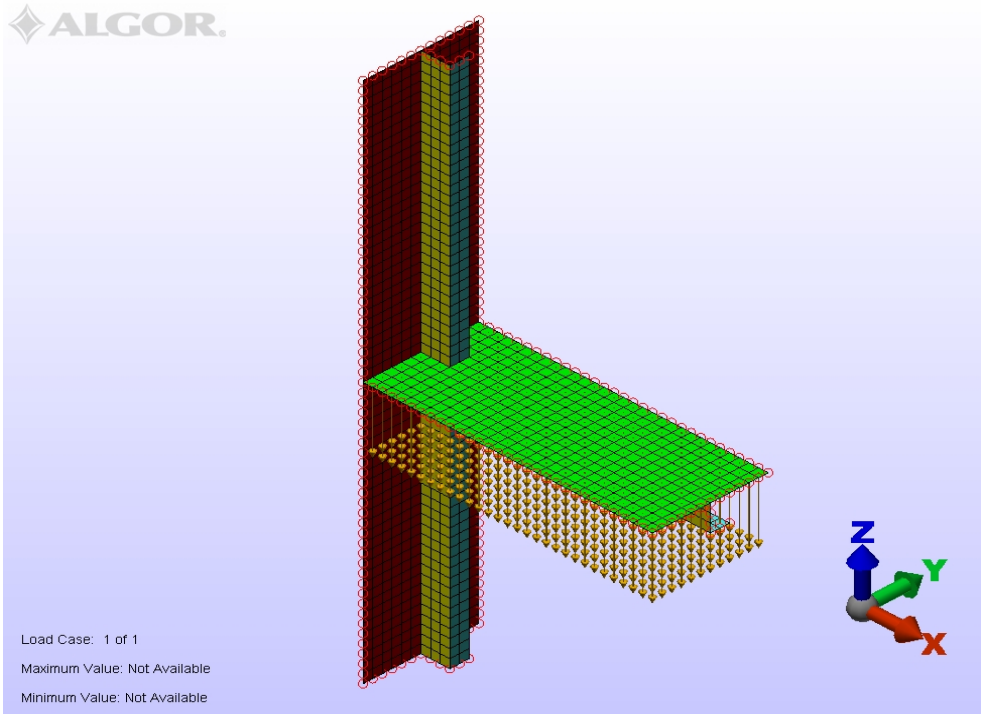

Figure 37 - Tapered Chock FEA Model - Plan View

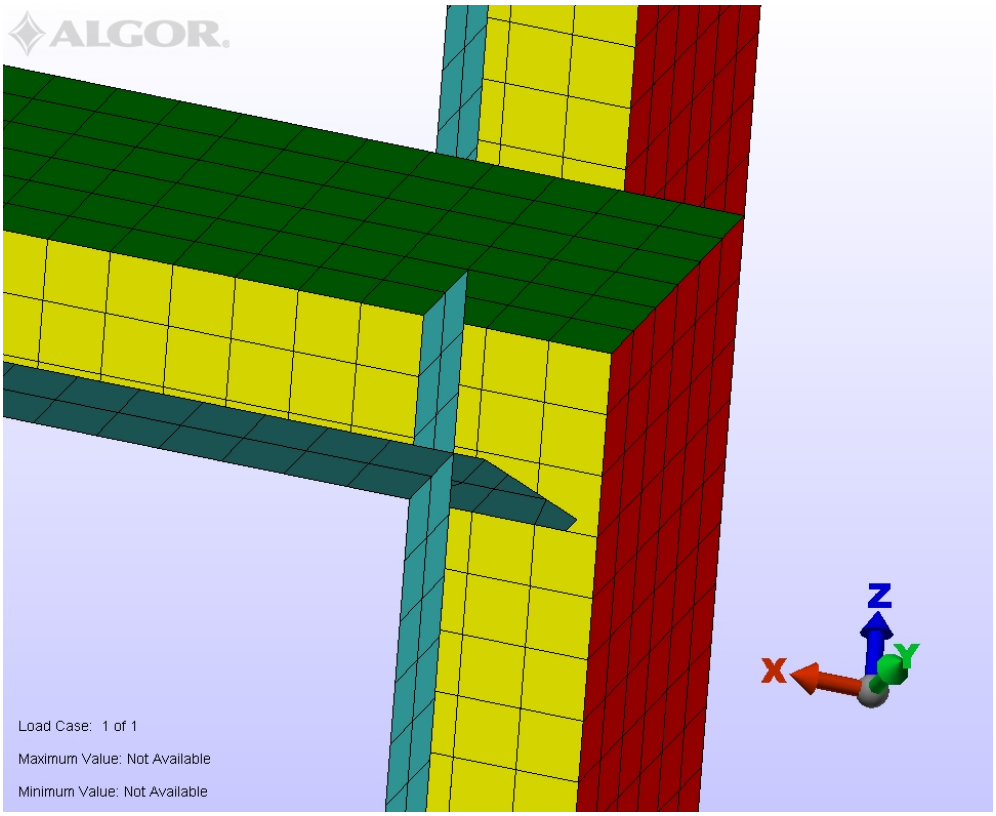

Figure 38 - Tapered Chock FEA Model -Connection View

The Von Mises stress results are shown in figures below (39), (40), and (41).

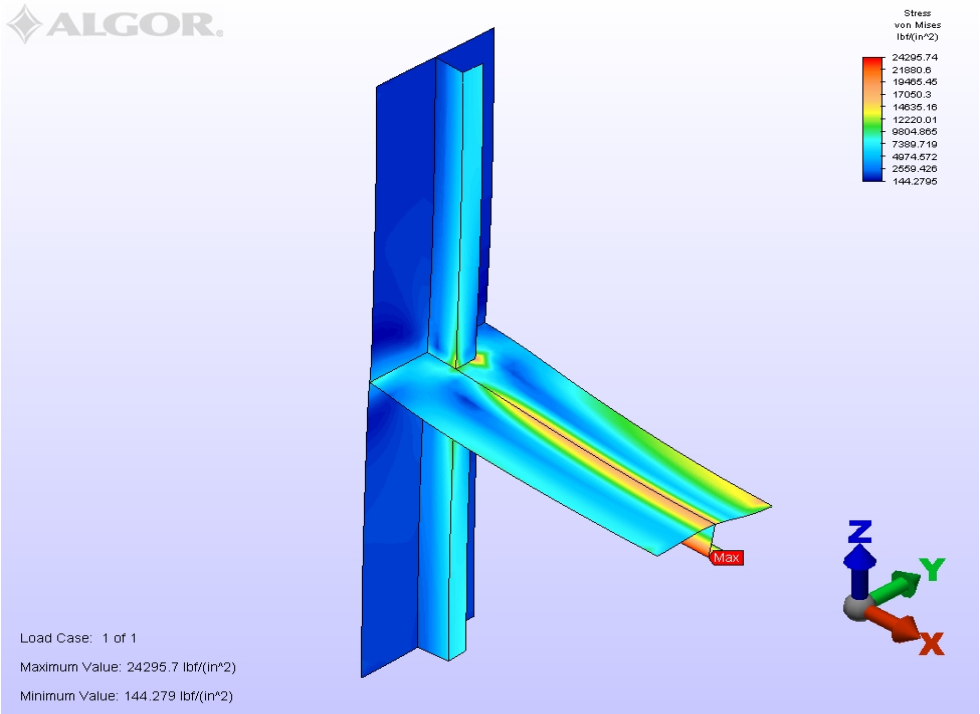

Figure 39 - Tapered Chock FEA Model -Stress Plot

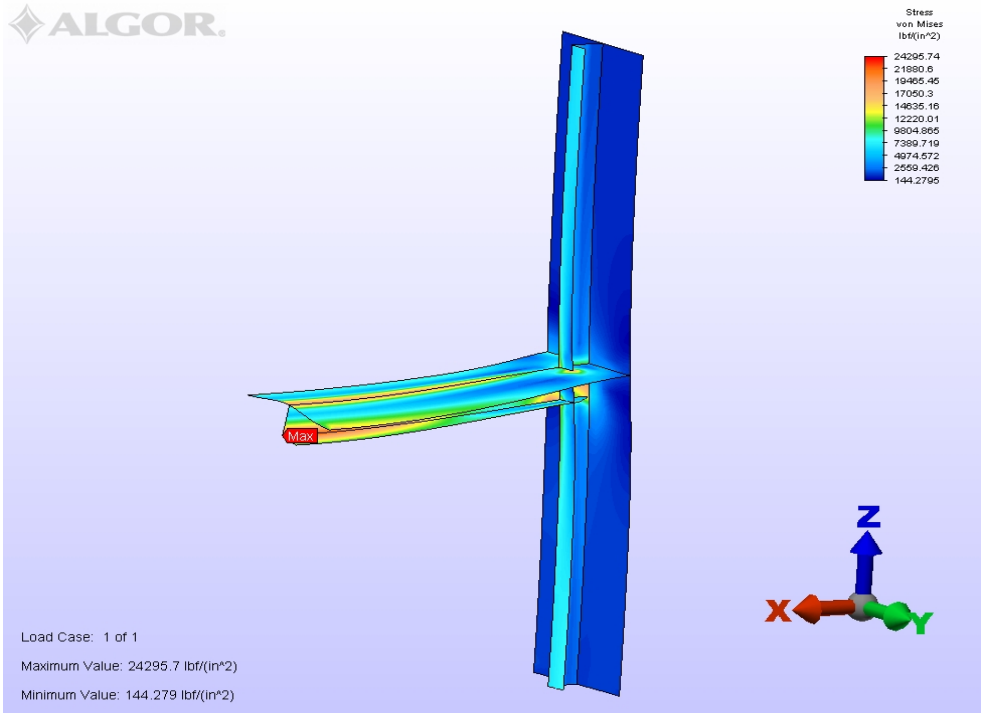

Figure 40 - Tapered Chock FEA Model -Stress Plot

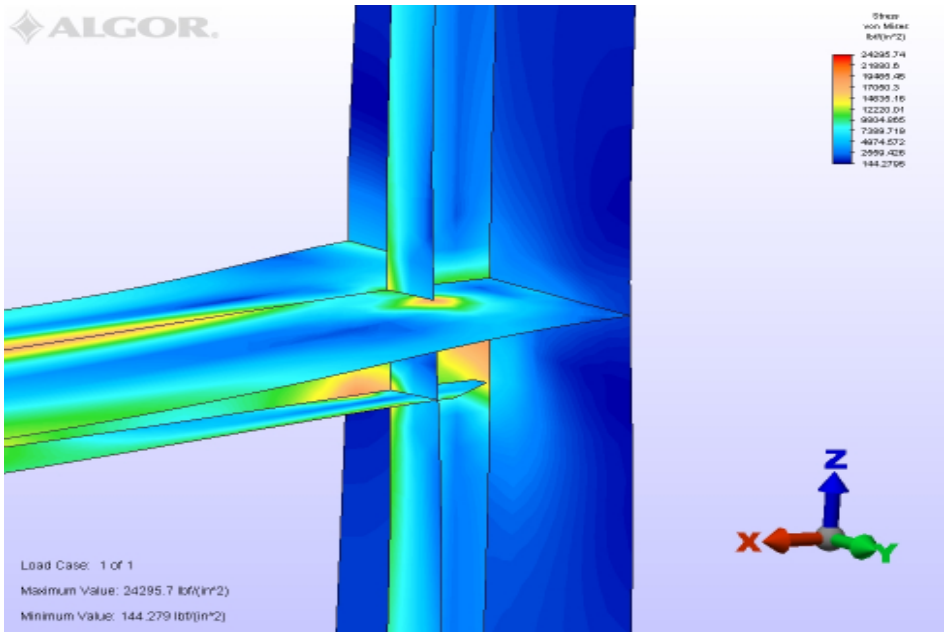

Figure 41 - Tapered Chock FEA Model -Stress Plot

The following data was collected for comparison,

Max Stress at the Connection	21,468.53	psi
Max Stress at Midspan	24,295.74	psi
Max Rotation Angle at the Connection	0.5249	degrees
Max Rotation Angle at Midspan	0.7312	degrees
Max Deck Uniform load to Yield	14.82	psi

Table 19 - Tapered Chock FEA Model -Summary

Like the flat bar chock, the max stress occurs at the midspan of the stiffener, where the web of the member joins the flange of the member.

Lap Connection

A lap connection can be classified as another economical and easy to fabricate end connection used throughout the marine industry. In this end connection, the flange of the deck stiffener is cut back at either 30 to 45 degrees angle like the snipe connection, but the snipe occurs approximately 3 to 4 inches behind the end cut of the stiffener. This allows for the web of the deck stiffener to overlap the vertical bulkhead stiffeners web. Also, for this end connection to work, the flanges of the deck stiffener and vertical bulkhead stiffener must be on opposite hands of each other. Since one flange will be forward, and the other aft, a bit of eccentricity will occur with the load path of the uniform load. This type of connection requires neither NC cutting of a bracket, nor a skilled laborer to cut the chock out of plate. The snipes will have to be cut by hand or machine, but the fit up is extremely easy, making this end connection very cost effective. For the purpose of this analysis, the deck stiffener is shifted half of the web thickness, and the lapped part of the deck stiffener web is connected to the vertical bulkhead stiffener web via a weld element. The weld element is a 3/8" plate element joining only the nodes that would be

connected via a weld. Welding is simplified due to the openness of the connection, as shown in figure (41) displayed below.

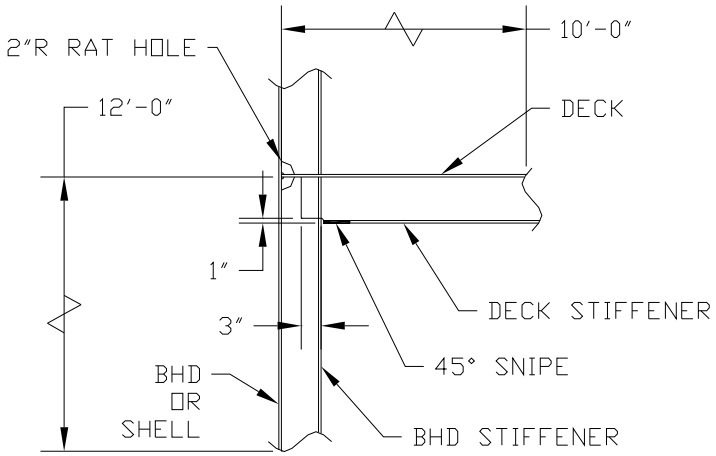

Figure 42 - Lap Connection Detail Sketch

The following model was produced to obtain results in Von Mises stress, node rotation, and max deck uniform load to produce material yielding.

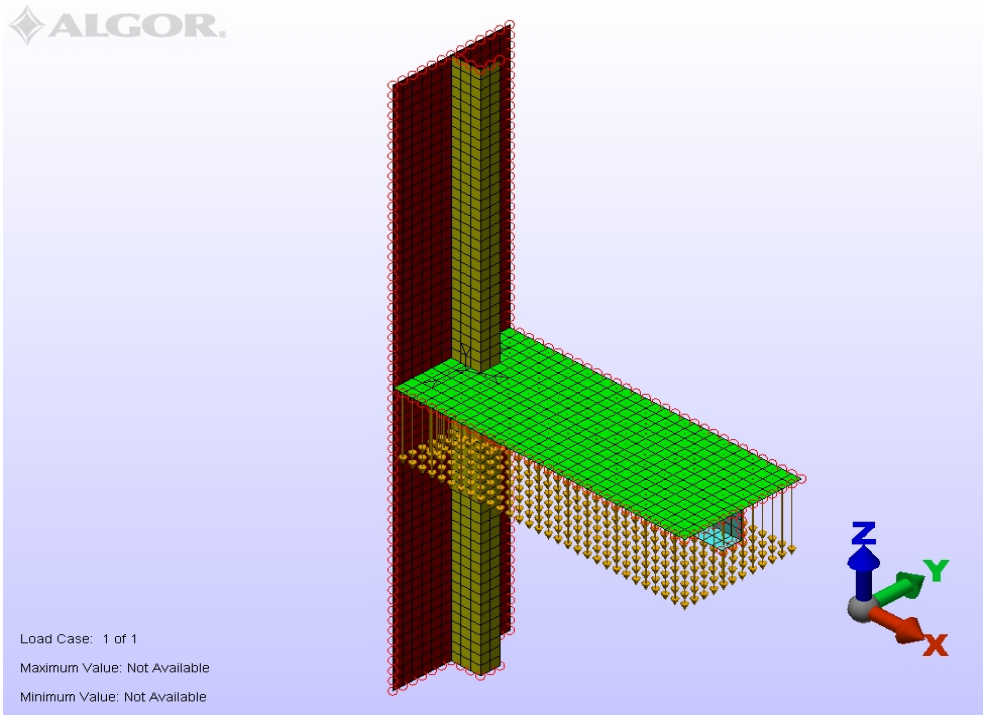

Figure 43 - Lap Connection FEA Model - Plan View

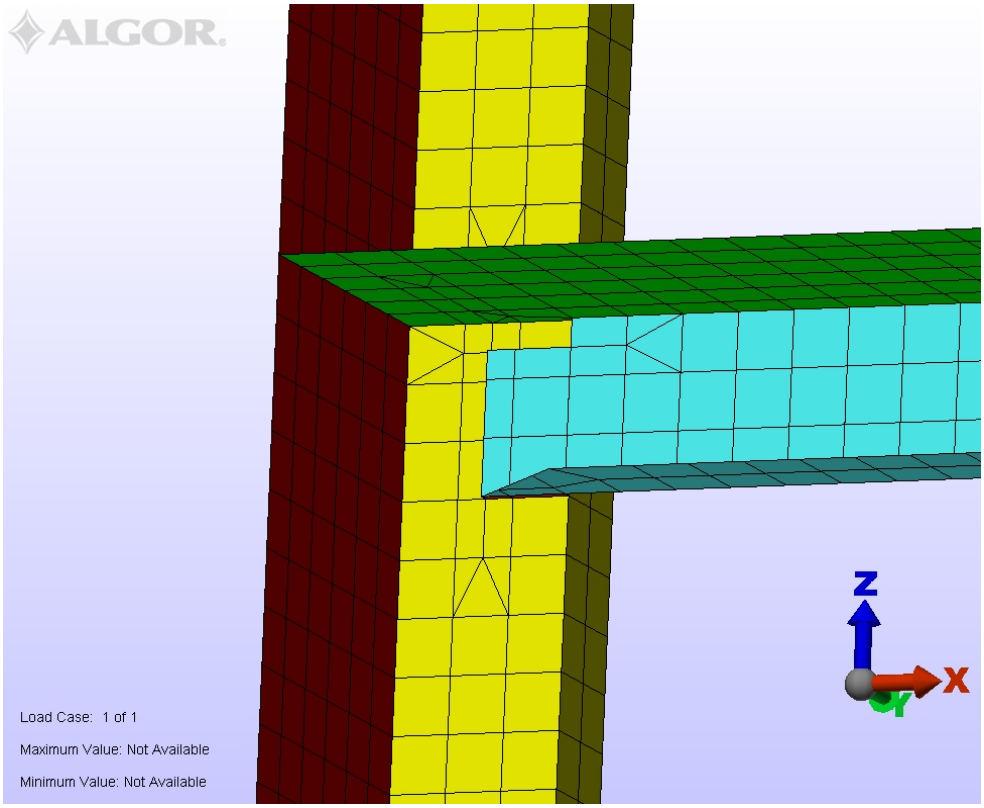

Figure 44 - Lap Connection FEA Model - Connection View

The Von Mises stress results are shown in figures (45), (46), and (47).

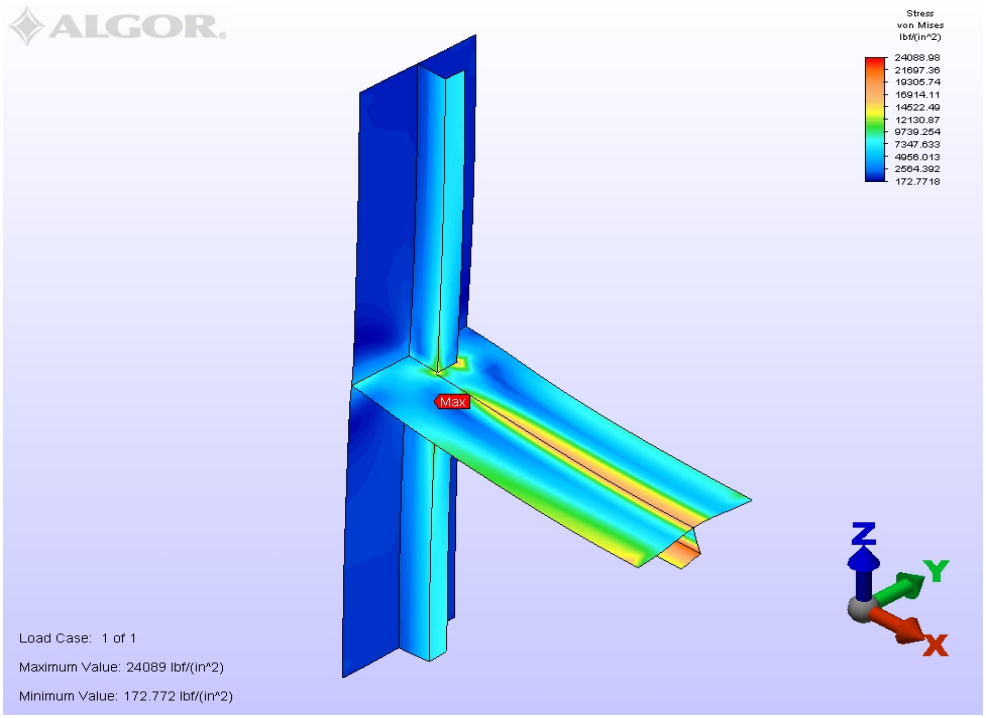

Figure 45 - Lap Connection FEA Model - Stress Plot

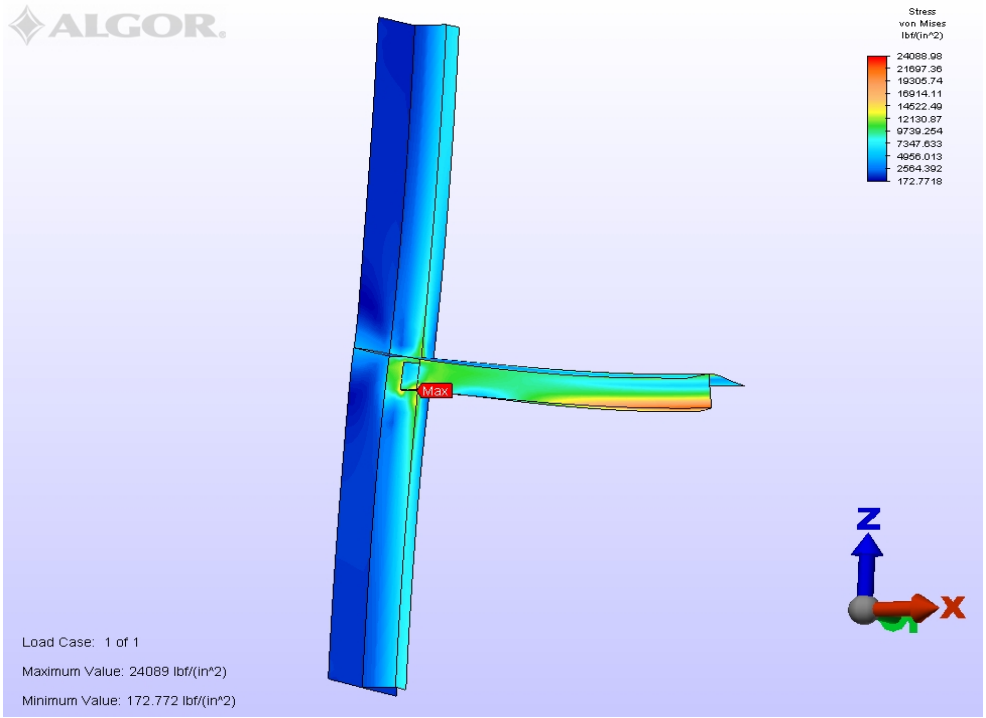

Figure 46 - Lap Connection FEA Model - Stress Plot

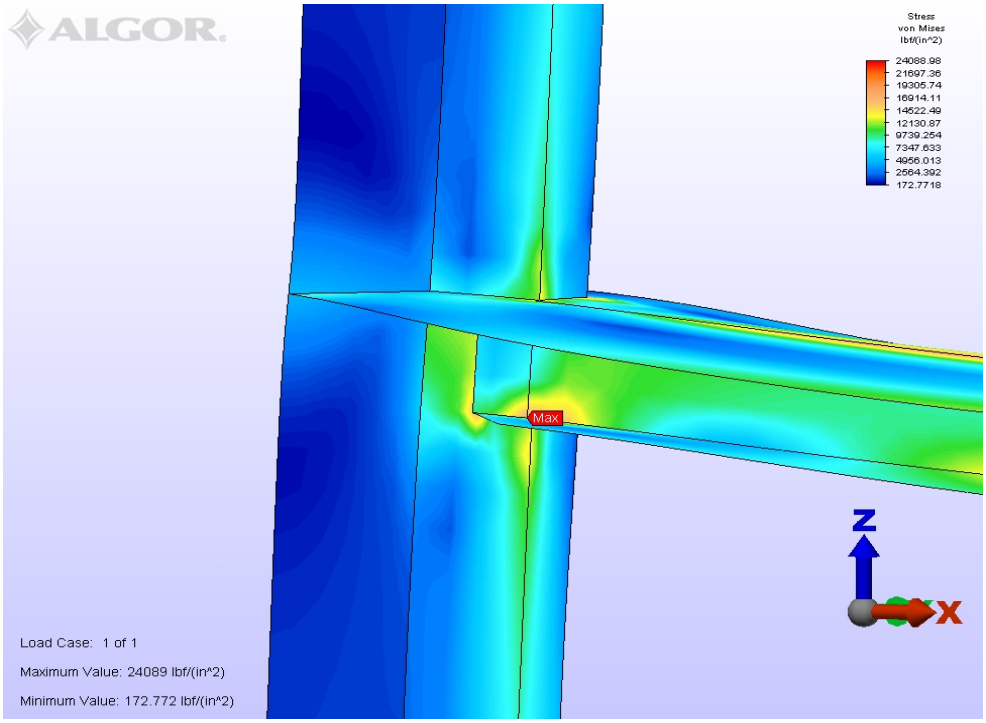

Figure 47 - Lap Connection FEA Model - Stress Plot

The following data was collected for comparison'.

Max Stress at the Connection	21,466.70	psi
Max Stress at Midspan	23,493.88	psi
Max Rotation Angle at the Connection	0.5337	degrees
Max Rotation Angle at Midspan	0.7346	degrees
Max Deck Uniform load to Yield	14.95	psi

Table 20 - Lap Connection FEA Model - Summary

Like the sniped connection, the max stress occurs where the extreme fiber of the deck stiffener meets the web of the vertical bulkhead stiffener.

Brackets

A more efficient end connection is to utilize a bracket. A bracket is a triangular cut piece of steel, either butt welded or lapped from the deck stiffener to the web of the vertical bulkhead

stiffener. The bracket dimensions may vary due to space restrictions, or designer preference. The flange of the deck stiffener is typically sniped 30 to 45 degrees like the snipe or lap connection. The web of the deck stiffener may hit hard to the web of the vertical bulkhead stiffener, or may be cut short by an inch. One might think that since there is no direct flange connection, from the vertical bulkhead stiffener to the deck stiffener, a moment transfer will not be 100 percent. A conclusion can be drawn from the summarized information displayed in chapter 7.

For the purpose of this thesis, three types of brackets were analyzed. The three types of brackets analyzed are Butt Bracket #1, Butt Bracket #2, and Lap Bracket.

Butt bracket #1 has the web of the deck stiffener cut short by one inch from hitting the web of the vertical bulkhead stiffener, and the flange of the web snipped at 45 degrees. The web of the deck stiffener is cut short for ease of construction. The deck with attached stiffeners can be lifted and placed without any objects binding. The vertical bulkhead stiffener will hit the deck hard, allowing for the deck to be placed directly on top making fit up easier. The bracket hits hard in-line with the web of the deck stiffener and the web of the vertical bulkhead stiffener. This type of connection is costly due to fit up in the field, and butt welds are required to attach the bracket to the deck stiffener and vertical bulkhead stiffener. Figure (48) displays the details of Butt Bracket #1.

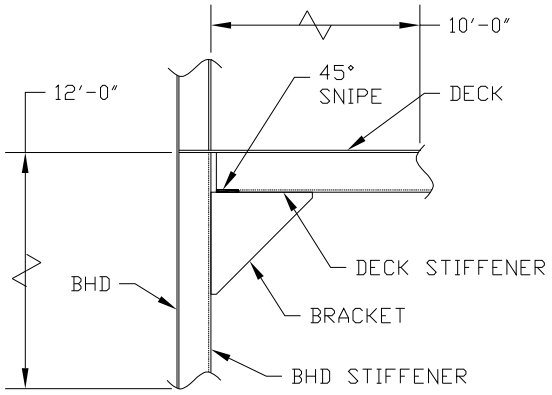

Figure 48 - Butt Bracket #1 Detail Sketch

Butt Bracket #2 is almost identical for Butt Bracket #1 except for the web of the deck stiffener. The web of the deck stiffener is not cut short from the web of the vertical bulkhead stiffener, but hits hard instead. This allows for a more direct load path from the deck stiffener to the vertical bulkhead stiffener. Fit up becomes an issue due to the tolerances required to attach the deck and stiffeners to the vertical bulkhead and stiffeners. Figure (49) displays the details of Butt Bracket #2.

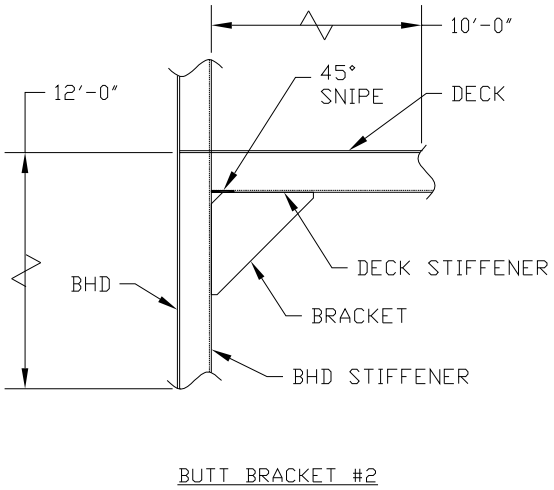

Figure 49 - Butt Bracket #2 Detail Sketch

Lap bracket connections give a lot more freedom to fit up in the field. The web of the deck stiffener is cut short by an inch from the vertical bulkhead stiffener like Butt Bracket #1, for ease of construction. The bracket contains three additional inches of extra material on the straight sides, called ears. The additional three inches of material allow for the bracket to be lapped to the web of the deck stiffener and to the web of the vertical bulkhead stiffener. Since the bracket is lapped to the stiffeners, field fit-up is easier, and the use of fillet welds around the perimeter of the bracket can be utilized. The fillet weld is a much cheaper and easier weld to produce. For the purpose of this analysis, the bracket is shifted half of the plate thickness, and the lapped part of the bracket is connected to the vertical bulkhead stiffener and deck stiffener web via a weld element. The weld element is a 3/8" plate element joining only the nodes that would be connected via a weld. Figure (50) displays the details of the Lap Bracket.

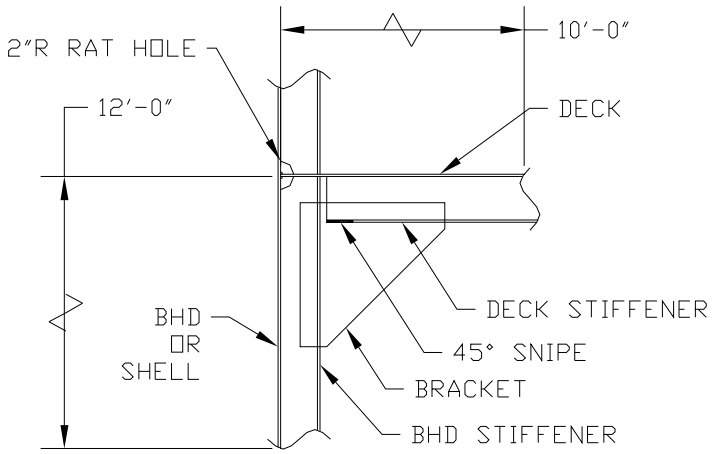

Figure 50 - Lap Bracket Detail Sketch

For each of these three types of bracket analyzed, three different sizes of brackets were checked. The bracket sizes are as follows; small (12”x12”x3/8”), medium (18”x18”x3/8”), and large (24”x24”x3/8”).

In the following sub sections, the results and models are displayed.

Butt Bracket #1; Small (12”x12”x3/8”)

The following model was produced to obtain results in Von Mises stress, node rotation, and max deck uniform load to produce material yielding.

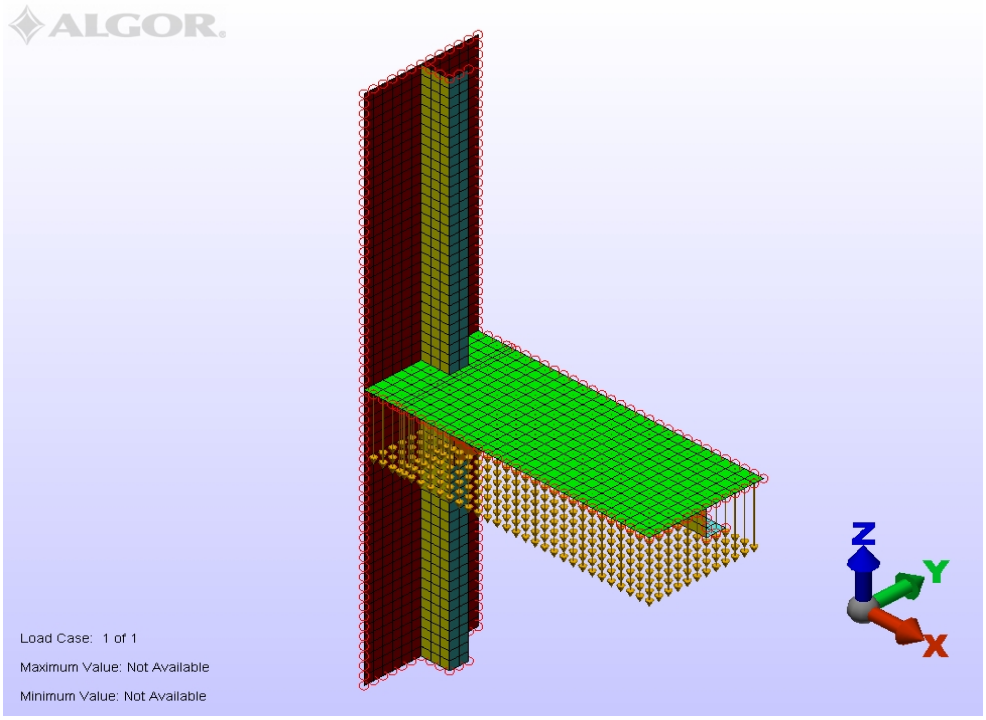

Figure 51 - Butt Bracket #1; Small Connection - Plane View

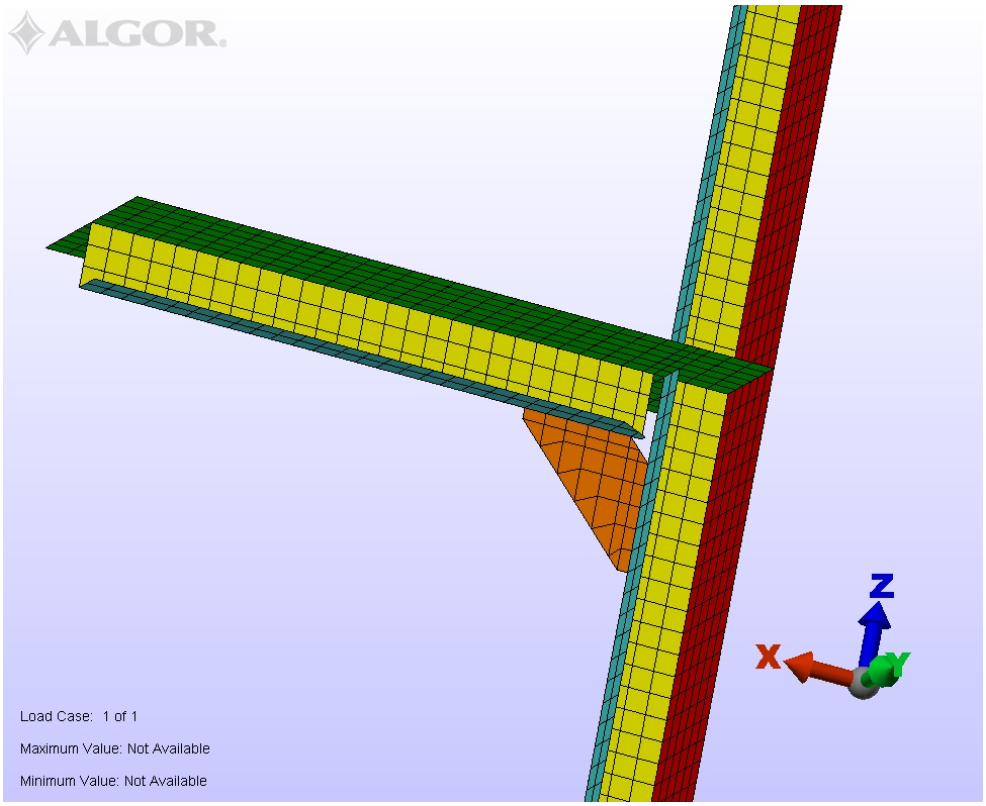

Figure 52 - Butt Bracket #1; Small Connection - Connection View

The Von Mises stress results are shown in figures (53) and (54).

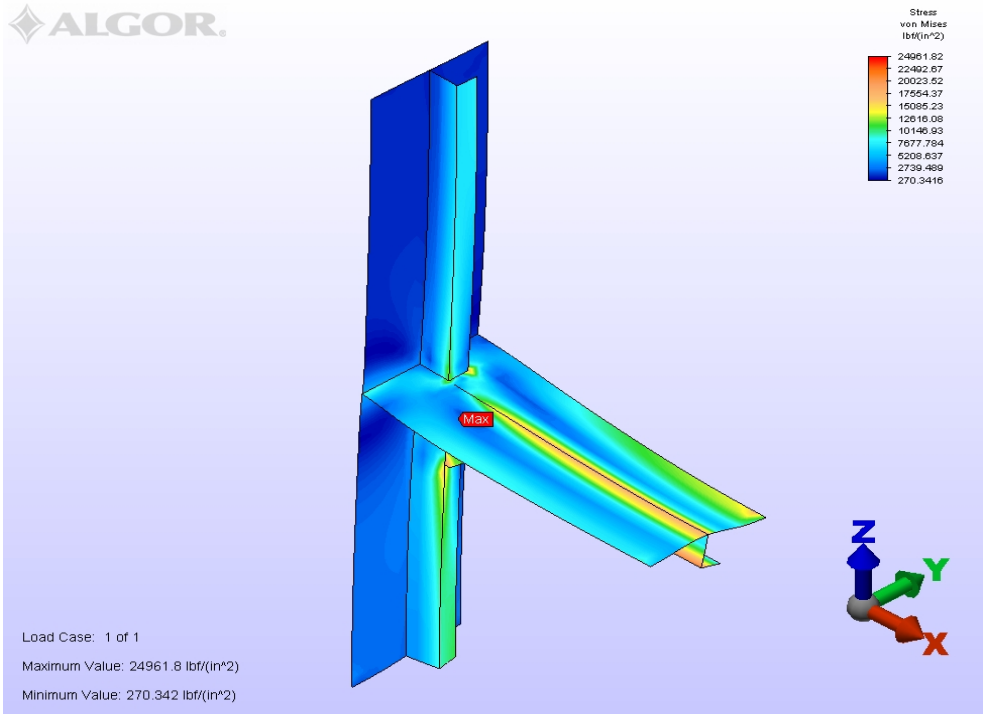

Figure 53 - Butt Bracket #1; Small Connection - Stress Plot

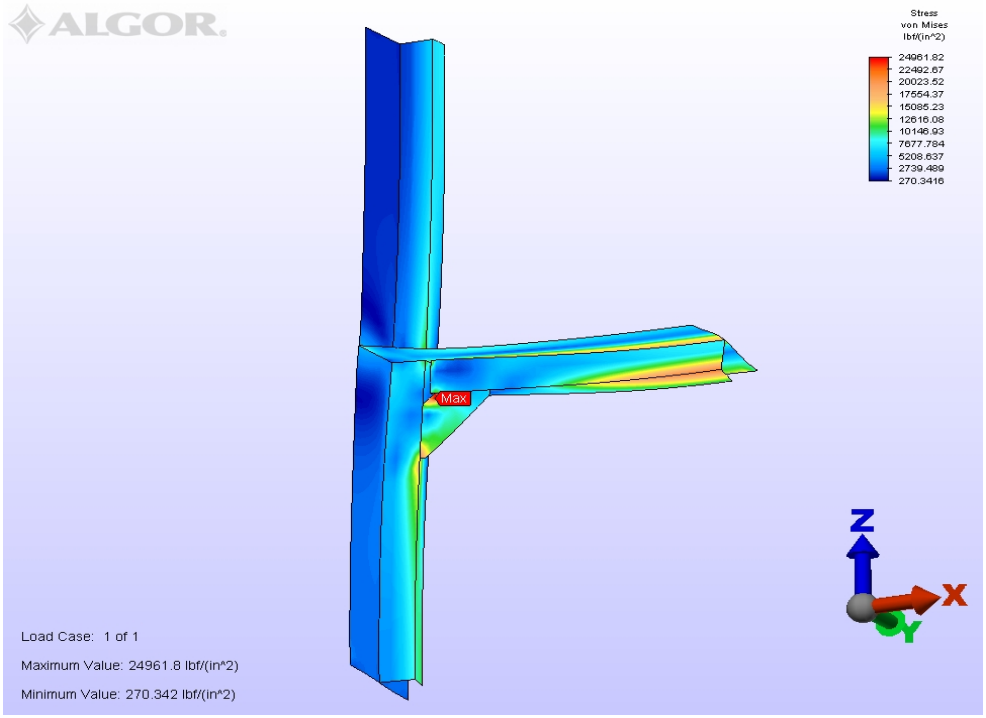

Figure 54 - Butt Bracket #1; Small Connection - Stress Plot

The following data was collected for comparison,

Max Stress at the Connection	24,961.82	psi
Max Stress at Midspan	21,669.92	psi
Max Rotation Angle at the Connection	0.5404	degrees
Max Rotation Angle at Midspan	0.7255	degrees
Max Deck Uniform load to Yield	14.42	psi

Table 21 - Butt Bracket #1; Small Connection - Summary

The maximum stress concentration occurs at the upper edge of snipe of the bracket, where the bracket separates from the extreme fiber of the deck stiffener.

Butt Bracket #1; Medium (18”x18”x3/8”)

The following model was produced to obtain results in Von Mises stress, node rotation, and max deck uniform load to produce material yielding.

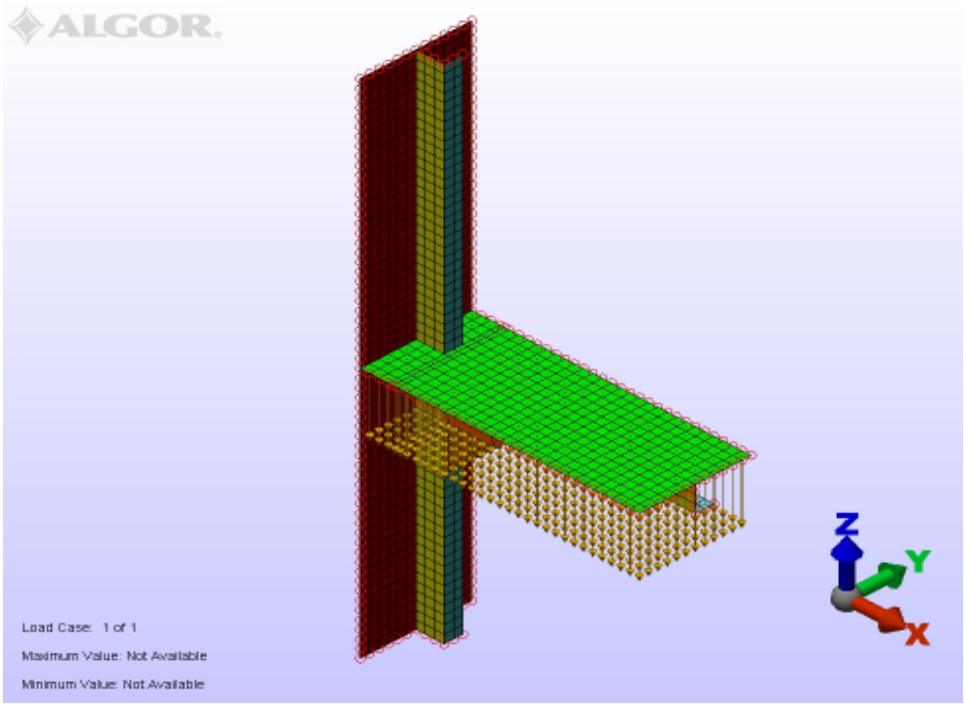

Figure 55 - Butt Bracket #1; Medium Connection – FEA Model – Plan View

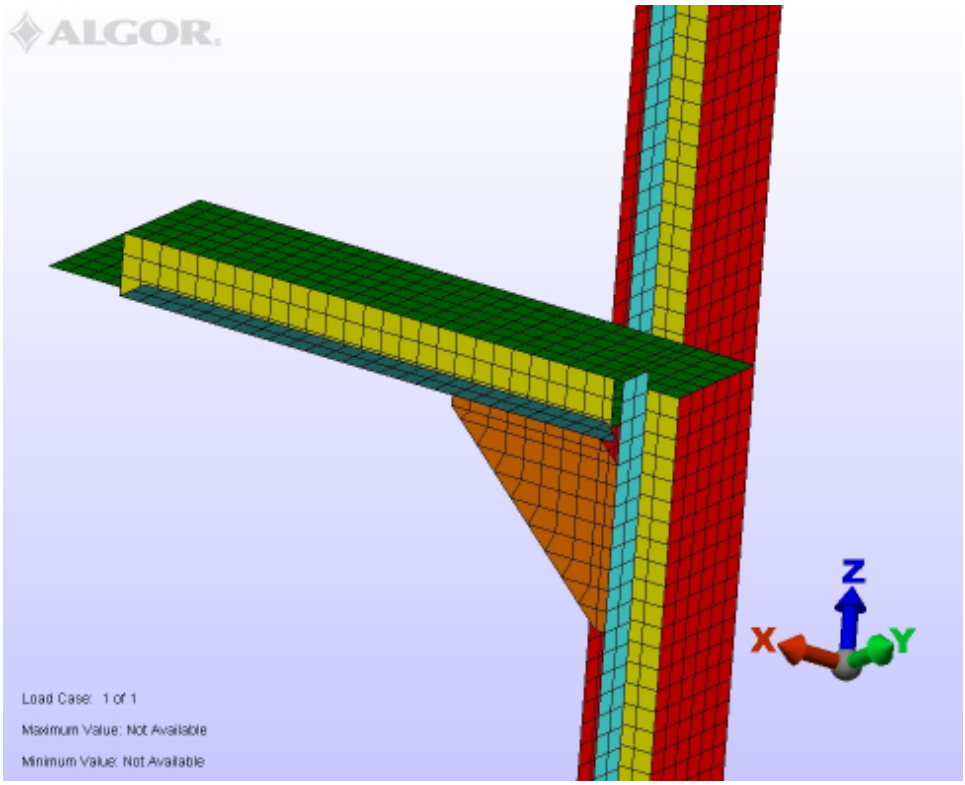

Figure 56 - Butt Bracket #; Medium Connection – FEA Model – Connection View

The Von Mises stress results are shown in figures (57) and (58).

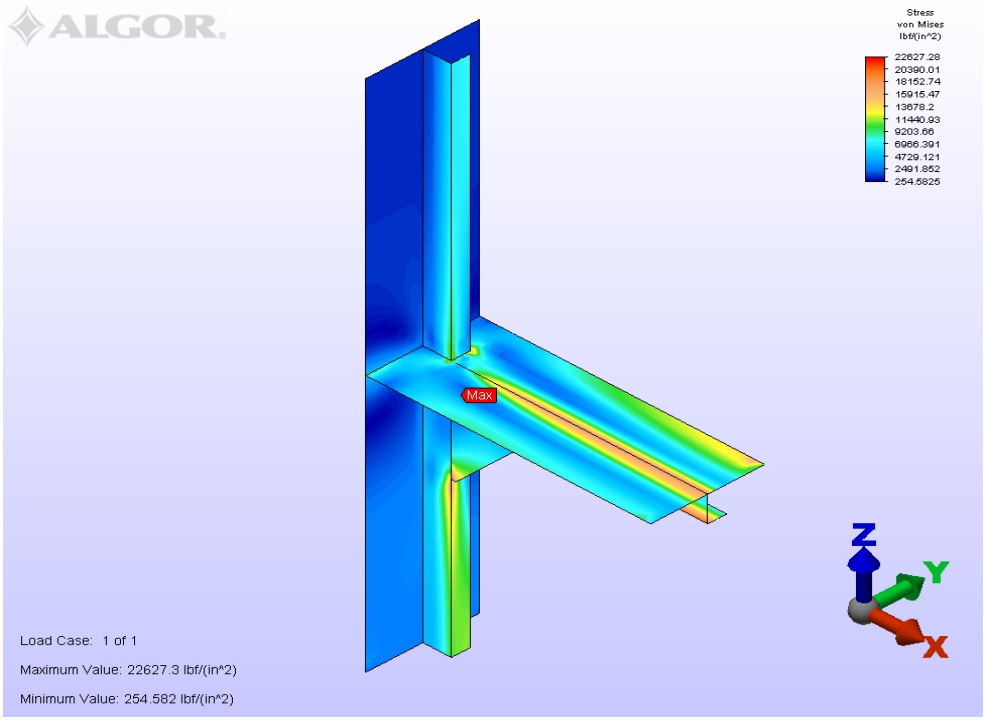

Figure 57 - Butt Bracket #1; Medium Connection – FEA Model – Stress Plot

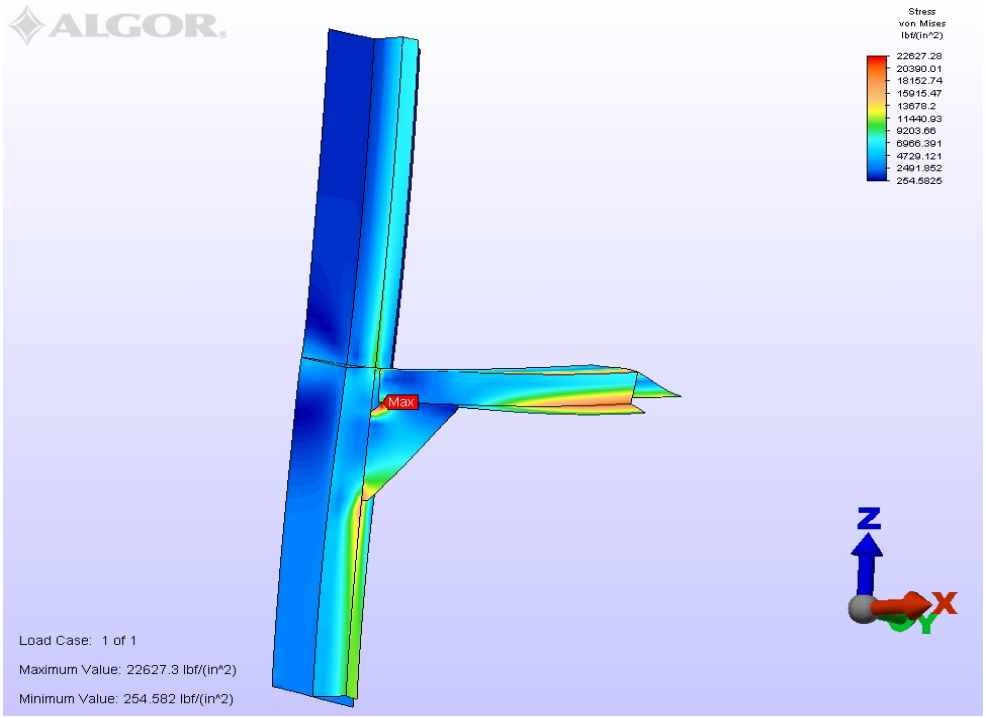

Figure 58 - Butt Bracket #1; Medium Connection – FEA Model – Stress Plot

The following data was collected for comparison,

Max Stress at the Connection	22,627.30	psi
Max Stress at Midspan	20,516.79	psi
Max Rotation Angle at the Connection	0.5479	degrees
Max Rotation Angle at Midspan	0.7020	degrees
Max Deck Uniform load to Yield	15.91	psi

Table 22 - Butt Bracket #1; Medium Connection – FEA Model – Summary

Again the maximum stress concentration occurs at the upper edge of snipe of the bracket, where the bracket separates from the extreme fiber of the deck stiffener.

Butt Bracket #1; Large (24”x24”x3/8”)

The following model was produced to obtain results in Von Mises stress, node rotation, and max deck uniform load to produce material yielding.

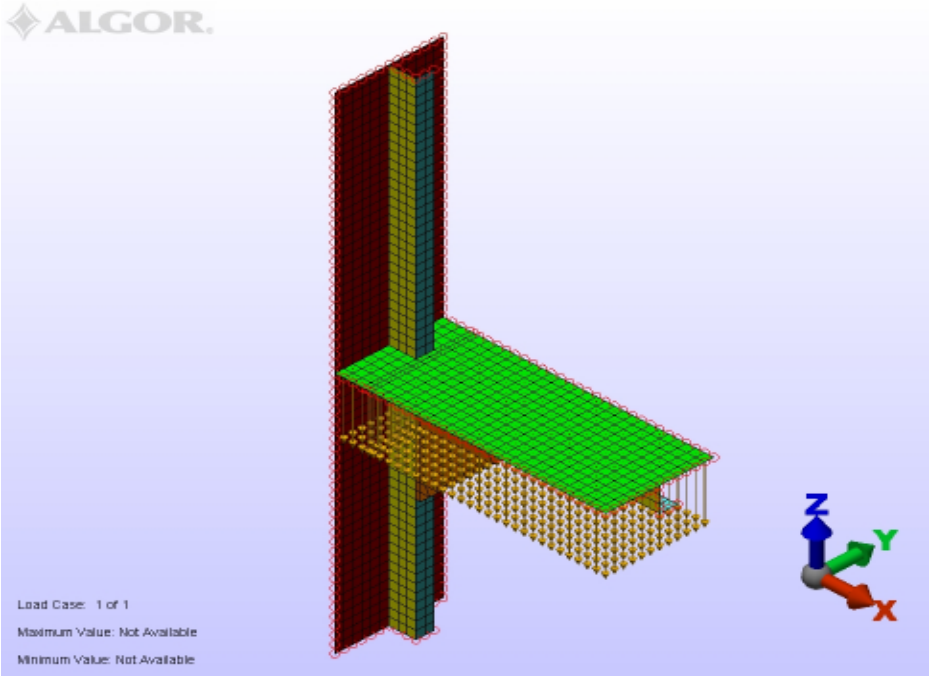

Figure 59 - Butt Bracket #1; Large Connection - FEA Model - Plane View

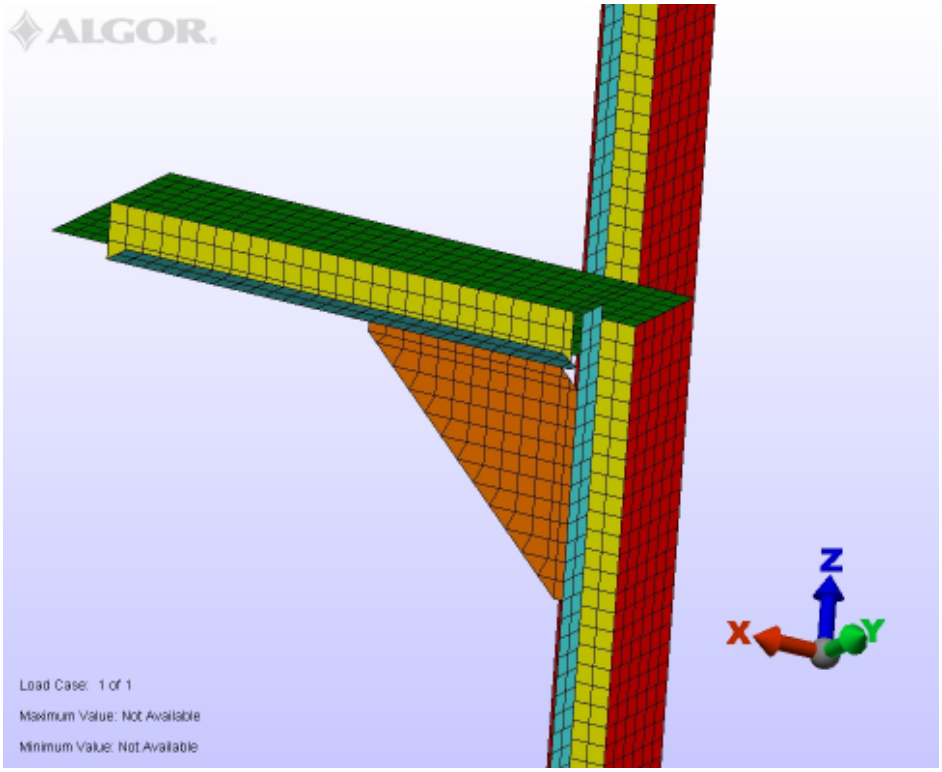

Figure 60 - Butt Bracket #1; Large Connection - FEA Model - Connection View

The Von Mises stress results are shown in figures (61) and (62).

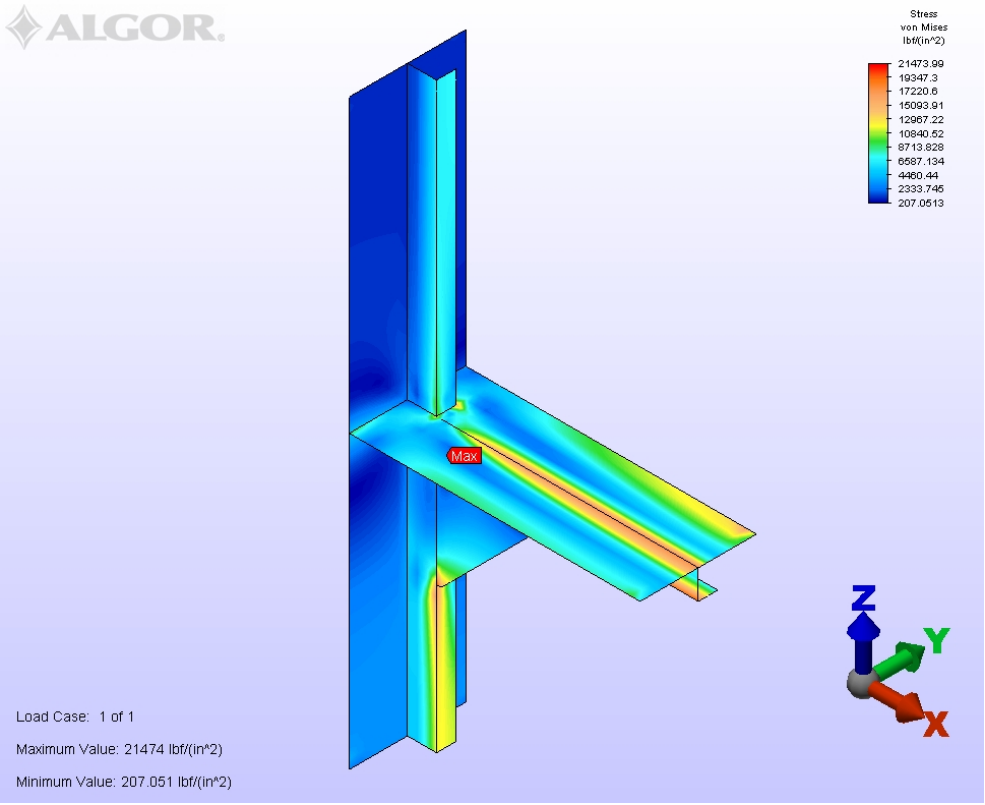

Figure 61 - Butt Bracket #1; Large Connection - FEA Model - Stress Plot

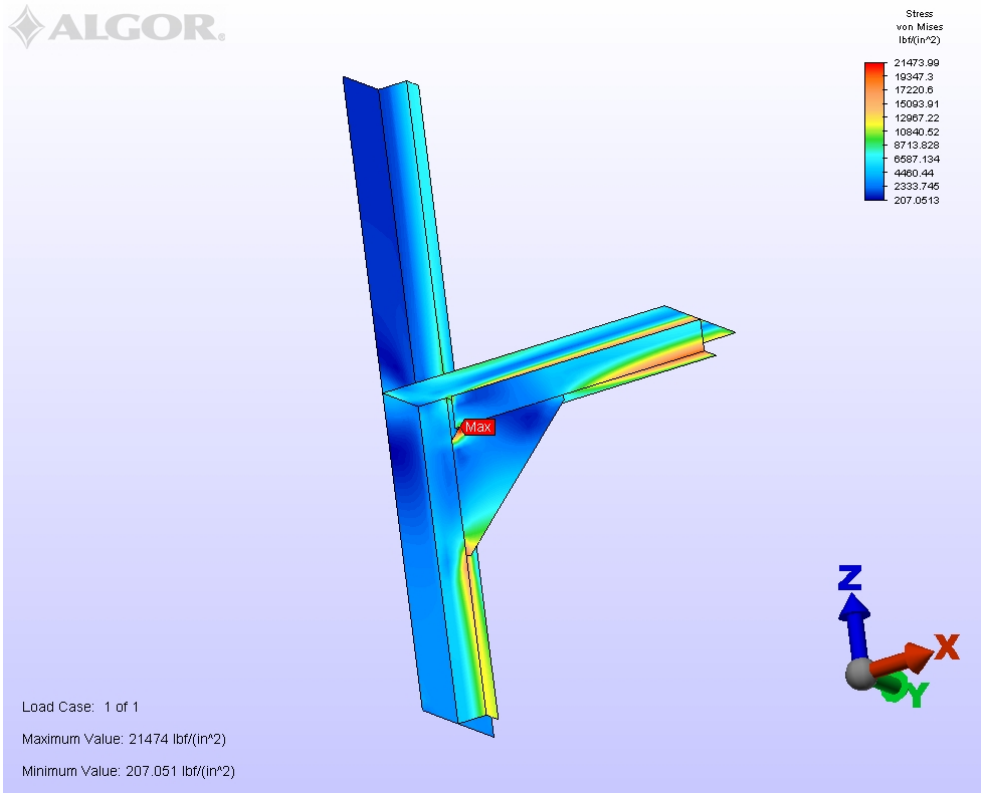

Figure 62 - Butt Bracket #1; Large Connection - FEA Model - Stress Plot

The following data was collected for comparison

Max Stress at the Connection	21,473.99	psi
Max Stress at Midspan	19,665.23	psi
Max Rotation Angle at the Connection	0.5740	degrees
Max Rotation Angle at Midspan	0.6831	degrees
Max Deck Uniform load to Yield	16.76	psi

Table 23 - Butt Bracket #1; Large Connection - FEA Model - Summary

Again the maximum stress concentration occurs at the upper edge of snipe of the bracket, where the bracket separates from the extreme fiber of the deck stiffener.

Butt Bracket #2; Small (12”x12”x3/8”)

The following model was produced to obtain results in Von Mises stress, node rotation, and max deck uniform load to produce material yielding.

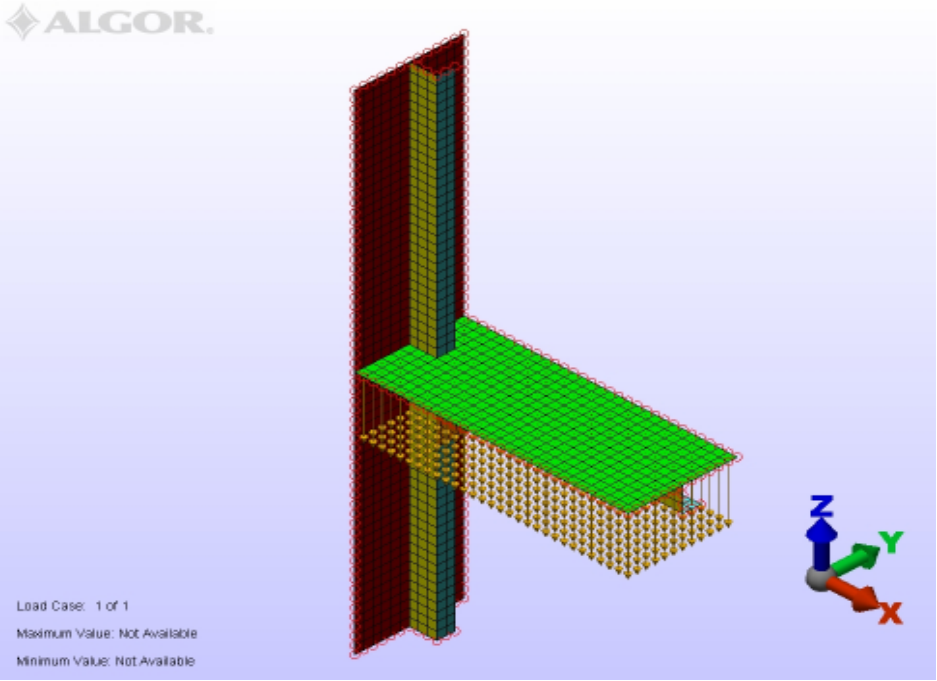

Figure 63 - Butt Bracket #2; Small Connection - FEA Model - Plane View

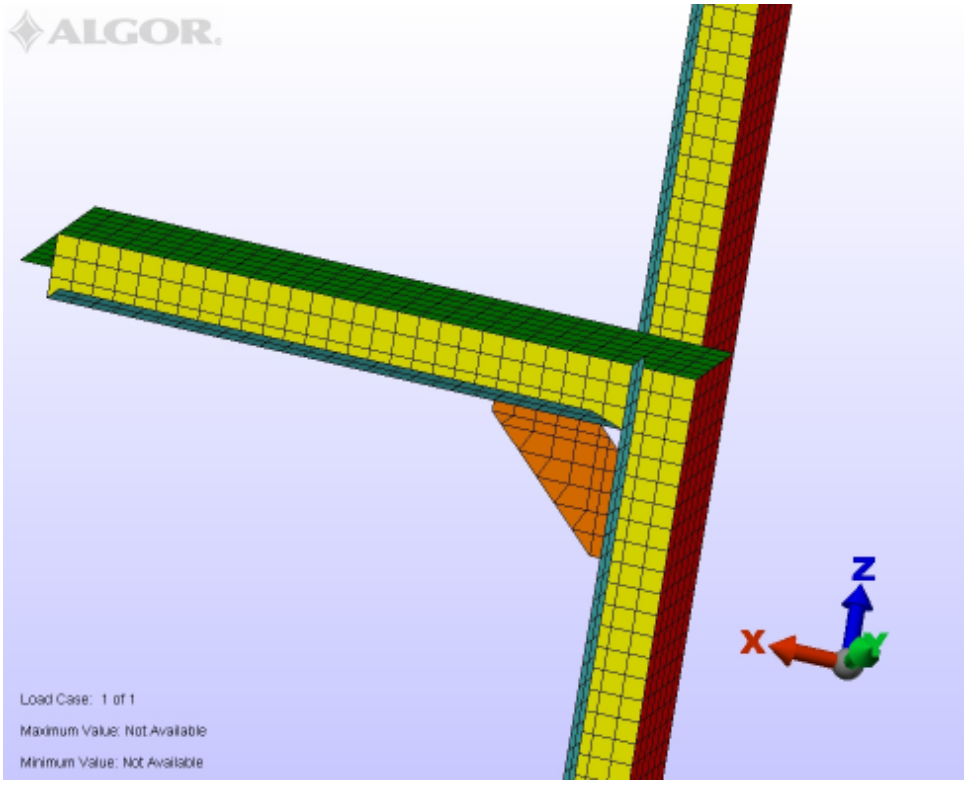

Figure 64 - Butt Bracket #2; Small Connection - FEA Model - Connection View

The Von Mises stress results are shown in figures (65) and (66).

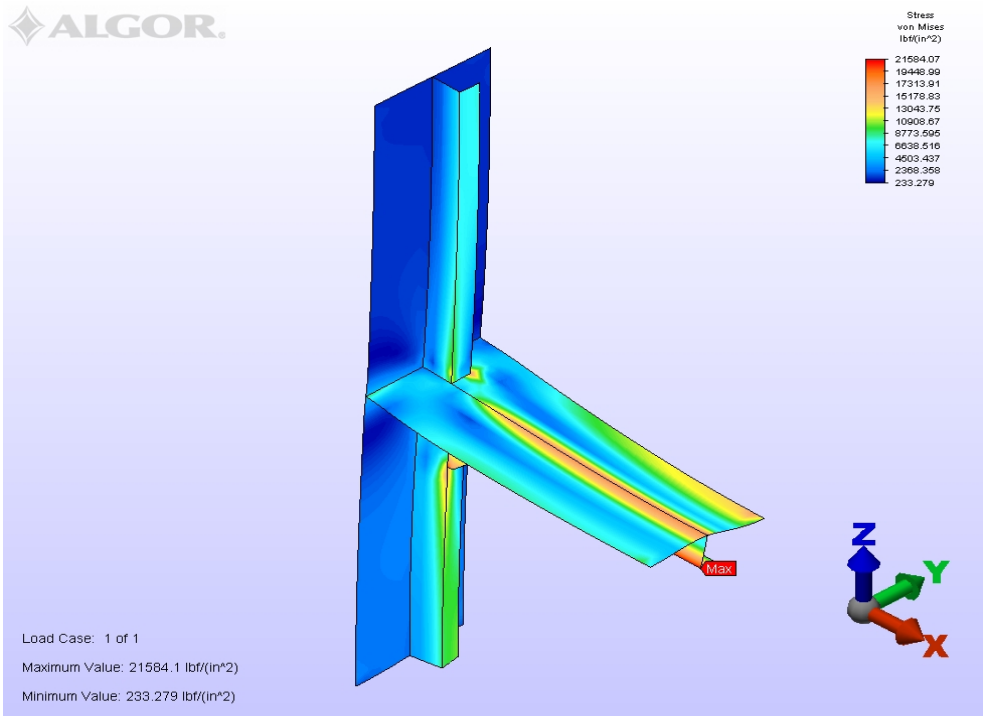

Figure 65 - Butt Bracket #2; Small Connection - FEA Model - Stress Plot

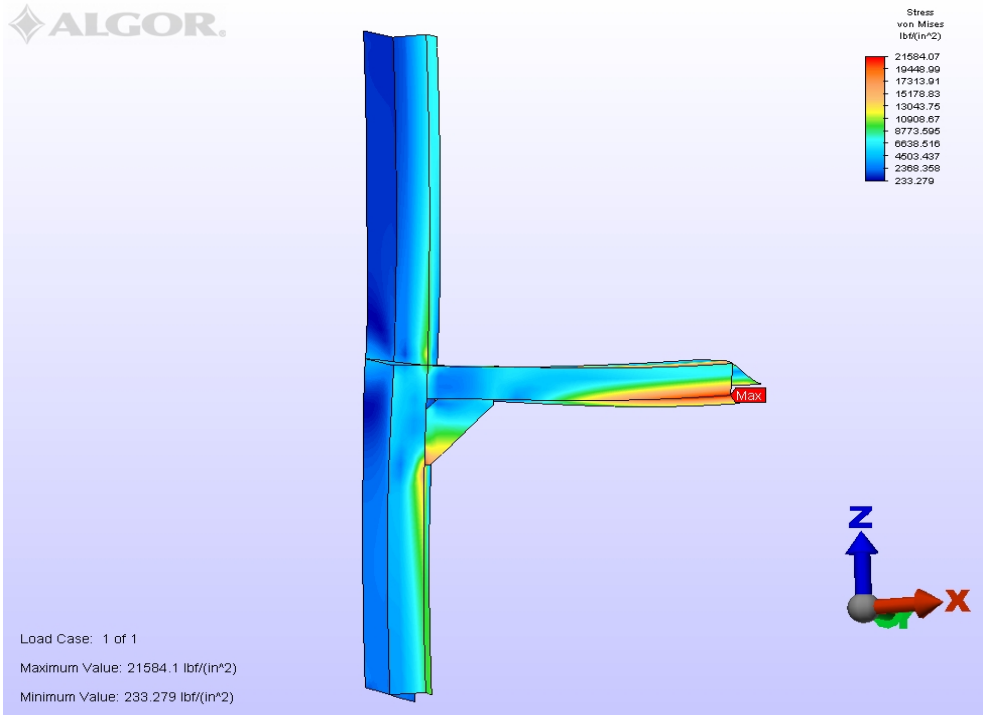

Figure 66 - Bracket #2; Small Connection - FEA Model - Stress Plot

The following data was collected for comparison,

Max Stress at the Connection	20,450.36	psi
Max Stress at Midspan	21,584.07	psi
Max Rotation Angle at the Connection	0.5288	degrees
Max Rotation Angle at Midspan	0.7178	degrees
Max Deck Uniform load to Yield	16.68	psi

Table 24 - Bracket #2; Small Connection - FEA Model - Summary

The maximum stress concentration occurs at midspan of the deck stiffener, at the lower extreme fiber of the member where the flange meets the web. It can be stated that the connection is efficient in obtaining the maximum moment the deck member can support.

Butt Bracket #2; Medium (18”x18”x3/8”)

The following model was produced to obtain results in Von Mises stress, node rotation, and max deck uniform load to produce material yielding.

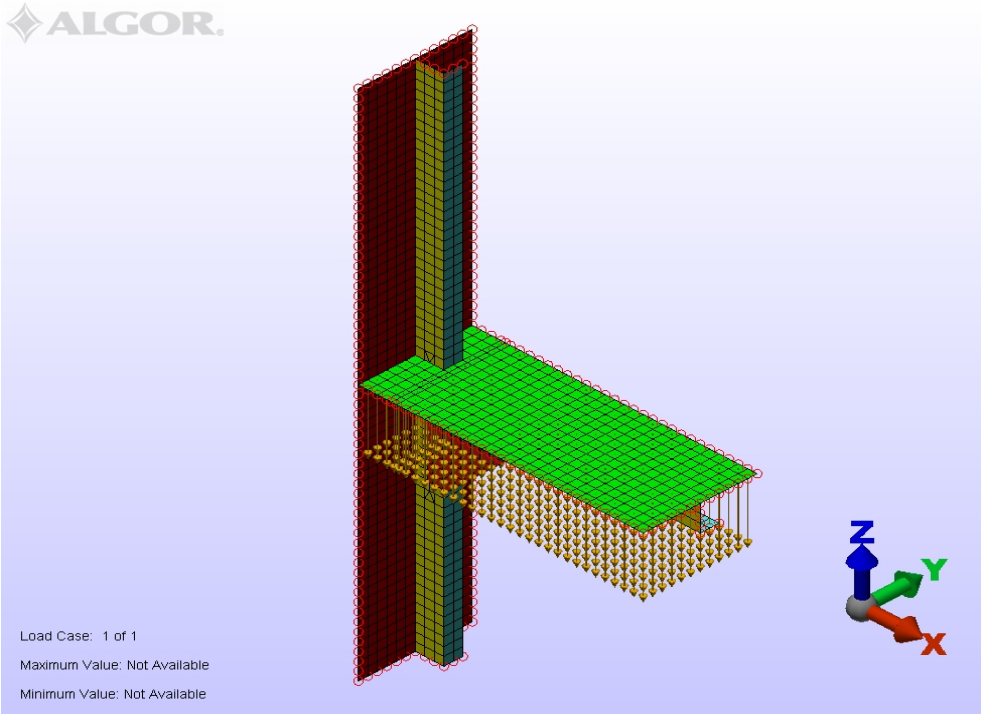

Figure 67 - Bracket #2; Medium Connection - FEA Model - Plan View

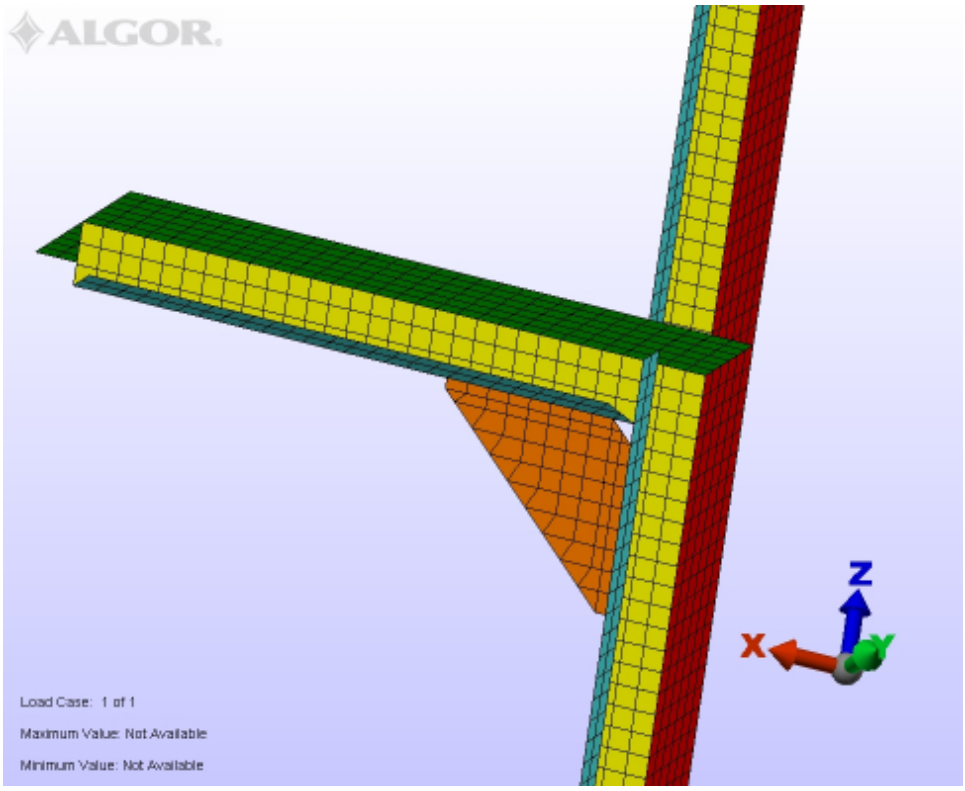

Figure 68 - Bracket #2; Medium Connection - FEA Model - Connection View

The Von Mises stress results are shown in figures (69) and (70).

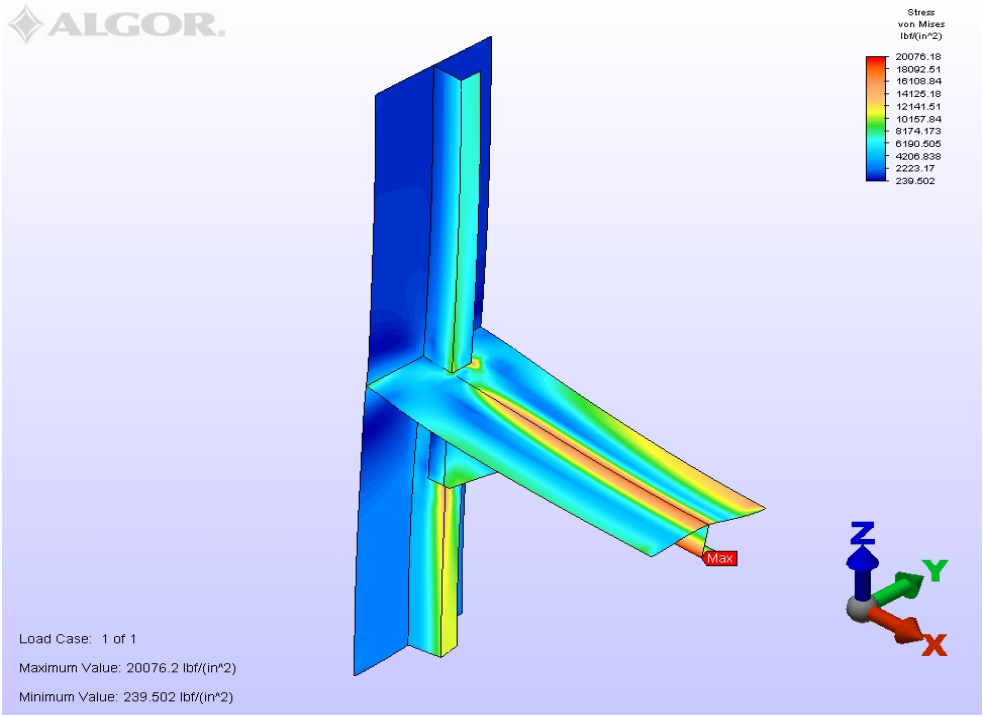

Figure 69 - Bracket #2; Medium Connection - FEA Model - Stress Plot

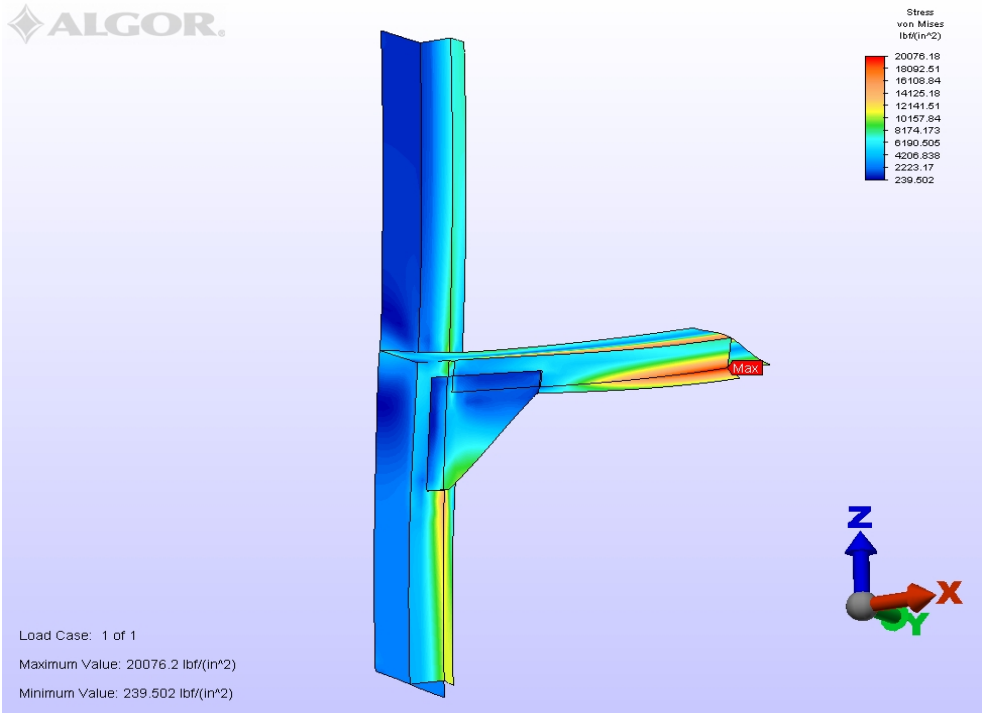

Figure 70 - Bracket #2; Medium Connection - FEA Model - Stress Plot

The following data was collected for comparison,

Max Stress at the Connection	19,749.43	psi
Max Stress at Midspan	20,421.30	psi
Max Rotation Angle at the Connection	0.5556	degrees
Max Rotation Angle at Midspan	0.6934	degrees
Max Deck Uniform load to Yield	17.63	psi

Table 25 - Bracket #2; Medium Connection - FEA Model - Summary

Like the smaller version of this connection, the maximum stress concentration occurs at midspan of the deck stiffener, at the lower extreme fiber of the member where the flange meets the web. It can be stated that the connection is efficient obtaining the maximum moment the deck member can support.

Butt Bracket #2; Large (24”x24”x3/8”)

The following model was produced to obtain results in Von Mises stress, node rotation, and max deck uniform load to produce material yielding.

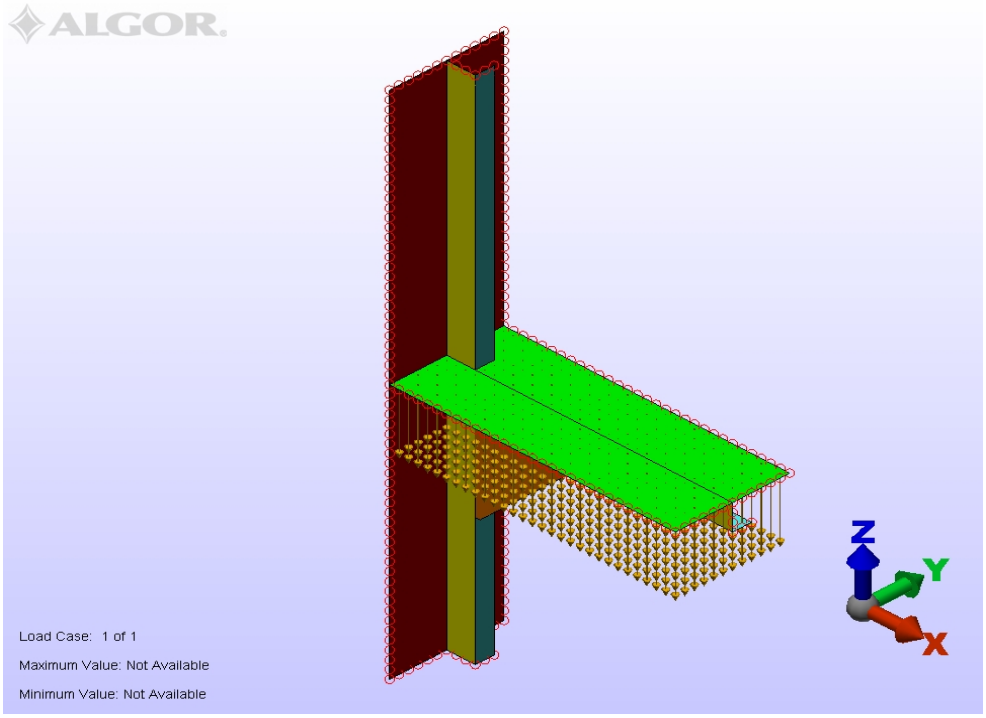

Figure 71 - Bracket #2; Large Connection - FEA Model - Plane View

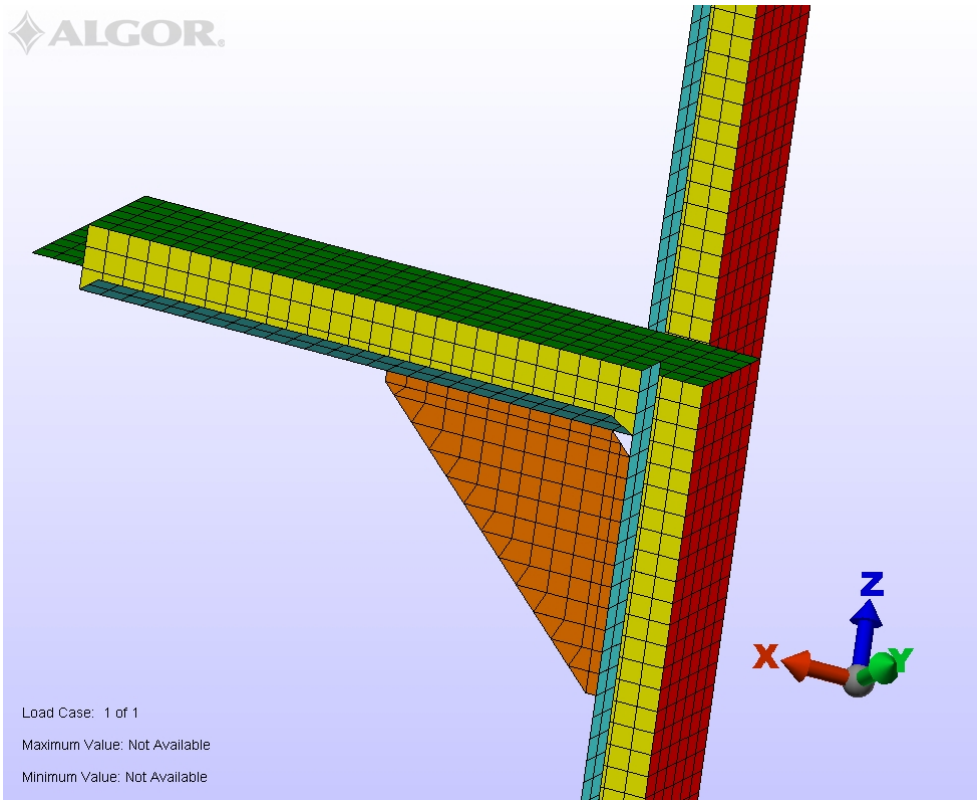

Figure 72 - Bracket #2; Large Connection - FEA Model - Connection View

The Von Mises stress results are shown in figures (73) and (74).

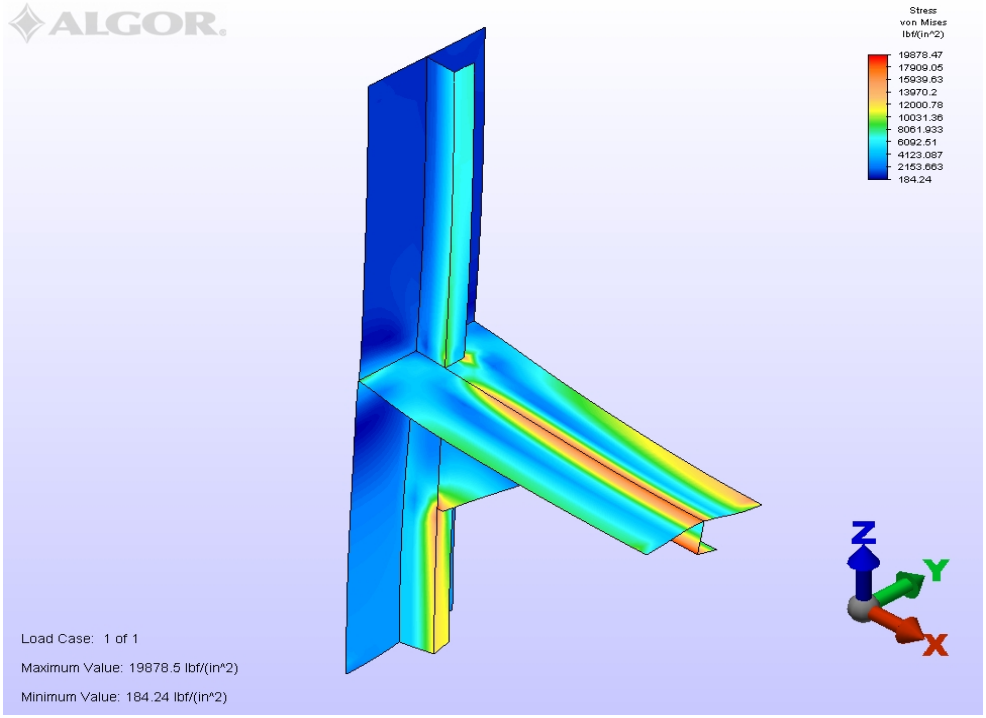

Figure 73 - Bracket #2; Large Connection - FEA Model - Stress Plot

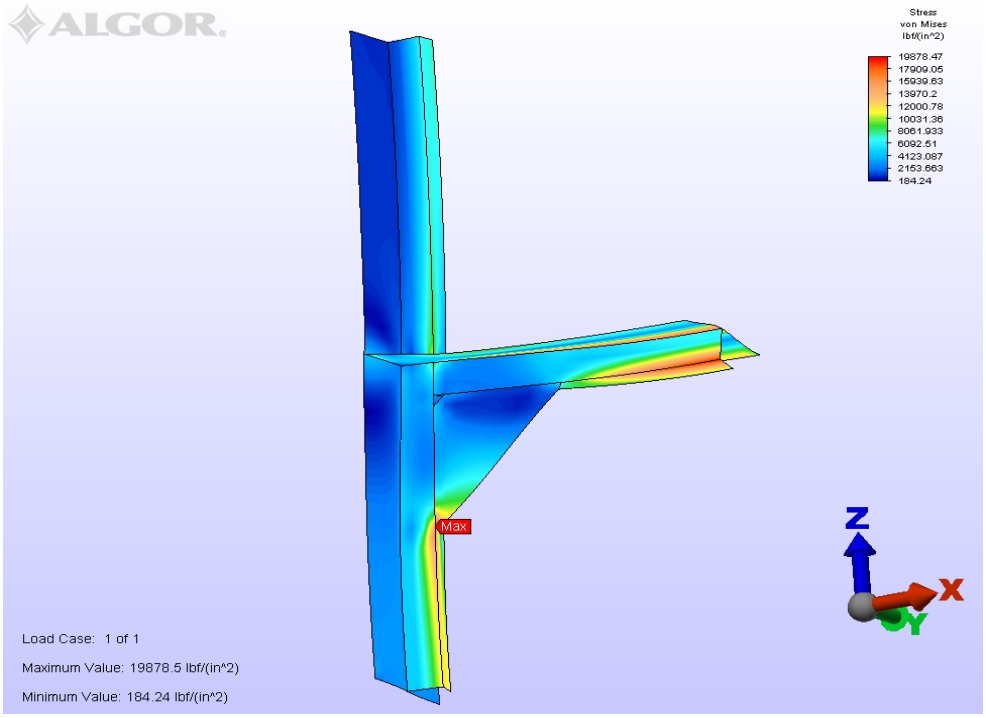

Figure 74 - Bracket #2; Large Connection - FEA Model - Stress Plot

The following data was collected for comparison,

Max Stress at the Connection	19,878.47	psi
Max Stress at Midspan	19,543.36	psi
Max Rotation Angle at the Connection	0.5833	degrees
Max Rotation Angle at Midspan	0.6742	degrees
Max Deck Uniform load to Yield	18.11	psi

Table 26 - Bracket #2; Large Connection - FEA Model - Summary

Like the smaller versions of this connection, the maximum stress concentration occurs at midspan of the deck stiffener, at the lower extreme fiber of the member where the flange meets the web. It can be stated that the connection is efficient in obtaining the maximum moment the deck member can support.

Lap Bracket; Small (12”x12”x3/8”)

The following model was produced to obtain results in Von Mises stress, node rotation, and max deck uniform load to produce material yielding.

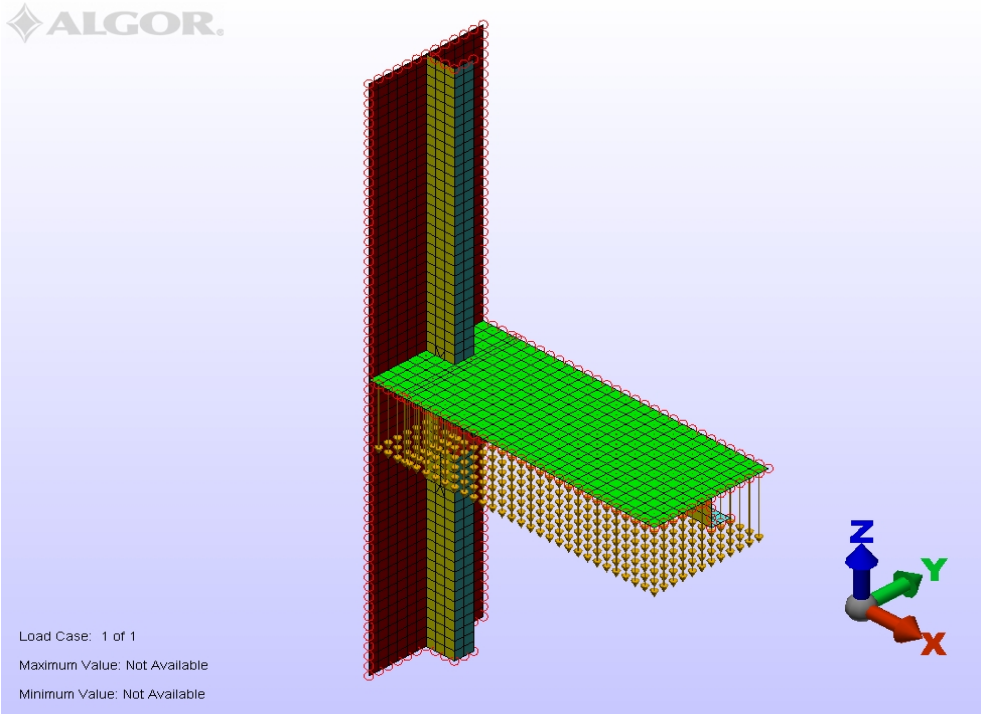

Figure 75 - Lap Bracket; Small Connection - FEA Model - Plane View

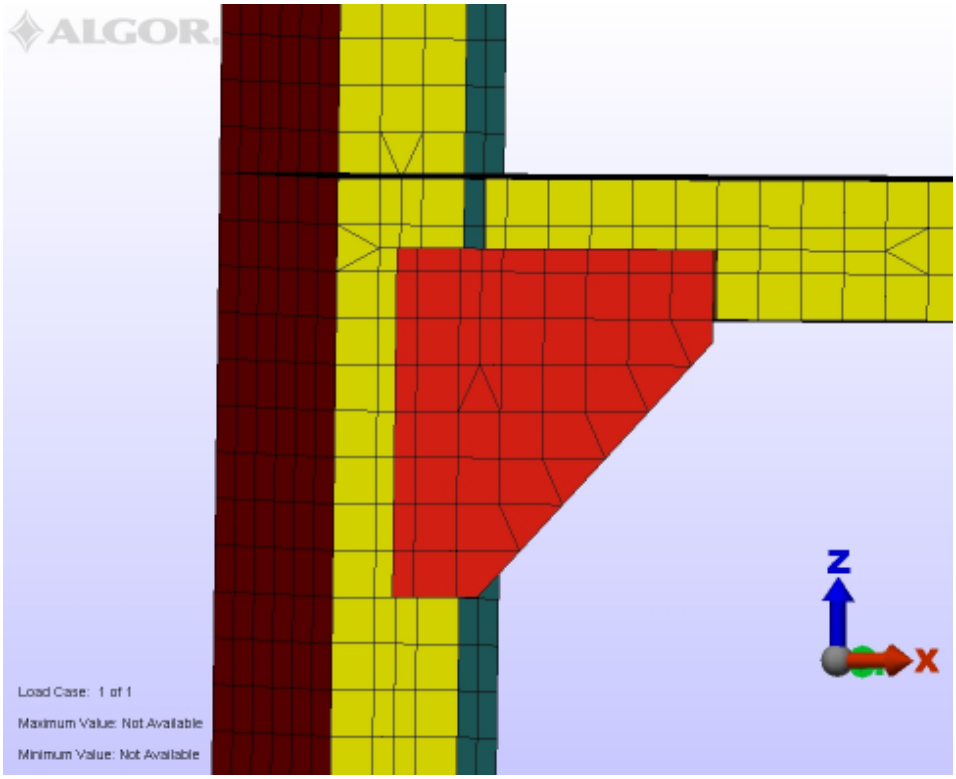

Figure 76 - Lap Bracket; Small Connection - FEA Model - Connection View

The Von Mises stress results are shown in figures (77) and (78).

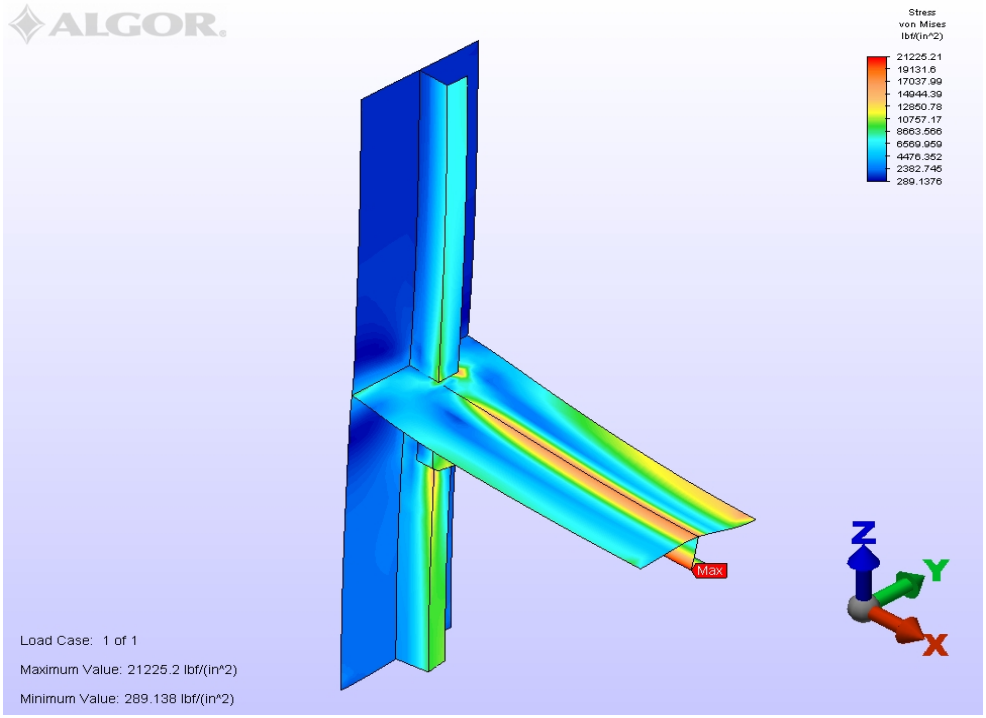

Figure 77 - Lap Bracket; Small Connection - FEA Model - Stress Plot

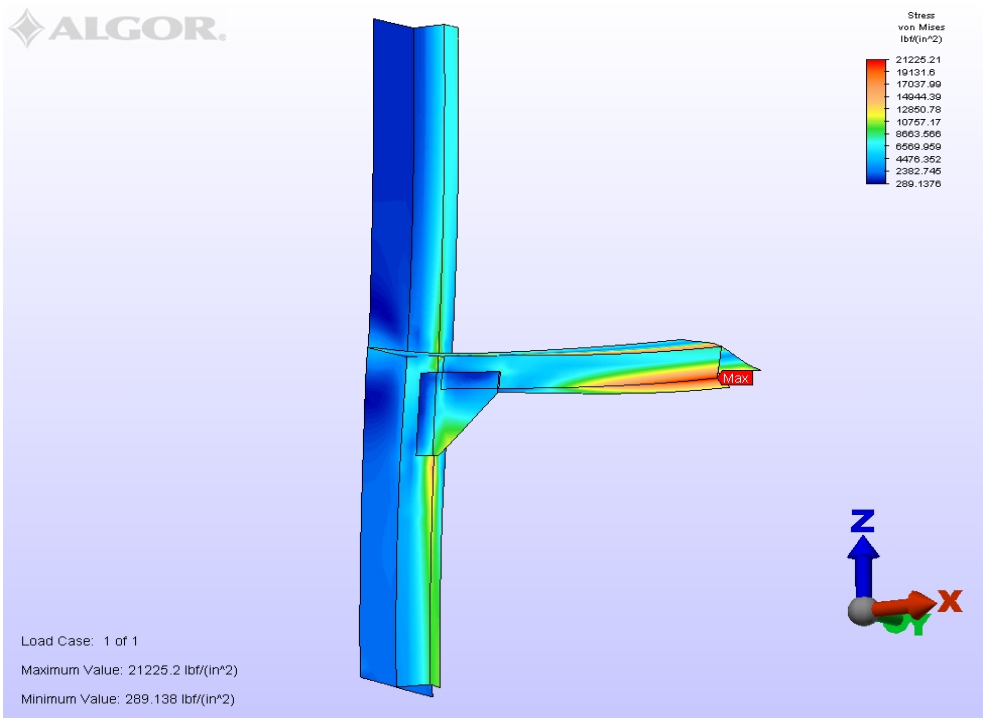

Figure 78 - Lap Bracket; Small Connection - FEA Model - Stress Plot

The following data was collected for comparison,

Max Stress at the Connection	17,039.96	psi
Max Stress at Midspan	21,225.21	psi
Max Rotation Angle at the Connection	0.5301	degrees
Max Rotation Angle at Midspan	0.7288	degrees
Max Deck Uniform load to Yield	16.96	psi

Table 27 - Lap Bracket; Small Connection - FEA Model - Summary

The maximum stress concentration occurs at midspan of the deck stiffener, at the lower extreme fiber of the member where the flange meets the web. From the results of the analysis, it can be

stated that the connection is efficient obtaining the maximum moment the deck member can support.

Lap Bracket; Medium (18”x18”x3/8”)

The following model was produced to obtain results in Von Mises stress, node rotation, and max deck uniform load to produce material yielding.

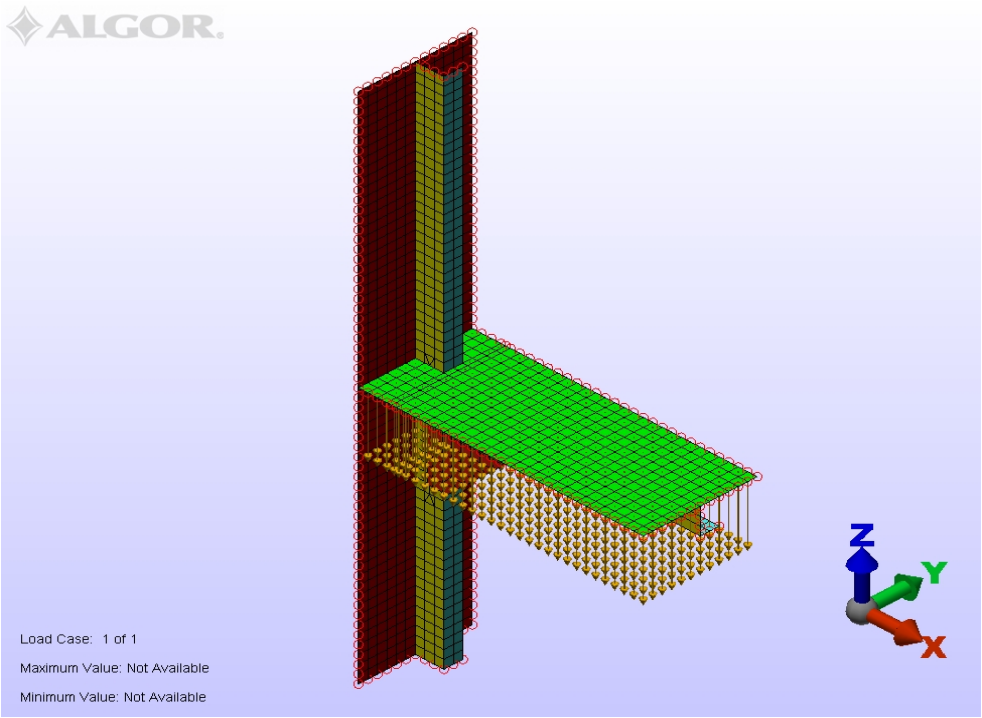

Figure 79 - Lap Bracket; Medium Connection - FEA Model - Plane View

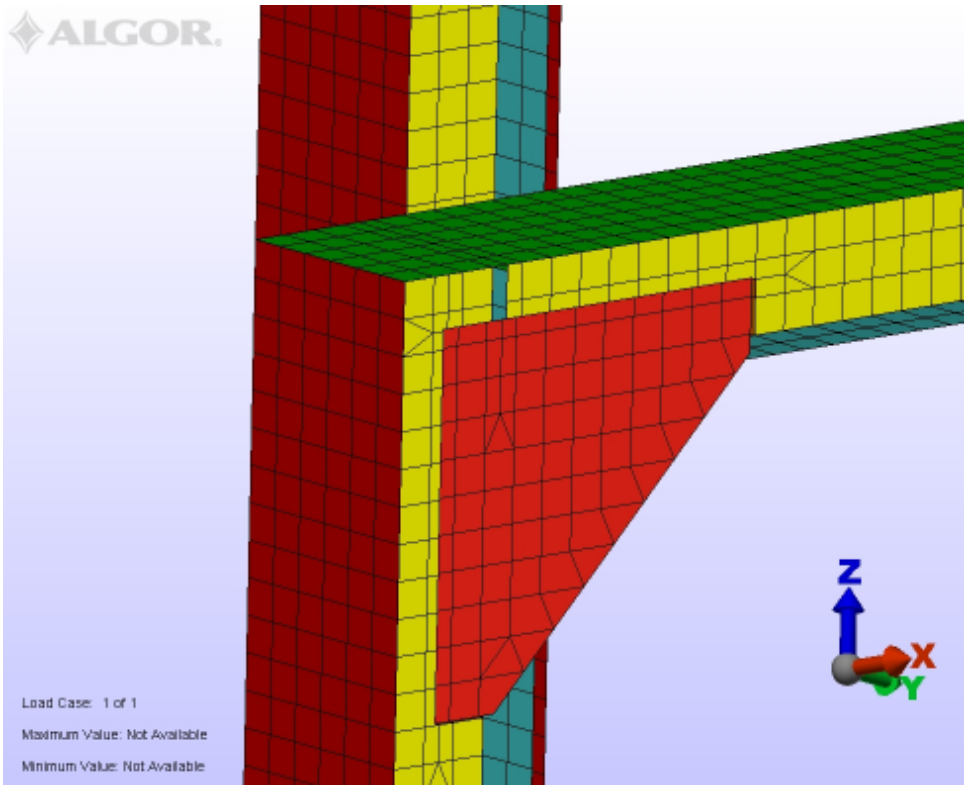

Figure 80 - Lap Bracket; Medium Connection - FEA Model - Connection View

The Von Mises stress results are shown in figures (81) and (82).

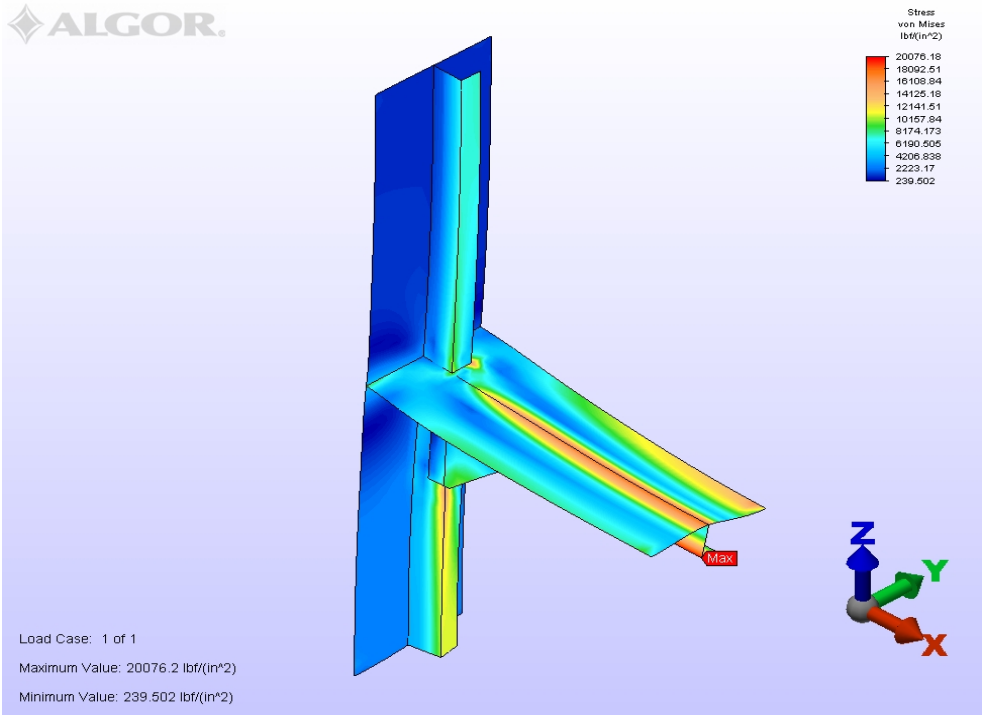

Figure 81 - Lap Bracket; Medium Connection - FEA Model - Stress Plot

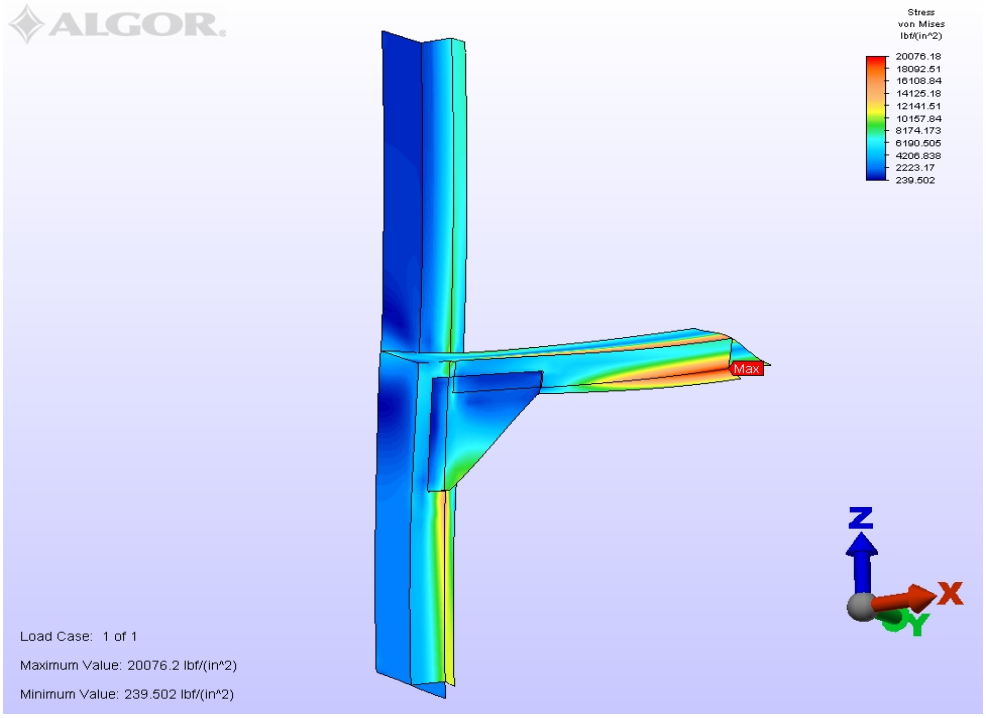

Figure 82 -Lap Bracket; Medium Connection - FEA Model - Stress Plot

The following data was collected for comparison,

Max Stress at the Connection	17,271.07	psi
Max Stress at Midspan	20,076.18	psi
Max Rotation Angle at the Connection	0.5652	degrees
Max Rotation Angle at Midspan	0.7173	degrees
Max Deck Uniform load to Yield	17.94	psi

Table 28 -Lap Bracket; Medium Connection - FEA Model - Summary

Like the smaller version of this connection, the maximum stress concentration occurs at midspan of the deck stiffener, at the lower extreme fiber of the member where the flange meets the web. From the analysis, it can be stated that the connection is efficient obtaining the maximum moment the deck member can support.

Lap Bracket; Large (24”x24”x3/8”)

The following model was produced to obtain results in Von Mises stress, node rotation, and max deck uniform load to produce material yielding.

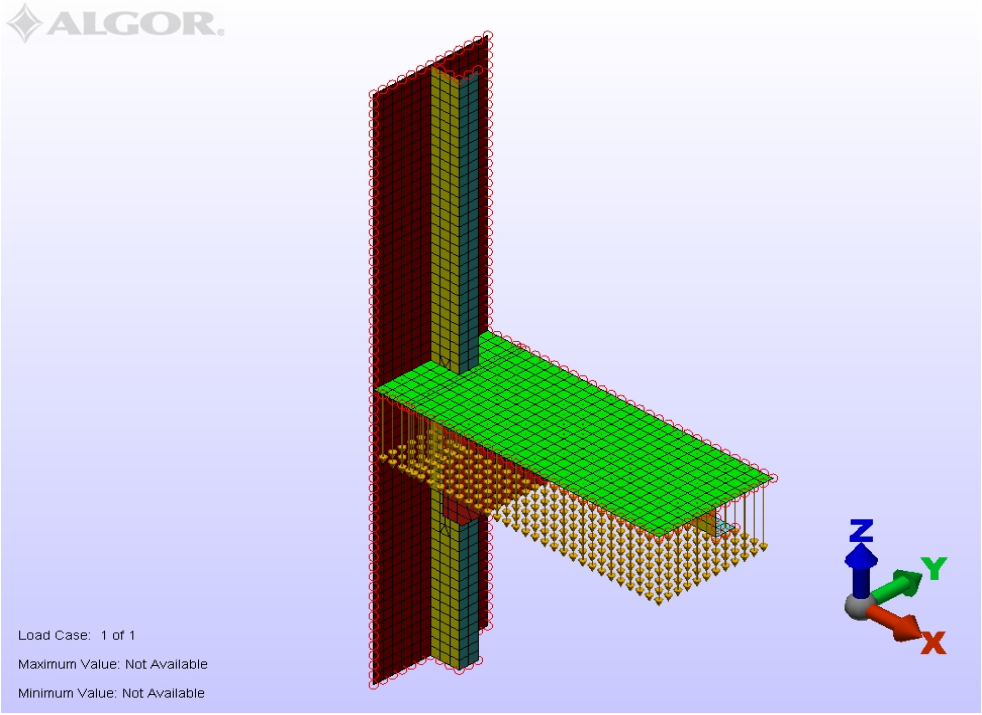

Figure 83 - Lap Bracket; Large Connection - FEA Model - Plane View

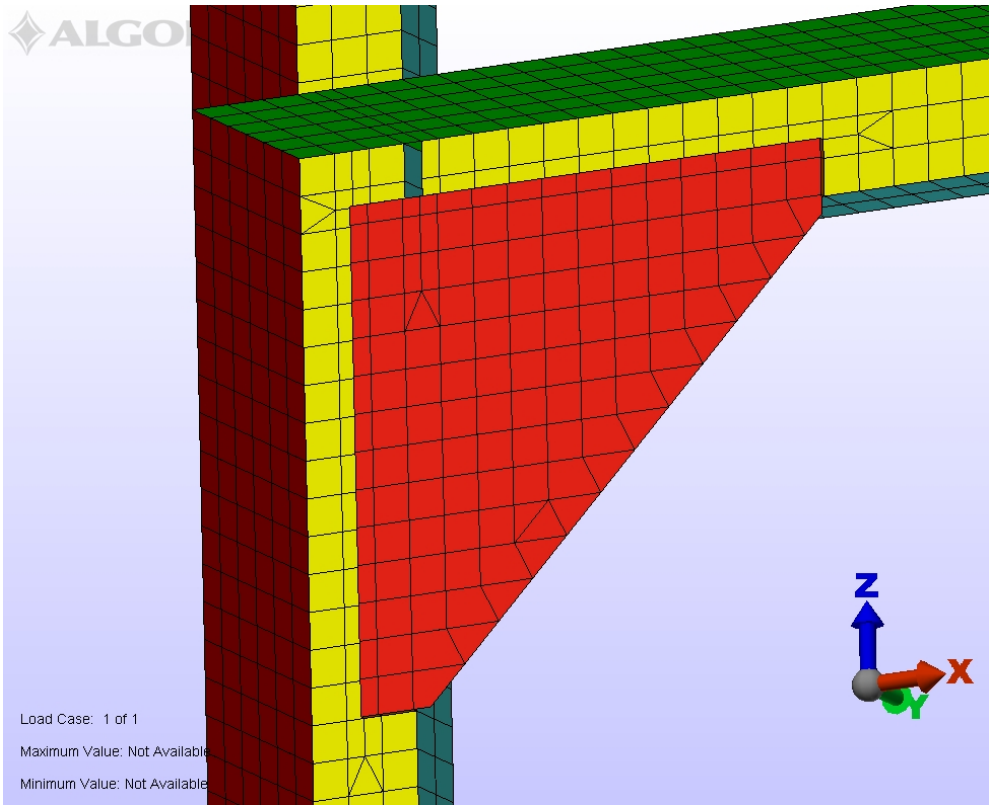

Figure 84 - Lap Bracket; Large Connection - FEA Model - Connection View

The Von Mises stress results are shown in figures (85) and (86).

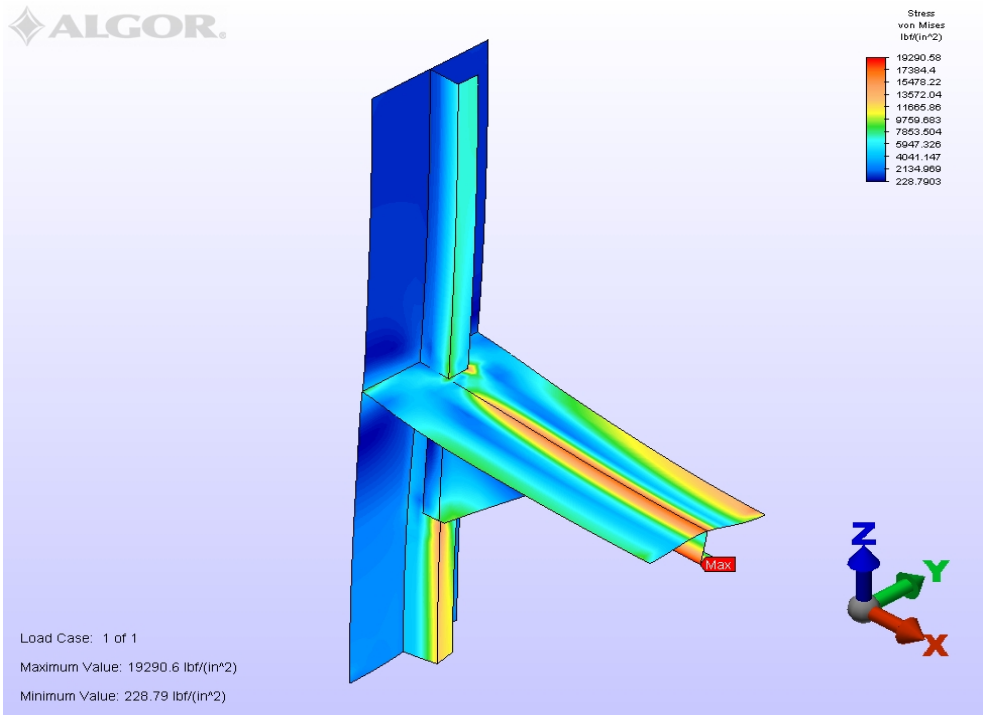

Figure 85 - Lap Bracket; Large Connection - FEA Model - Stress Plot

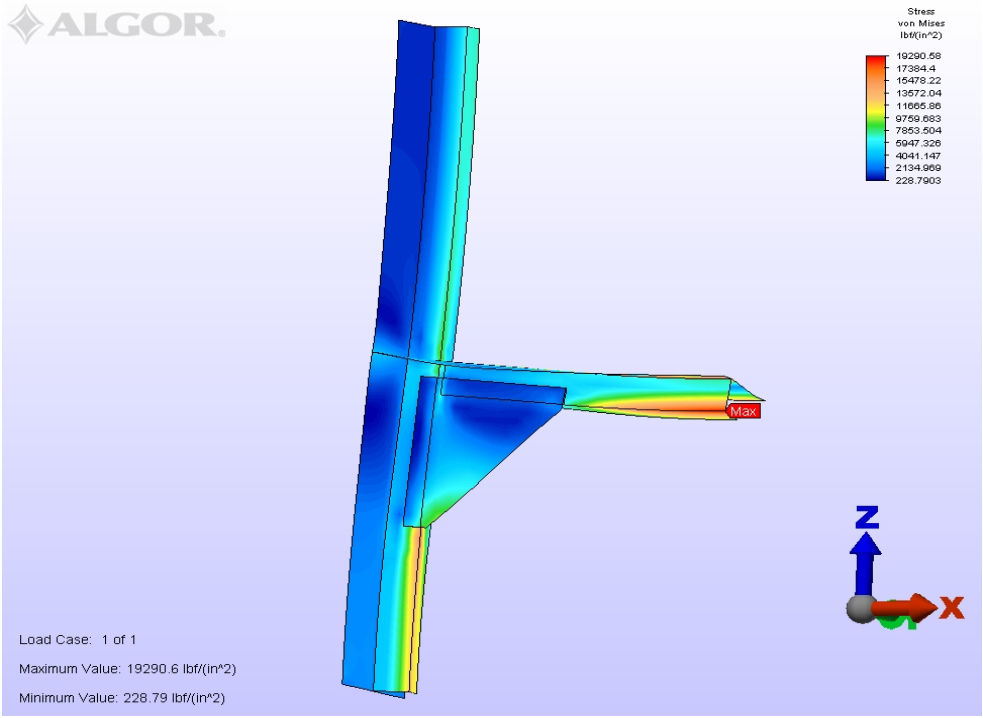

Figure 86 - Lap Bracket; Large Connection - FEA Model - Stress Plot

The following data was collected for comparison,

Max Stress at the Connection	17,320.57	psi
Max Stress at Midspan	19,290.58	psi
Max Rotation Angle at the Connection	0.6041	degrees
Max Rotation Angle at Midspan	0.7077	degrees
Max Deck Uniform load to Yield	18.66	psi

Table 29 - Lap Bracket; Large Connection - FEA Model - Summary

Like the smaller versions of this connection, the maximum stress concentration occurs at midspan of the deck stiffener, at the lower extreme fiber of the member where the flange meets the web. It can be stated that the connection is efficient in obtaining the maximum moment the deck member can support.

Chapter 7 – Summary

In this thesis, the author has presented the reader with three criteria and the evaluation of each for determining the efficiency of various structural end connections utilized in the marine industry. Chapter 4 introduced the three criteria used in developing the findings of this thesis paper. Chapter 5 introduced the baseline models used as the contrast for determining the comparisons of the various end connections analyzed. Finally chapter 6 explained the 13 various end connections analyzed and offered the reader the results per individual analysis.

In the Stress Criteria, the individual models were subjected to a 10 psi deck pressure and the stress at the connection and at the mid-span of the deck beam were obtained. Table (16) displays the findings of the Stress Criteria per location and displays the percent difference of the Von Mises stress at the location to the Von Mises stress of the baseline model with edge supports at the same location. As stated in reference [1], "there are no perfectly rigid connections nor completely flexible ones, all connections really are partly restrained, or PR, to one degree or another." Therefore no end connection analyzed by this thesis should have a percent equal to 100 or 0.

	@ Connection	@ Mid-Span	@ Connection	@ Mid-Span
End Connection	**Max HVM Stress (psi)** *10 psi Dist Load*	**Max HVM Stress (psi)** *10 psi Dist Load*	**% Difference**	**% Difference**
Baseline Fixed	38,375.2	27,575.4	-	-
Baseline Fixed Edge Support	32,616.8	17,311.8	-	-
Flat Bar Chock Connection	22,613.9	24,344.8	31%	-41%
Snipe Connection	24,311.8	24,147.0	25%	-39%
Tapered Chock Connection	21,468.5	24,295.7	34%	-40%
Lap Connection	21,466.7	23,493.9	34%	-36%
Butt Bracket #1 Small	24,961.8	21,669.9	23%	-25%
Butt Bracket #1 Medium	22,627.3	20,516.8	31%	-19%
Butt Bracket #1 Large	21,474.0	19,665.2	34%	-14%
Butt Bracket #2 Small	20,450.4	21,584.1	37%	-25%
Butt Bracket #2 Medium	19,749.4	20,421.3	39%	-18%
Butt Bracket #2 Large	19,878.5	19,543.4	39%	-13%
Lap Bracket Small	17,040.0	21,225.2	48%	-23%
Lap Bracket Medium	17,271.1	20,076.2	47%	-16%
Lap Bracket Large	17,320.6	19,290.6	47%	-11%

Table 30 - Stress Criteria Summary

When the stresses at the end connection and midspan of the 2 baseline models and 13 end connection models are plotted on a chart, the stress ranges between the various end connections is evident. For example, using the light blue line of the baseline fixed edge support model as the contrast, and the brown line representing the lap bracket large model, the difference of stress obtained at the end connection and at the midspan can be clearly seen. Please note that the area between the support end and midspan do **NOT** represent the actual stress at that location, but a straight line from point to point. If the stresses at a consistent interval along the entire length of beam were plotted, each model would have a non linear line. At the connection, the lap bracket large model has lower stresses at the connection than the baseline fixed edge support model. At the midspan, the baseline edge support model has lower stresses than the lap bracket large model. Other stress variances can be obtained in a similar method for the various end connection analyzed.

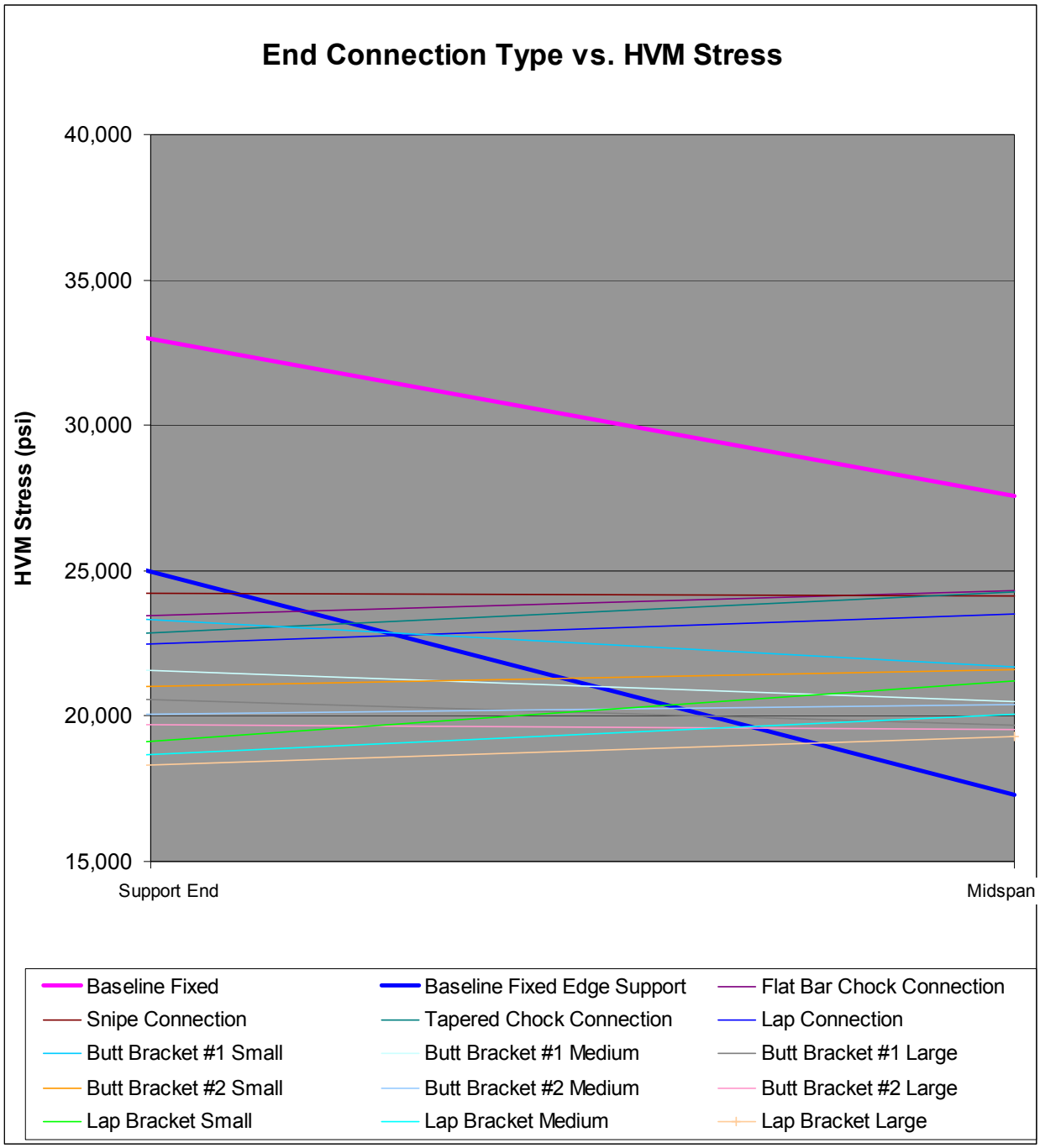

Figure 87 - Stress Criteria - End Connection Type vs. HVM Stress – Line Graph

Another method for drawing conclusions on the variances of stress at the end connection or midspan of the baseline models to the end connection models is to plot a bar graph. The two

baseline models are at the left of the graph, and if a line drawn horizontal to the x-axis was plotted one can see the differences of stress at the connection and at the midspan clearly.

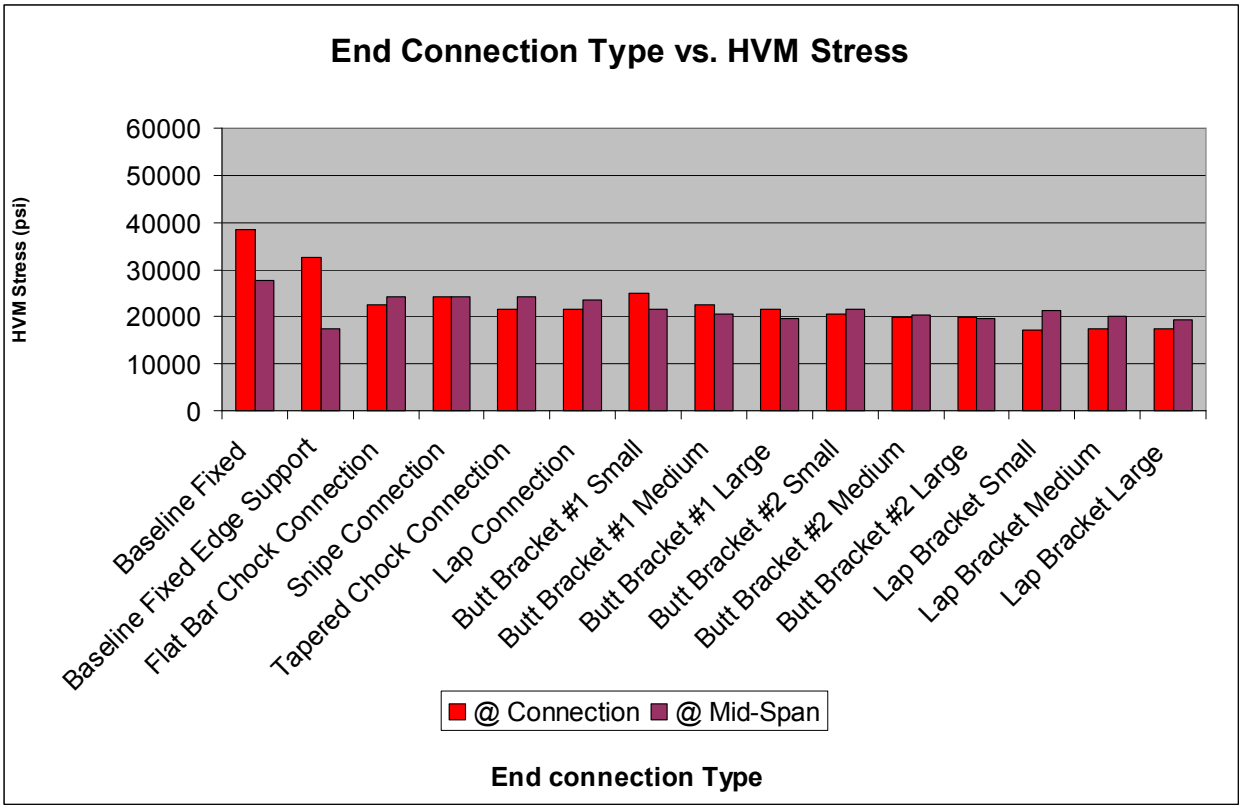

Figure 88 - Stress Criteria - End Connection Type vs. HVM Stress - Bar Graph

In the Rotation Criteria, the individual models were subjected to a 10 psi deck pressure and the nodal rotation at the general location of the connection and the mid-span of the deck beam were obtained. Table (17) displays the findings of the Rotation Criteria per location and displays the percent difference of the nodal rotation at the location to the nodal rotation of the baseline model with edge supports at the same location. A similar approach of comparisons as stated in the Stress Criteria can be used for the following tables and graphs for nodal rotation.

End Connection	@ Connection Max Rotation (degrees) *10 psi Dist Load*	@ Mid-Span Max Rotation (degrees) *10 psi Dist Load*	@ Connection % Difference	@ Mid-Span % Difference
Baseline Fixed	1.71733	1.96403	-	-
Baseline Fixed Edge Support	0.43426	0.89733	-	-
Flat Bar Chock Connection	0.52890	0.71307	-22%	21%
Snipe Connection	0.56372	0.78705	-30%	12%
Tapered Chock Connection	0.52491	0.73120	-21%	19%
Lap Connection	0.53372	0.73457	-23%	18%
Butt Bracket #1 Small	0.54040	0.72547	-24%	19%
Butt Bracket #1 Medium	0.54786	0.70205	-26%	22%
Butt Bracket #1 Large	0.57398	0.68311	-32%	24%
Butt Bracket #2 Small	0.52876	0.71777	-22%	20%
Butt Bracket #2 Medium	0.55562	0.69336	-28%	23%
Butt Bracket #2 Large	0.58326	0.67424	-34%	25%
Lap Bracket Small	0.53007	0.72881	-22%	19%
Lap Bracket Medium	0.56519	0.71734	-30%	20%
Lap Bracket Large	0.60413	0.70767	-39%	21%

Table 31 - Rotation Criteria Summary

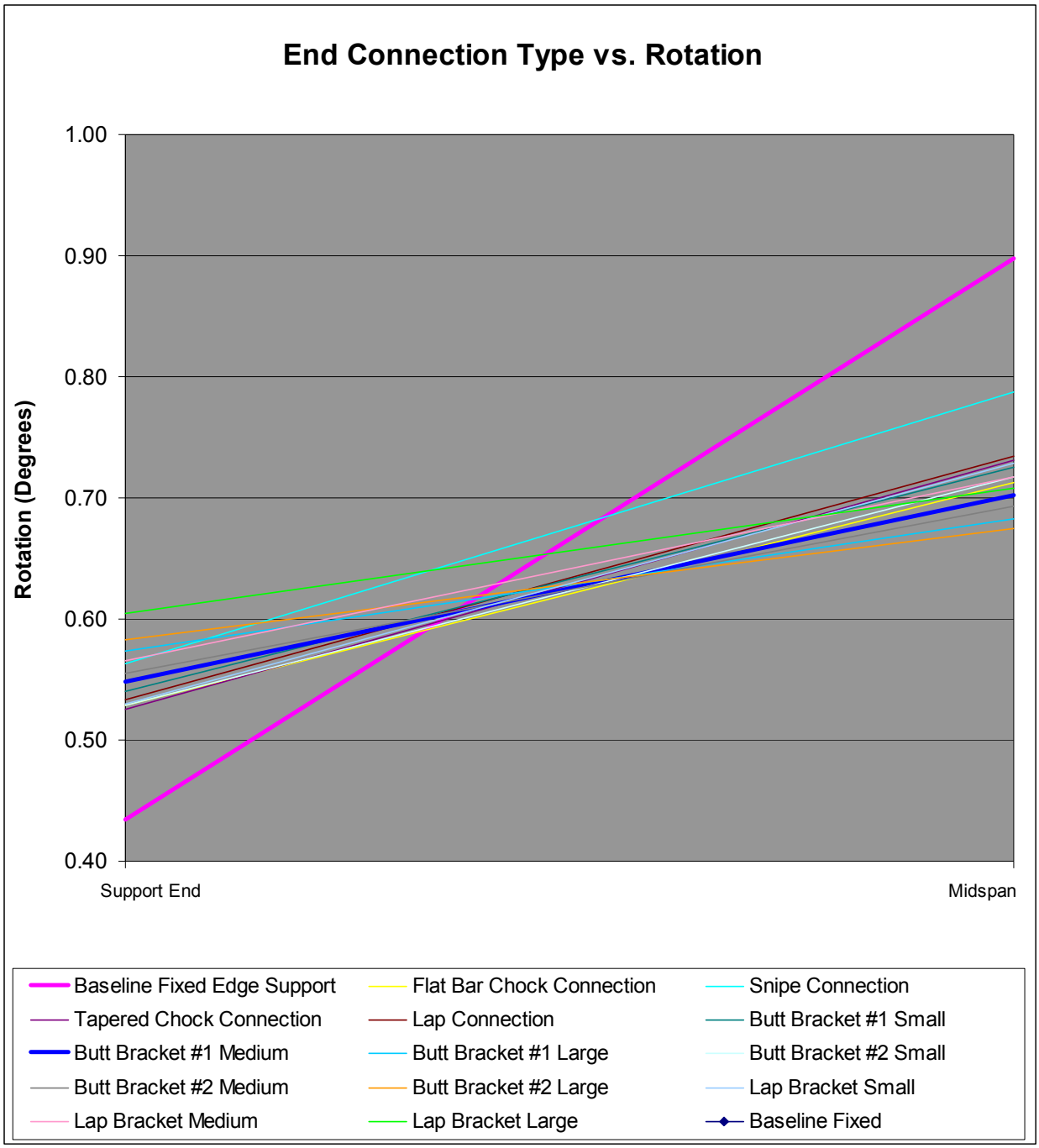

Figure 89 - Rotation Criteria - End Connection Type vs. Nodal Rotation – Line Graph

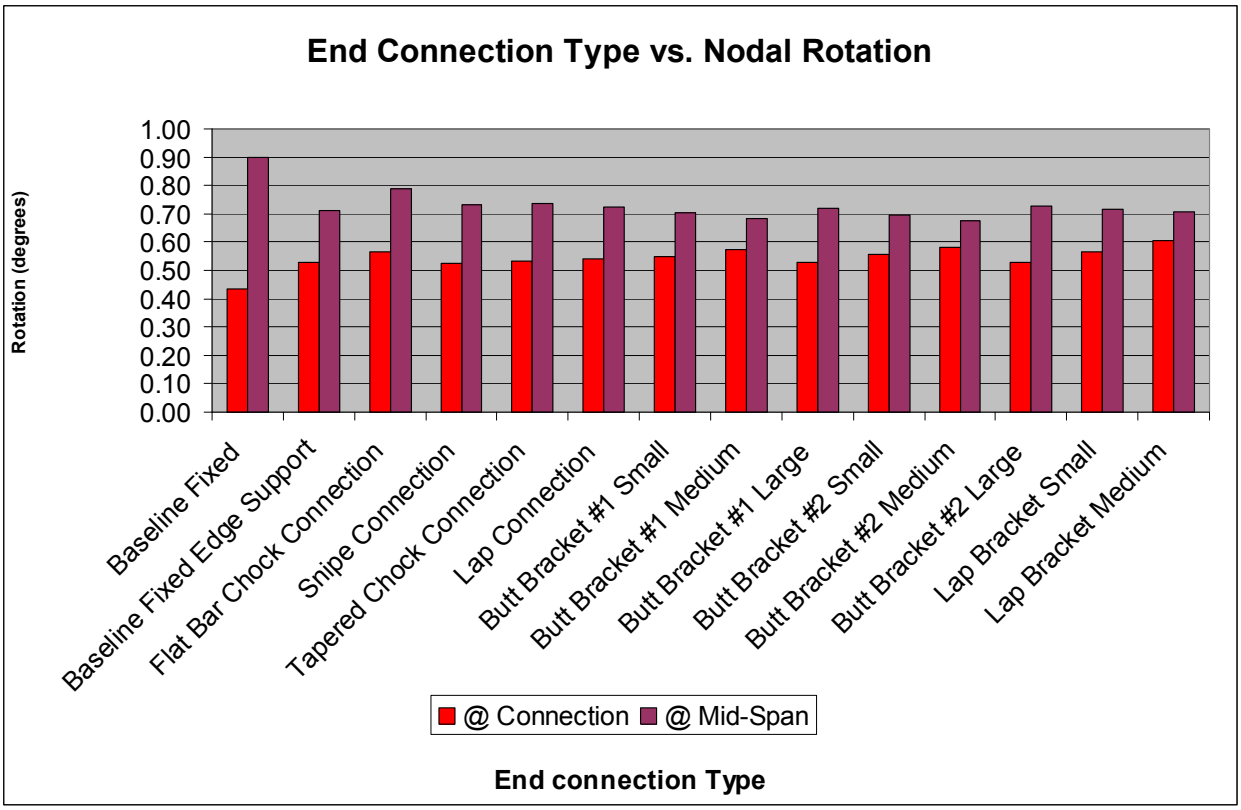

Figure 90 - Stress Criteria - End Connection Type vs. Nodal Rotation - Bar Graph

The final criterion was the "c" factor criterion. For this criterion, the individual models were subjected to a uniform load placed on the deck of the model and increased until yield of any part of the model occurred. The uniform load that produced material yielding was then recorded and used in a series of equations, stated in chapter 4. The "c" factor was then backed out, and used to draw comparisons for each end connection. Table (18) displays the findings of the "c" Factor criteria.

End Connection	Distributed Load for Failure (36 ksi) (lbs/in^2)	Line Load for Failure (lbs/in)	Constant (unitless)	Constant Correction (FEA - 1st Princ) (unitless)
Baseline Fixed	9.381	225.14	7.53	12.00
Baseline Fixed Edge Support	11.655	279.72	9.35	14.91
Flat Bar Chock Connection	14.79	354.96	11.87	18.92
Snipe Connection	14.81	355.44	11.89	18.94
Tapered Chock Connection	14.82	355.68	11.89	18.96
Lap Connection	14.945	358.68	12.00	19.12
Butt Bracket #1 Small	14.422	346.13	11.58	18.45
Butt Bracket #1 Medium	15.91	381.84	12.77	20.35
Butt Bracket #1 Large	16.764	402.34	13.46	21.44
Butt Bracket #2 Small	16.679	400.30	13.39	21.34
Butt Bracket #2 Medium	17.63	423.12	14.15	22.55
Butt Bracket #2 Large	18.11	434.64	14.54	23.17
Lap Bracket Small	16.961	407.06	13.61	21.70
Lap Bracket Medium	17.935	430.44	14.39	22.94
Lap Bracket Large	18.662	447.89	14.98	23.87

Table 32 - "c" Factor Criteria Summary

As shown below in figure (88), a straightforward method for drawing conclusions on the variances of “c” factors is to plot a bar graph. Again, the two baseline models are at the left of the graph, and if a line drawn horizontal to the x-axis was plotted one can see the differences of stress at the connection and at the midspan clearly.

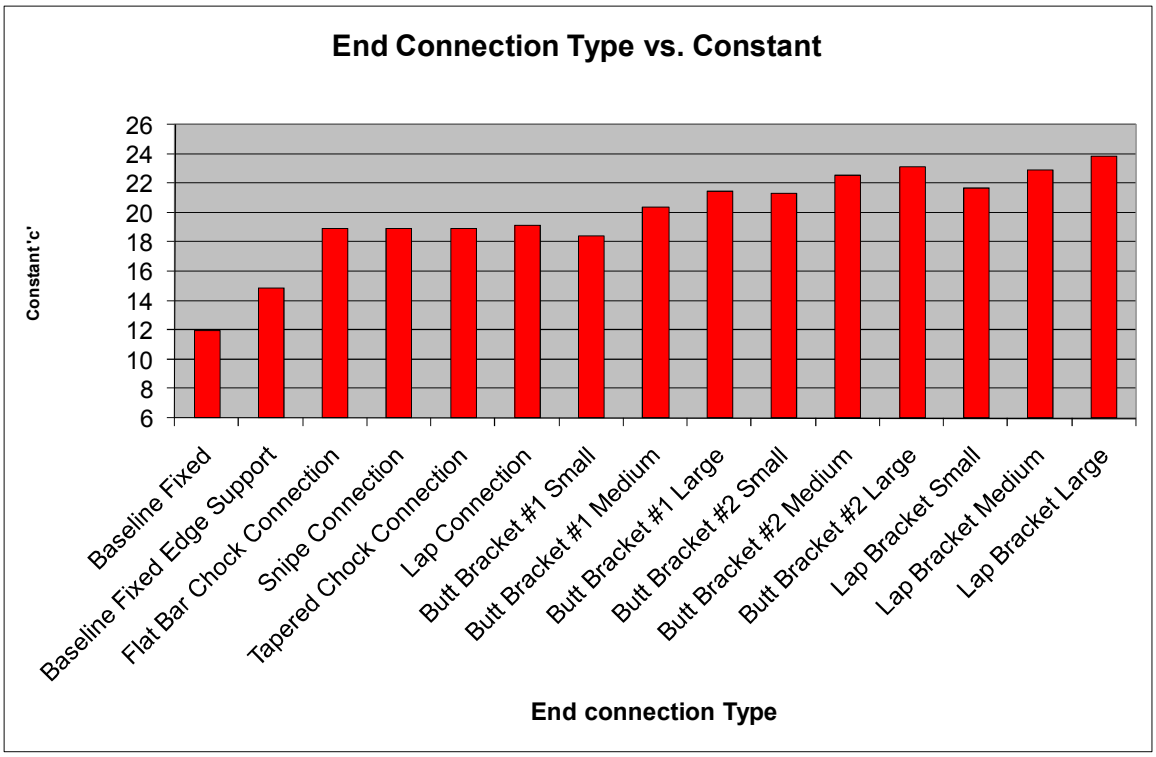

Figure 91 - Stress Criteria - End Connection Type vs. "c" Factor - Bar Graph

Chapter 8 – Conclusion

After completing the comparison of the three criteria, it is clear to see that the utilization of an efficiently sized bracket will offer the designer the optimum end connection for moment and shear transfer. This can be justified with the simple increase of section modulus and shear area at the connection. The larger the bracket, the more moment and shear transfer will occur.

Not only will the size of the bracket affect the amount of shear and moment transfer, but the type of connection the bracket makes with the deck stiffener and the vertical bulkhead stiffener will affect the transfer. The lap bracket connection offered the best results in the Stress Criteria and "c" Factor Criteria, yet for the Rotation Criteria, the results are comparable to the rest for other the 10 end connections analyzed. The commonality of the 10 end connections and the Lap Bracket connections is thought to have occurred because of the larger nodal sample area at the connection.

The Butt Bracket #2 connection which has the web of the deck stiffener hitting hard to the web of the vertical bulkhead stiffener, follows the Lap Bracket connection in the comparison of the bracket category. It is a stronger connection than the Butt Bracket #1 connection. The extra contact area created when both webs hit hard give the Butt Bracket #2 connection a lower Von Mises stress at the connection and midspan of the deck stiffener. The differences between all three bracket connection types in regards to the three comparison criteria are very minimal, and the use of the individual size and connection type should be decided upon the discretion of the designer for ease and cost of fabrication.

The efficiency of brackets can be linked to the American Bureau of Shipping allowable reduction of member span if a bracket is utilized. The American Bureau of Shipping allows a reduction in member length of twenty five percent from the toe of the bracket. This is significant

due to the length variable is squared in the moment equations as shown in figure (20). A well sized bracket can reduce member size dramatically therefore leading to material cost and weight savings

If the end connection under consideration is restricted by space, a chock connection may be utilized. Either the flat bar connection or a tapered chock connection yields very close results in the all three criteria. The chock connections offer lower moment and shear transfers than brackets. The tapered chock connection is slightly favorable in all three criteria, but the difference is not that great to state that one connection is far superior to the other. It is once again up to the designer for the selection of the type of chock to be used for ease and cost of fabrication.

For simplicity, the Snipe Connection can be used. These connections offered the worst results in the Stress Criterion and "c" Factor Criterion, but were comparable to the other 12 end connections analyzed for the Rotation Criteria. The stress at the connection and at midspan of the deck stiffener for this connection is almost the same. The trade off for this end connection is in the relative cost efficiency. A larger more costly deck stiffener will have to be used for shear and moment transfer.

The Lap Connection can be categorized better than the Snipe Connection, and chock connections. The Lap Connection offered the most favorable results behind the bracket connections. Due to the cost savings due to material and fabrication cost, the Lap Connection offers the designer a viable option.

In conclusion, the type of end connection utilized is a very important factor in structural design, and should not be under considered. The reduction of member sizes, fabrication cost, and material cost can be optimized by the proper selection of connection type. The selection of

connection type will often be governed by the location of the connection, and the cost of the connection to fabricate. It is the responsibility of the designer to adequately check the end connection for stress, ease of fabrication, and cost, before utilizing any connection.

The subject of structural end connections is an exciting topic in ship design. Although there has been much research in this area in the recent years, there are still many things yet to be explored.

References

[1] McCormac, Jack C., 2008, *Structural Steel Design,* Pearson Prentice Hall, Inc., Up Saddles Rivier, NJ

[2] American Institute of Steel Construction, Inc., 2005, *Steel Design 13th ed.*,

[3] Ship Structure Committee, 1990, "Design Guide for Ship Structural Details," SSC-331

[4] Ship Structure Committee, 1978, "In Service Performance of Structural Details," SSC-272

[5] Young, Warren C., Budynas, Richard G., 2002, *Roark's Formulas for Stress and Strain 7th ed,* McGraw Hill Book Company

[6] Kassimali, Aslam, 2005, *Structural Analysis,* Cengage Learning

[7] Beer, Ferdinand P., Johnston, E. Russell Jr., DeWolf, John T., 2002, *Mechanics of Materials 3rd ed.,* McGraw Hill Book Company

[8] Egeseli, Engin, 2007, "Advanced Steel Design", ENCE 6358 *Course Notes*, University of New Orleans School of Civil Engineering, Fall

[9] Boresi, Arthur P., Schmidt, Richard J., Sidebottom, Omar M., 1932, Advanced Mechanics of Materials 5th ed., John Wiley and Sons, Inc

[10] Boresi, Arthur P., Schmidt, Richard J., Sidebottom, Omar M., 1932, Advanced Mechanics of Materials 5th ed., John Wiley and Sons, Inc

[11] Algor Finite Element Suite, 2009, Algor User's Guide, Algor, Inc

[12] Timoshenko, 1995, "Strength of Materials, Part 1" Van Nostrand,

Vita

Bret Silewicz, born in Chicago, Illinois, obtained his High School Diploma from St. Thomas Aquinas High School (Hammond, Louisiana) in 1999 where he graduated in the top twenty percent of his class. He graduated in May 2004 from the University of New Orleans in New Orleans, Louisiana with a Bachelor of Science Degree in Naval Architecture and Marine Engineering. He is currently employed as a Naval Architect at Northrop Grumman Ship Building New Orleans Operations in Avondale, Louisiana.